

APPENDICES

Performance Characteristics of Modern Recycled Asphalt Mixes in Missouri,
Including Ground Tire Rubber, Recycled Roofing Shingles, and Rejuvenators

by

William G. Buttlar
Glen Barton Chair in Flexible Pavements

Jim Meister
Research Engineer

and

Behnam Jahangiri and Hamed Majidifard
Graduate Research Assistants

University of Missouri-Columbia

Missouri Department of Transportation Project #TR-201712
MU Project #00056783

February 16, 2018

See Main Report cmr 19-002

Table of Contents

Appendix A.	Field Sampling Details	A-1
Appendix B.	Development of DC(T) Creep Test	B-1
Appendix C.	Advanced Block Cracking Analysis Development	C-1
Appendix D.	Literature Review	D-1
Appendix E.	Acoustic Emission Testing	E-1

List of Figures

Figure A-1.	Google maps view of MO52_1	A-1
Figure A-2.	Location: MO52WB west of D. Section: MO52_1	A-2
Figure A-3.	Coring from MO52_1	A-2
Figure A-4.	Field cores from MO52_1	A-2
Figure A-5.	Google maps view of MO50_1	A-3
Figure A-6.	Location: US50WB 0.9w of Claas. Section: US50_1	A-4
Figure A-7.	Coring from MO52_1	A-4
Figure A-8.	Google maps view of US54_7	A-5
Figure A-9.	Location: US54WB w of United. Section: US54_7	A-5
Figure A-10.	Coring from US54_7	A-6
Figure A-11.	Google maps view of US54_8	A-7
Figure A-12.	Location: US54WB Wooded Hills Ln. Section: US54_8	A-7
Figure A-13.	Coring from US54_8	A-8
Figure A-14.	Coring from US63_2	A-9
Figure B-1.	Simplified model used to verify creep and relaxation tests: (a) loading and boundary conditions and (b) finite element mesh	B-1
Figure B-2.	Numerical vs. experimental values for: (a) relaxation modulus and (b) creep compliance	B-3
Figure B-3.	Three-dimensional DC(T) model used for simulation of creep compliance test: (a) geometry, loading, and boundary conditions and (b) finite element mesh	B-4
Figure B-4.	Cohesive fracture surface used to simulate fracture in the DC(T)	B-5
Figure B-5.	Creep compliance values obtained using Eq. (3) and based on simulation results obtained from 3D DC(T) models	B-6
Figure B-6.	Numerical vs. Experimental fracture test results obtained using (a) $E_{\infty}=0.741$ GPa (Table B-2) and (b) $E_{\infty}=1.033$ GPa	B-7
Figure B-7.	Simulated creep/recovery tests obtained from DC(T) models	B-7
Figure B-8.	Results of simulated fracture tests obtained after conducting a creep/recovery test for rest times of (a) 0 hours, (b) 1 hour, (c) 12 hours, and (d) 24 hours	B-8
Figure C-1.	Block cracks on US63 near La Plata, MO in July 2017, after 9 years of service ...	C-1
Figure C-2.	Load-CMOD curve of the surface mix	C-2
Figure C-3.	Creep compliance results from US63 La Plata field cores, at a reference temperature of -24°C	C-3

Figure C-4. Discrete element model of the pavement system of US 63 at La Plata, Missouri in PFC software.....	C-5
Figure C-5. Crack propagation patterns at various stages in the DEM simulation.....	C-6
Figure D-1. Reclaimed asphalt pavement (RAP)	D-2
Figure D-2. Production temperatures of asphalt concrete	D-3
Figure D-3. (a) HMA placement (b) WMA placement (11).....	D-6
Figure D-4. Asphalt milling machine and dump trailer	D-7
Figure D-5. Fractionated RAP stockpiles	D-7
Figure D-6. Sasobit pellets.....	D-9
Figure D-7. Rediset WMX pastilles.....	D-10
Figure D-8. Aspha-min Zeolite.....	D-11
Figure D-9. Astec double barrel green foaming drum.....	D-12
Figure D-10. Asphalt binder testing plan.....	D-13
Figure D-11. Mixture testing suite.....	D-14
Figure D-12. Virgin and 45% RAP mixture design gradations	D-17
Figure D-13. Hamburg Wheel Tracking device	D-19
Figure D-14. Hamburg gyratory specimen molds	D-20
Figure D-15. Typical DC(T) load-CMOD plots	D-20
Figure D-16. DC(T) testing arrangement.....	D-21
Figure D-17. Tank and RTFO binder M-Values	D-22
Figure D-18. Advera tank and RTFO binder stiffness.....	D-22
Figure D-19. Evotherm tank and RTFO binder stiffness.....	D-23
Figure D-20. Sasobit tank and RTFO binder stiffness.....	D-24
Figure D-21. Virgin Mixture rut depth profiles	D-25
Figure D-22. Virgin mixture wheel passes to maximum rut depth.....	D-26
Figure D-23. Moisture sensitivity of virgin mixture specimen.....	D-26
Figure D-24. 45% RAP mixture rut depth profiles.....	D-27
Figure D-25. 45% RAP mixture rut Depths at 10,000 wheel passes	D-28
Figure D-26. RAP Sasobit Hamburg Specimen	D-28
Figure D-27. TSR results for virgin HMA and WMA mixtures.....	D-30
Figure D-28. (a) Unconditioned Evotherm TSR sample and (b) Conditioned Evotherm TSR sample	D-30
Figure D-29. 45% RAP HMA and WMA mixture TSR results	D-31
Figure D-30. DC(T) results for virgin HMA and WMA mixtures	D-32
Figure D-31. DC(T) results for 45% RAP HMA and WMA mixtures.....	D-33
Figure D-32. Asphalt shingle composition	D-38
Figure D-33. Post-consumer RAS	D-38
Figure D-34. Summary of sections investigated in Chicago area.....	D-41
Figure D-35. Sample fracture energy results from cores tested in DC(T): High traffic SMA mixes	D-42
Figure D-36. DC(T) test results at -12°C.....	D-51
Figure D-37. Acoustic emission embrittlement temperature test results.....	D-51
Figure D-38. Hamburg-DC(T) plot concept and Performance zones.....	D-52
Figure D-39. Hamburg-DC(T) plot with typical specification limits superimposed.....	D-53
Figure D-40. Hamburg DC(T) Plot showing typically Illinois' mixture data, along with 4 data points collected in this study (located at the beginning and ends of red arrows)	D-54

Figure D-41. Paving of the Grand Avenue test sections in May, 2015	D-57
Figure D-42. Hamburg test results.....	D-59
Figure D-43. DC(T) test results	D-62
Figure D-44. SCB load-displacement plots	D-66
Figure D-45. Hamburg-DC(T) plot with typical specification limits superimposed.....	D-67
Figure D-46. Hamburg-DC(T) plot for N70 CHI mixes and N30 reference mixes	D-68
Figure E-1. Schematic representation of Acoustic Emission testing setup	E-1
Figure E-2. (a) AE testing setup for asphalt binders (b) AE asphalt binder sample (thin film of asphalt binder bonded to granite substrate) (c) AE testing setup for asphalt mixtures (d) AE asphalt mixture sample	E-3
Figure E-3. Typical AE test result for asphalt materials.....	E-4
Figure E-4. Embrittlement Temperatures of X and Y Specimens for all mixture samples	E-6
Figure E-5. Acoustic Emission Energy and Event Count versus Temperature for specimen Y of US54-3-1 Sample. Horizontal axis denotes temperature in °C.....	E-7
Figure E-6. Embrittlement Temperatures in °C of A, B, C specimens for all binder samples. See Table 3.	E-8
Figure E-7. Acoustic Emission Energy and Event Count versus Temperature for specimen B of US63-1 Binder Sample. Horizontal axis denotes temperature in °C.....	E-9
Figure E-8. Embrittlement temperature from Acoustic Emission test compared to the DC(T) fracture energy	E-9

List of Tables

Table B-1. Parameters for creep model	B-2
Table B-2. Parameters for relaxation model	B-2
Table B-3. Cohesive contact properties used to simulate fracture in DC(T) specimens	B-5
Table C-1. Block crack areas of US63 at La Plata, MO - analytical solution vs. observed pattern	C-4
Table D-1. RAP gradations.....	D-15
Table D-2. Virgin mixture blend	D-16
Table D-3. 45% RAP blend	D-18
Table D-4. Sasobit tank and RTFO binder stiffness	D-25
Table D-5. 45% RAP Hamburg WTD results	D-28
Table D-6. Virgin mixture TSR results.....	D-29
Table D-7. 45% RAP mixture TSR results.....	D-31
Table D-8. (a) D-1 RAP/RAS specification, (b) Statewide RAP/RAS specification.....	D-41
Table D-9. Mixture design gradations	D-46
Table D-10. Mixture volumetrics in RAS availability study	D-47
Table D-11. 2.5% RAS pulp mixture design	D-48
Table D-12. 5.0% RAS pulp mixture design	D-48
Table D-13. Hamburg test results	D-50
Table D-14. DC(T) Grand Ave. mixture results.....	D-61
Table D-15. Summary DC(T) and SCB results	D-63
Table D-16. Detailed DC(T) and SCB comparison.....	D-64
Table D-17. Detailed SCB results.....	D-65
Table D-18. Superpave binder grade determination results for N70 CHI mixtures	D-69
Table D-19. Summary of GTR technologies and asphalt binder types	D-79
Table D-20. Location of GTR Test sections on Reagan Memorial Tollway (I-88)	D-79
Table E-1. Asphalt mixture samples tested using Acoustic Emission.....	E-5
Table E-2. Acoustic Emission testing results for asphalt mixture samples	E-6
Table E-3. Acoustic Emission testing results for asphalt binder samples	E-8

Appendix A. Field Sampling Details

A.1. MO52_1

Contract J5P0925

MO52 west of Versailles in Morgan County

TWay ID: 53 MO 52 W

Propose coring take place between the intersection with highway D on the east end and the intersection with highway T on the west end. The total distance between these endpoints is approximately 1.2 miles. There is a small hill leading up to highway T. We will defer to the core rig operator and safety crew to determine if we must avoid this hill.

Junction with highway D: log mile – 52.132

Junction with highway T: log mile – 53.389

PLAN: to core west bound direction away from Versailles on April 3, 2017



Figure A-1. Google maps view of MO52_1



Figure A-2. Location: MO52WB west of D. Section: MO52_1



Figure A-3. Coring from MO52_1



Figure A-4. Field cores from MO52_1

A.2. US50_1

Contract: J5P0961

US50 west of Tipton in Moniteau County

TWay ID: 3507 US 50 E

Proposed coring to take place between 0.3 miles east of Claas Crossing Road intersection on the east end and 1.0 mile west of Claas Crossing Road on the west end. The total distance between these endpoints is about 1.25 miles. Claas Crossing Road is approximately 2.3 miles west of the MO5/US50 junction in Tipton, and approximately 2.1 miles east of the MO5/US50 junction in Morgan County.

End of curve 0.3 miles east of Claas Crossing: log mile – 103.063

County line Morgan/Moniteau, 1 mile west of Claas Crossing: log mile – 101.957

-There are gentle curves at each end of this area. It is relatively flat and farmland around the pavement, so the sight distances are good even in the curves.

PLAN: to core west bound direction away from Tipton on April 3, 2017



Figure A-5. Google maps view of MO50_1



Figure A-6. Location: US50WB 0.9w of Claas. Section: US50_1



Figure A-7. Coring from MO52_1

A.3. US54_7

Contract: J5P0769

US54 WBL west of Brazito in Cole County

TWay ID: 1986 US 54 W

Proposed coring to take place between 0.1 miles west of the intersection with Quail Drive on the east and 0.2 mile west of the intersection with Penny Hollow Road on the west. Google maps measures this distance at 2.7 miles.

Quail Drive intersection: log mile – 118.285

Penny Hollow Road intersection: log mile – 120.74

- There are several areas to be careful around in between these boundaries. There are intersections at United Road and at Clark Fork Road. Additionally, there are some hills on 54

that seem to have good sight distances, but we will defer to the judgment of the safety crew and coring operator.



Figure A-8. Google maps view of US54_7



Figure A-9. Location: US54WB w of United. Section: US54_7



Figure A-10. Coring from US54_7

A.3. US54_8

Contract: J5D0600A

US54 west of Jeff City in Cole County

TWay ID: 1986 US 54 W

Proposed coring to take place between the intersection with Hamman Drive on the east and the intersection with Monticello Road on the west. Google maps measures this distance at 1.6 miles.

Hamman Drive intersection: log mile – 108.178

Monticello Road intersection: log mile – 110.13

- There are several areas to be careful around in between these boundaries. There are intersections at highway CC and at Wooded Hill Lane as well as a bridge crossing Neighorn Creek. In addition to these intersections, there are some hills on 54 that seem to have good sight distances, but we will defer to the judgment of the safety crew and coring operator.

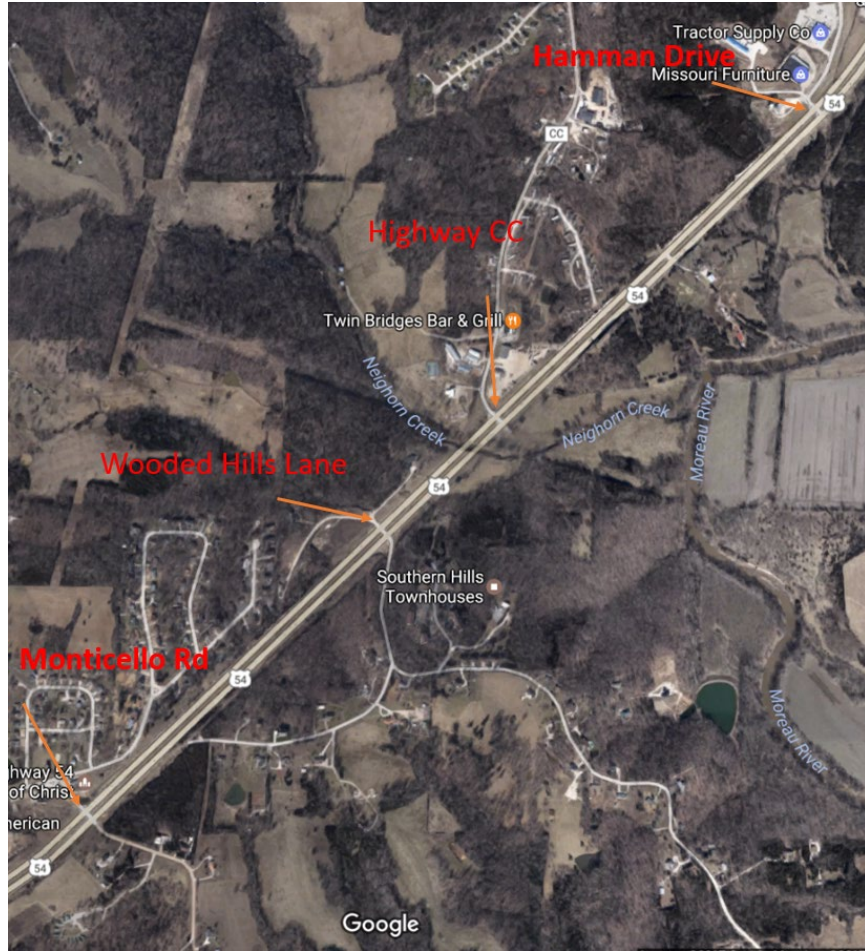


Figure A-11. Google maps view of US54_8



Figure A-12. Location: US54WB Wooded Hills Ln. Section:US54_8



Figure A-13. Coring from US54_8

A.3. US63_2

Project short label: US63_2

Coring date/time: Monday November 11, 2016 / 1000-1130. Weather: Partly cloudy, temp = 73F.

Contract: J2P0733

Cores taken from US63 SBL near between La Plata and Atlanta in Macon County

TWay ID: 57 = US 63 S; 56 = US 63 N

MoDOT Mobile Log Finder information:

Core	Tway 57	Tway 56	Accu	Location Description
63_2-1	44.481	293.264	10	500 ft S of Katydid, MODOT station 400
63_2-2	44.452	293.225	10	200 ft further S, MODOT station 600
63_2-3	44.564	293.181	5	200 ft further S, MODOT station 800
63_2-4	44.599	293.147	5	200 ft further S, MODOT station 1000
63_2-5	45.202	292.544	5	50 ft N of sign "NN next intersection"
63_2-6	45.836	291.910	5	No good landmark ~1/2 mi N of next intersection
63_2-7	46.340	291.405	5	75 ft N of Jockey St.
63_2-8	46.823	290.922	5	50 ft N of guardrail
63_2-9	47.593	290.152	5	150 ft N of Joliet Rd
63_2-10	48.361	289.384	5	100 ft N of Landmark Rd

63_2-11	48.862 288.886	5	100 ft N of Kangaroo Rd
63_2-122	49.730 288.016	5	Adjacent to sign "R and J next right"



Figure A-14. Coring from US63_2

Appendix B. Development of DC(T) Creep Test

B.1. A simplified Abaqus model to obtain creep and relaxation data

The finite element program Abaqus was employed to simulate creep compliance and fracture tests conducted on DC(T) specimens. This was done in an effort to obtain formulas to turn raw test data into fundamental creep compliance data, accounting for the non-uniaxial specimen geometry of the DC(T). In addition, modeling was used to determine maximum creep load levels that would ensure predominantly linear viscoelastic response and statistically insignificant specimen damage at the notch tip. The latter was necessary to enable test specimens to be reused for subsequent fracture energy testing. Before simulation of the DC(T) creep compliance and fracture tests, both creep and relaxation tests were performed in Abaqus on a simple uniaxial geometry to verify that the viscoelastic parameters used in the models were applied correctly. The simplified finite element (FE) model for the creep and relaxation simulation is shown in Figure B-1.

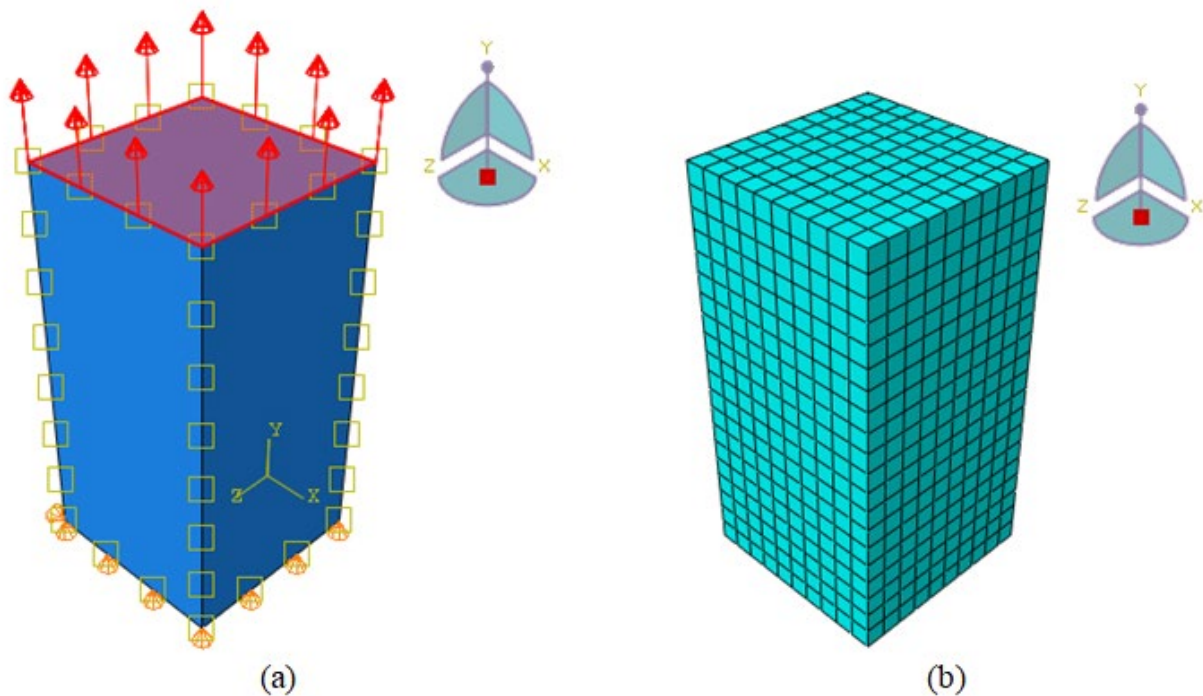


Figure B-1. Simplified model used to verify creep and relaxation tests: (a) loading and boundary conditions and (b) finite element mesh

The viscoelastic material model form used in Abaqus corresponds to a Generalized Maxwell relaxation model. The Maxwell model parameters used in Abaqus were obtained via interconversion, as derived from experimental creep compliance values obtained from DC(T) creep testing. The experimental creep compliance data was fitted with a generalized Voight-Kelvin model, having the functional form:

$$D(t) = D_0 + \eta t + \sum_{i=1}^N D_i (1 - e^{-\lambda_i t}) \quad (1)$$

where parameters $D_i, \lambda_i, i = 0, \dots, N$ and η , correspond to the material simulated in the simplified model depicted in Figure B-1, which are shown in Table B-1.

The creep compliance function given by Eq. (1) can be transformed to obtain a generalized Maxwell, a.k.a. Prony series representation of the relaxation modulus function:

$$E(t) = E_\infty + \sum_{i=1}^N E_i e^{-t/\tau_i} \quad (2)$$

where parameters E_∞, E_i , and $\tau_i, i = 1, \dots, N$ are given in Table B-2.

Table B-1. Parameters for creep model

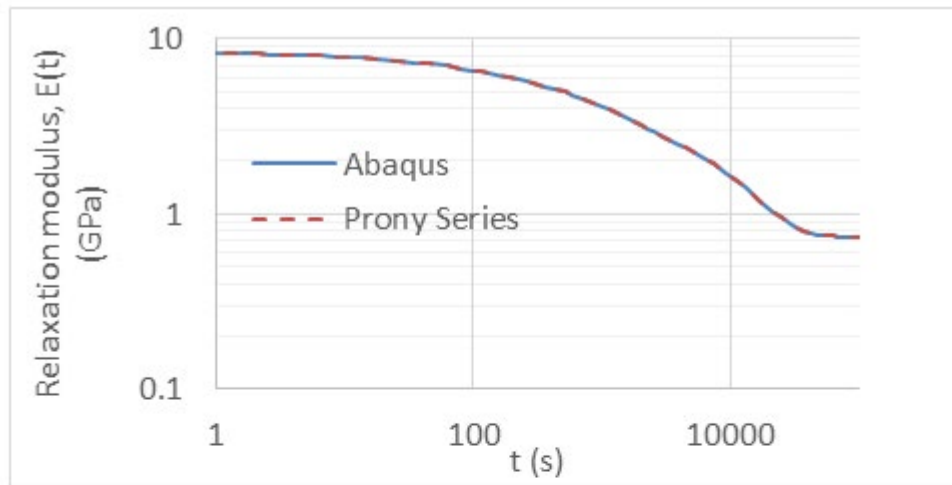
Coefficient	Coefficient λ_i (s^{-1})	
D_0 (1/GPa)	0.07031	
η (1/GPa · s)	9.25E-06	
D_1 (1/GPa)	0.005027	1
D_2 (1/GPa)	0.01008	0.1
D_3 (1/GPa)	0.001437	10
D_4 (1/GPa)	0.02853	0.01
D_5 (1/GPa)	0.003245	100
D_6 (1/GPa)	0.07879	0.001
D_7 (1/GPa)	4.6E-06	1000
D_8 (1/GPa)	0.252	0.0001
D_9 (1/GPa)	0.0271	10000

Table B-2. Parameters for relaxation model

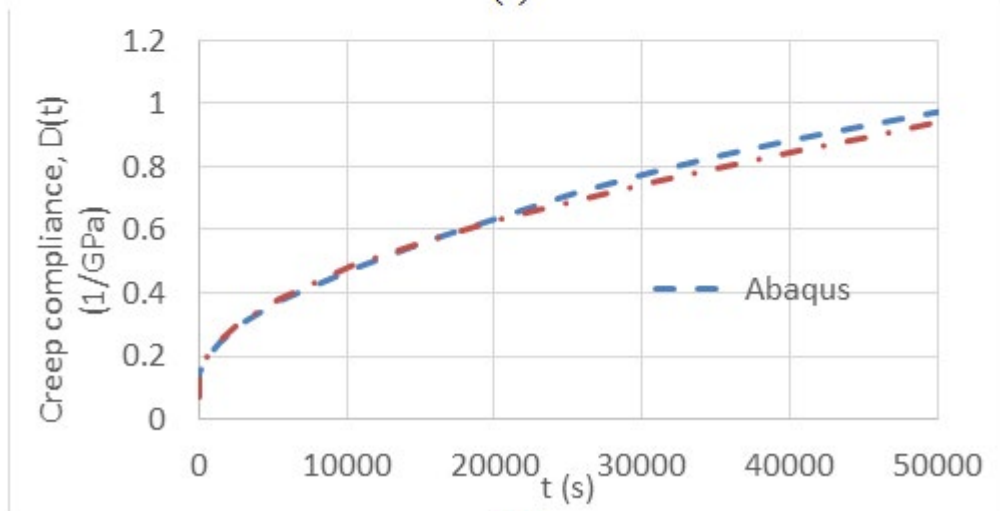
i	τ_i (s)	E_i (GPa)
∞	-	0.741
1	1	0.473
2	10	0.2793
3	0.1	0.1195
4	100	1.634
5	0.01	0.7502
6	1000	3.061
7	0.001	0.1171

i	τ_i (s)	E_i (GPa)
8	10000	2.502
9	0.0001	0.3023

The numerical and experimental results for both creep and relaxation modulus are presented in Figure B-2. The experimental and numerical results agree well for the relaxation modulus, while minor discrepancies were observed for the creep compliance, due to the approximate nature of the interconversion technique used.



(a)



(b)

Figure B-2. Numerical vs. experimental values for: (a) relaxation modulus and (b) creep compliance

B.2. Obtaining creep compliance from DC(T) Abaqus models

Using the material parameters given in Table B-2, the simulation of the DC(T) creep compliance test was carried out with Abaqus, using the boundary conditions and finite element mesh shown in Figure B-3. To simulate the experimental setup, the bottom pin of the DC(T) was fixed, while the load P was applied at the top of the upper loading hole. Additional boundary conditions were applied to the top loading pin to enforce pure vertical movement. The results from the 3D DC(T) creep test simulations were used to obtain a creep compliance formula for use with raw test data, according to the following expression:

$$D(t) = C_f \frac{CMOD(t) \times B}{P} \quad (3)$$

where $C_f = 0.0538$ is a so-called correction factor obtained through trial-and-error, by adjusting C_f in such a manner as to bring the simulated DC(T) creep compliance values in agreement with the creep compliance function used in the Abaqus model. $CMOD(t)$ corresponds to the crack mouth opening displacements, which are function of time; B is the thickness of the DC(T) specimen; and P is the applied load.

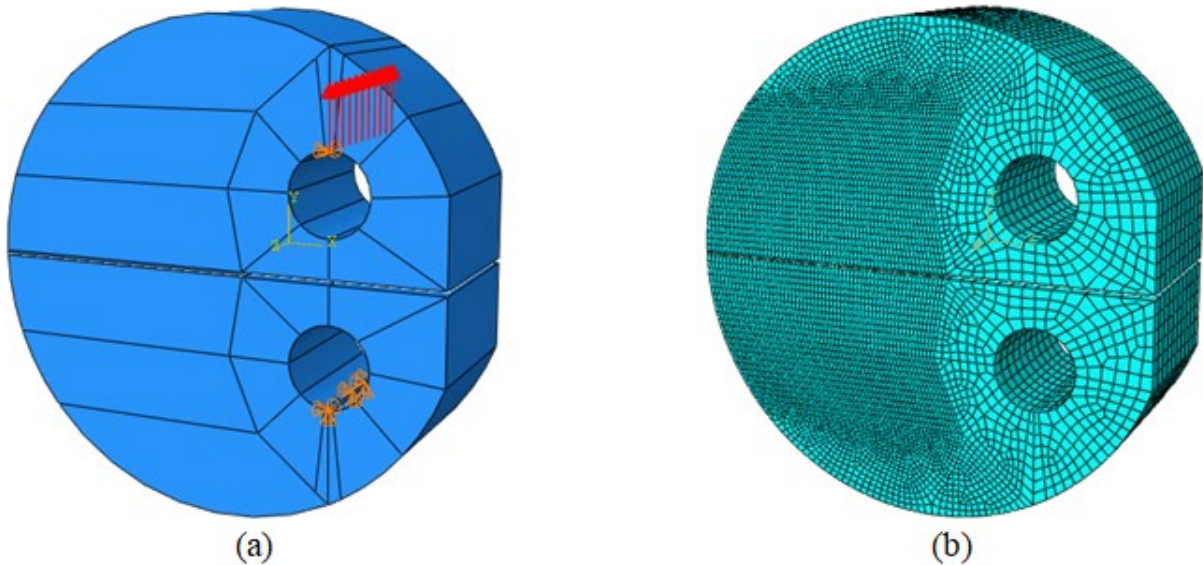


**Figure B-3. Three-dimensional DC(T) model used for simulation of creep compliance test:
(a) geometry, loading, and boundary conditions and (b) finite element mesh**

In order to study the effect of the magnitude of the applied load, P , on the creep compliance values obtained from the DC(T) models, cohesive zone fracture elements were inserted along the ligament length (Song et al. 2006), where the fracture is expected to propagate, as shown in Figure B-4. A linear softening cohesive contact model was used (Song et al., 2006) with the parameters shown in Table B-3.

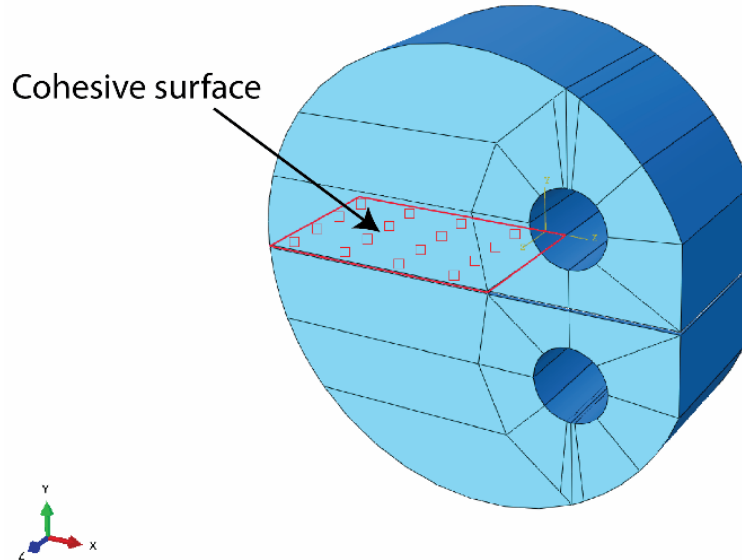


Figure B-4. Cohesive fracture surface used to simulate fracture in the DC(T)

Next, creep compliance simulations were used to obtain creep compliance values for various levels of applied load, P , to determine the threshold where significant damage occurs at the notch tip. The creep test responses obtained from these simulations are shown in Figure B-4. Clearly, the simulated DC(T) creep compliance curves are very close to those from the simplified (non-fracture) Abaqus model across the entire range of applied loads P that were considered. This indicates that using applied loads below 0.8 kN are acceptable to conduct DC(T) creep tests without inducing significant damage to the test specimens.

Table B-3. Cohesive contact properties used to simulate fracture in DC(T) specimens

Cohesive behavior

K_{nn} (MPa/mm)	K_{ss} (MPa/mm)	K_{tt} (MPa/mm)
5000	5000	5000

Damage initialization: Quadratic traction

Normal (MPa)	Shear-1 (MPa)	Shear-2 (MPa)
3.5	3.5	3.5

Damage Evolution: Linear

Fracture energy (J/m ²)
318

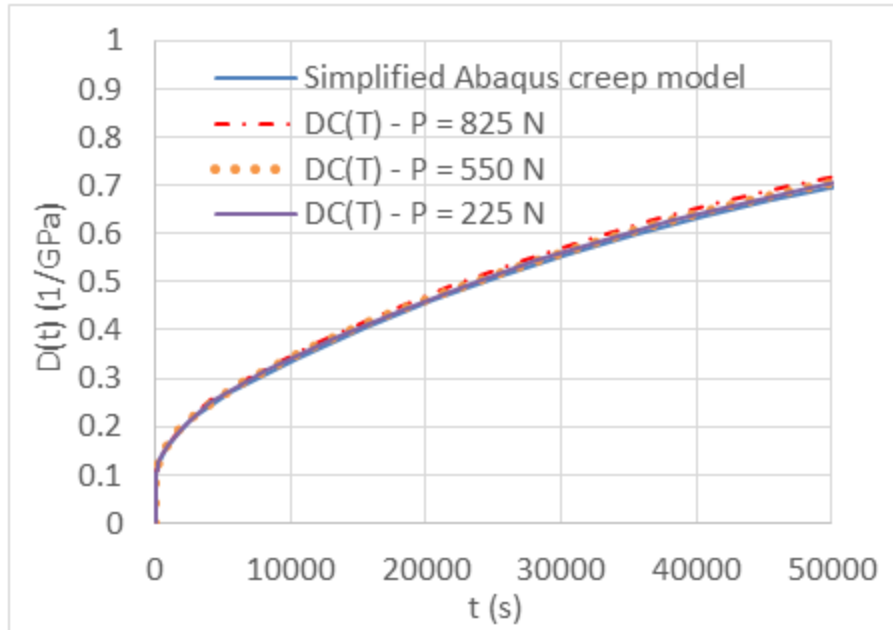


Figure B-5. Creep compliance values obtained using Eq. (3) and based on simulation results obtained from 3D DC(T) models

B.3. Fracture simulation of the DC(T) test

Next, fracture simulations were performed using the 3D DC(T) model shown in Figure B-3. The bulk material was again modeled using the Prony series data given in Table B-2, and the cohesive contact model again used the properties reported in Table B-3. Fracture simulations were conducted by applying a velocity boundary condition in the direction indicated by the arrows in Figure B-3a. The applied velocity was 0.76 mm/min, which was chosen to be consistent with the experimental loading rate. The fracture simulation results are displayed in Figure B-5a. According to these results, we observe that the Abaqus model underestimates the initial slope obtained from the experimental DC(T) fracture test, which is not uncommon (Song et al., 2006). A possible explanation for this particular discrepancy is that the Abaqus model overestimates the measured creep compliance data (e.g., see Figure B-2b), which indicates that the material used in the actual models is more compliant than the actual material tested in our lab. In order to reduce such discrepancies, we increase set $E_{\infty} = 1.033$ GPa and re-run the simulations. Using this value for E_{∞} led to a slightly improved prediction of the initial slope. In order to achieve an even better fit, a more complex cohesive zone fracture model would need to be employed, such as the exponential softening-type model introduced by Song et al. (2006). However, for the purposes of the analysis being conducted herein, the simple linear softening model was deemed appropriate.

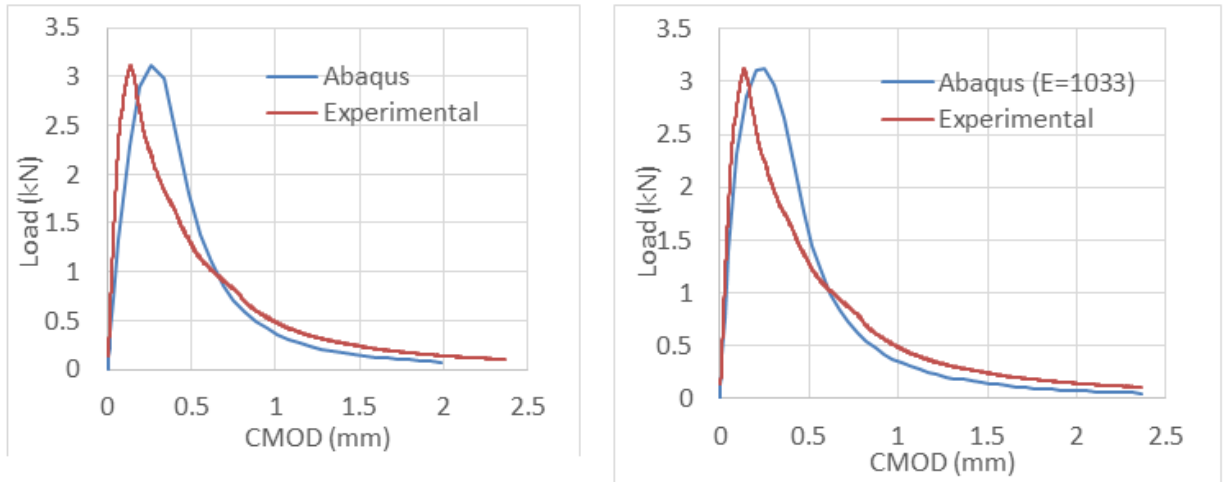


Figure B-6. Numerical vs. Experimental fracture test results obtained using (a) $E_{\infty}=0.741$ GPa (Table B-2) and (b) $E_{\infty}=1.033$ GPa

Finally, creep/recovery test simulations for various levels of the applied load, P , and compare the results against those obtained from the creep tests. After conducting the creep/recovery tests, we conduct fracture tests and study the effect that the rest time has on the fracture simulation results. Figure B-7 shows obtained numerical results for the creep/recovery tests, which are shown to agree with the creep tests results for all levels of applied loads up to the point in which the applied load is removed.

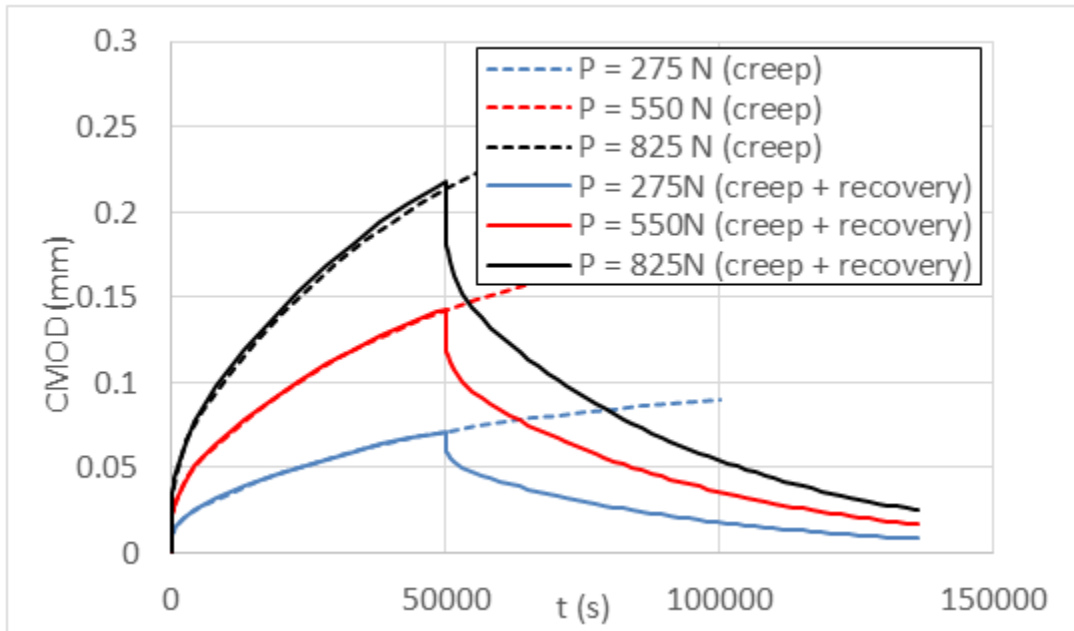


Figure B-7. Simulated creep/recovery tests obtained from DC(T) models

Figure B-8 shows the fracture simulation results obtained for various values of rest time. The results are compared against those obtained from fracture tests that were not preceded by a creep/recovery test. The results show that the fracture simulation results are independent of the rest time.

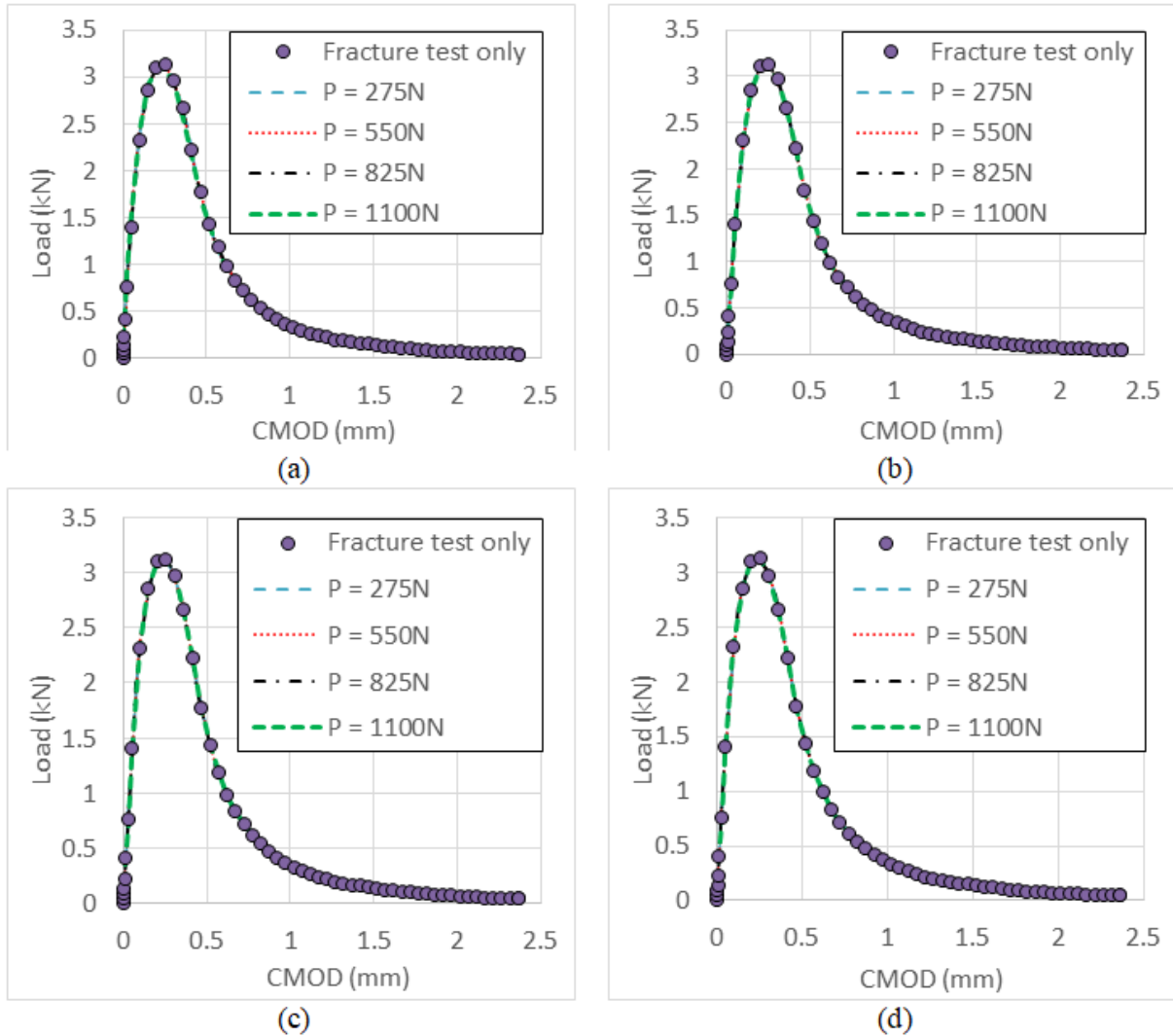


Figure B-8. Results of simulated fracture tests obtained after conducting a creep/recovery test for rest times of (a) 0 hours, (b) 1 hour, (c) 12 hours, and (d) 24 hours

Appendix C. Advanced Block Cracking Analysis Development

C.1. Introduction

Block cracking is a common type of distress observed in asphalt pavements. Similar to thermal cracking, block cracking is also considered as thermally-induced (non-load associated) form of cracking in asphalt pavements, usually occurring when the pavement surface becomes more vulnerable to cracking as a result of years of oxidative and steric hardening. The prevalence of block cracking on current asphalt pavement surfaces may be due to increased usage of recycled materials. Others speculate that increased cracking may be due to changes in asphalt supply, such as the inclusion of recycled engine oil bottoms or REOB (ref), polyphosphoric acid (PPA), and changes in refining techniques. Block cracking is most often found in climates with hot summers and/or large swings in surface temperatures, such as in mid-continental climates and deserts. Block cracking has not received much attention in research studies, and therefore, the precise mechanisms behind its development are not well understood. Integrated testing, modeling, and field studies are required to deepen our understanding of this unsightly, and often damaging cracking form.

In July 2017, a dense block cracking pattern was observed on US63 near La Plata, Missouri after nine years of service life, as shown in Figure C-1. In order to further investigate the cause of this advanced block cracking pattern, three performance test samples of the top layer were prepared from field cores. The viscoelastic behavior and fracture properties of the samples were examined to characterize the properties present in the aged asphalt surface. These test results were then utilized in analytical and computer simulation models to predict the block crack formation and density of US 63 at La Plata, as a means of model validation.



Figure C-1. Block cracks on US63 near La Plata, MO in July 2017, after 9 years of service

C-2. Material Properties Results and Discussion

The surface mixture was comprised of a PG 64-22 binder, used in a 12.5 mm nominal maximum aggregate size Superpave aggregate blend. The mix contained 26.8% asphalt binder replacement

achieved by using 18% reclaimed asphalt pavement (RAP) and 2% reclaimed asphalt shingles (RAS), by weight of mixture. In order to examine the relaxation behavior and low-temperature fracture properties of the surface mix, DC(T) fracture energy and DC(T) creep compliance tests were conducted in triplicate replication. The DC(T) fracture energy test follows ASTM D7313, and the DC(T) creep compliance was conducted based on the procedures introduced in Appendix B.

The average fracture energy value of the tested samples was 244J/m^2 , which was considerably below the fracture energy threshold, 400J/m^2 , as recommended in the FHWA pool fund study (Marasteanu et al., 2007) for a medium traffic level (under 30 million ESALs). The load versus crack mouth opening displacement (CMOD) curve of one of the replicates is presented in Figure C-2. As can be seen from this figure, the peak load of this sample was about 1.9kN , which was relatively low (which is a characteristic of highly aged, brittle mix) and clearly a component leading to the low fracture energy of this sample. In addition, a brittle (steep) post-peak softening curve was observed, which is also characteristic of highly aged, brittle mixes, further reducing mixture fracture energy. As a result of this high brittleness, a high density of block cracks would be expected to occur on a pavement comprised of this mixture, particularly if placed in a mid-continental climate. There are a number of other reasons why low peak load/fracture energy may be present, such as inclusion of recycling without a downward asphalt grade bump, low pavement density (high in-place voids), age-susceptible binder (containing REOB), low-ductility asphalt (for instance, containing PPA), weak/damaged aggregates, poor adhesion, or a combination of factors.

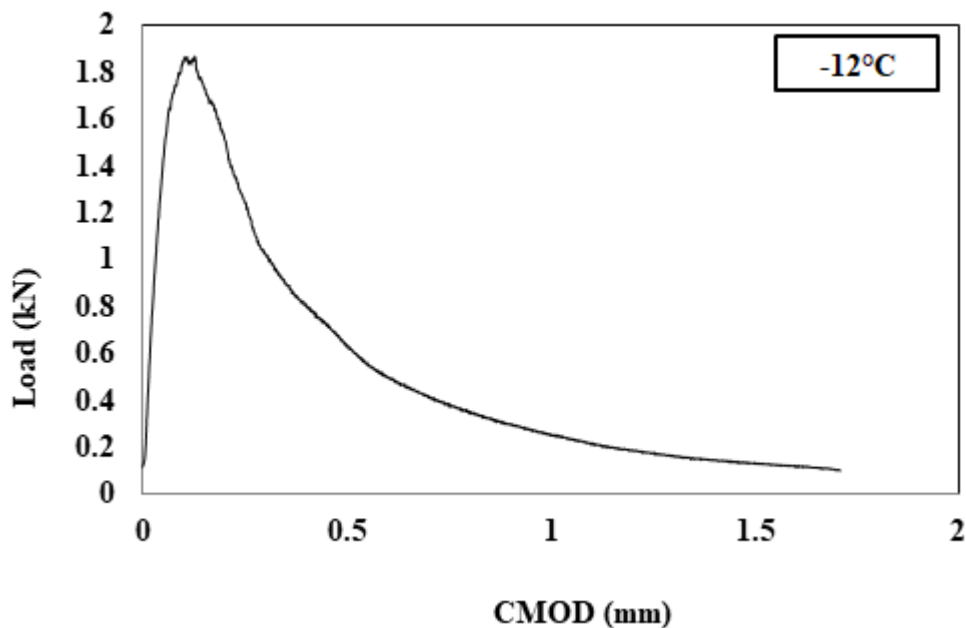


Figure C-2. Load-CMOD curve of the surface mix

Asphalt mixture is considered as viscoelastic material, even at low temperatures, so creep compliance testing is necessary to capture the response of the pavement under temperature

cycling for the purposes of simulation. The creep compliance curve of the tested asphalt material is shown in Figure C-3. Creep compliance test results were fitted with a power law function, and the obtained m-value of 0.395, was found to be within the normal range.

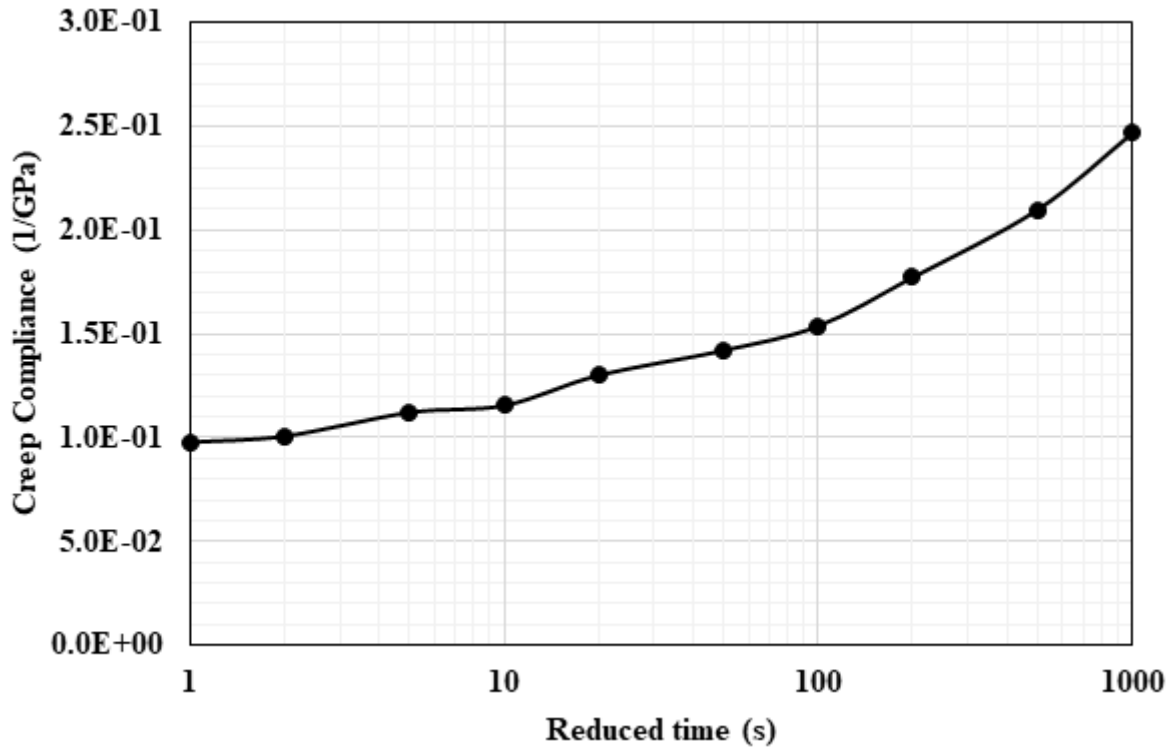


Figure C-3. Creep compliance results from US63 La Plata field cores, at a reference temperature of -24°C

C.3. Block crack dimension prediction using analytical models

Wang and Buttlar (2018) developed analytical solutions for displacement and stress fields of a three-dimensional asphalt pavement system subjected to constant thermal stresses, and presented methods to approximate the saturated block crack dimensions for a given asphalt pavement. Suppose the following conditions exist: asphalt material elastic modulus of 20GPa (low temperatures prevail), a spring coefficient of 2GPa, Poisson's ratio of 0.2, a coefficient of thermal expansion of $3E-5/^{\circ}C$, asphalt tensile strength of 3.5MPa, and a base layer with a thermal expansion coefficient of $1E-5/^{\circ}C$. Due to the elastic assumption of the analytical model, the instantaneous relaxation modulus was taken as the elastic modulus of the surface mix, which was obtained through interconversion of the creep compliance master curve at a reference temperature of -24°C. The tensile strength of the surface mixture was estimated from the peak load measured in the DC(T) test using Equation 1, which was obtained from ASTM E399-90(1997) and applied by Dave et al. (2013).

$$S_t = (2P (2W+a))/(B (W-a)^2) \quad (1)$$

Where, S_t represents the material tensile strength in MPa, P is the maximum load sustained by the sample in Newtons, B is the thickness of the sample (in mm), and W and a are geometric parameters of the DC(T) specimen, in mm, following the recommended values of 110mm and 27.5mm, accordingly (Wagoner et al., 2005). Due to the normal in-situ, top-down aging processes, the material properties in the aged surface layer vary through the thickness in a highly graded manner. However, note that the obtained laboratory results represent an ‘averaged’ or intermediate description of the material properties in the top 50 mm of the pavement section. To obtain graded properties, results from the studies of (Apegyei, 2006, Braham et al., 2009, Buttlar et al., 2006) were examined and applied. In summary, based on these test results along with engineering judgment derived from previous studies, material properties (elastic modulus and tensile strength of the surface layer) and material grading parameters across the 50 mm thickness were approximated, as shown in Table C-1.

Examining the temperature history of La Plata, MO from December 2016 to January 2017, the average daily winter air temperature change was about -15°C . Therefore, for full-depth, mid-depth and near-surface cracks, the corresponding saturated block crack dimensions were found to be $2.34\text{m} \times 2.34\text{m}$, $1.98\text{m} \times 1.98\text{m}$, and $1.67\text{m} \times 1.67\text{m}$, respectively. A visual observation of the field section (Figure C-1) revealed that the sizes of block cracks vary from $0.12\text{m} \times 0.15\text{m}$ to $1.54 \times 1.76\text{m}$. The ‘major’ block crack size observed in the field (larger blocks with notably wider cracks – likely the block cracks that formed first and have penetrated the deepest) was similar to the near-surface crack size predicted by the analytical model. The presence of smaller block cracks in the field suggests the strong near-surface cracking vulnerability of the highly-aged mixture containing RAP and RAS.

Therefore, the present analytical model is capable of providing a reasonable prediction of the primary, larger block crack pattern observed in the chosen field section. It was hypothesized that the smaller block cracking pattern could be captured with a more rigorous 3D numerical modeling scheme, including additional physical quantities such as bulk viscoelasticity, fracture property gradients, temperature cycling, and material morphological representation (aggregates, mastic, air voids). This motivation led to the modeling results presented in the following section.

Table C-1. Block crack areas of US63 at La Plata, MO - analytical solution vs. observed pattern

Crack depth	Elastic modulus multiplier	Elastic Modulus (MPa)	Tensile strength multiplier	Tensile strength (MPa)	Crack area (m^2)	Observed block crack dimensional range (m)
near-surface	1.55	2.15E+04	1.05	3.28	1.67^2	0.12×0.15^1 1.54×1.76
mid-depth	1.20	1.66E+04	1.01	3.16	1.98^2	-
full-depth	1.00	1.38E+04	1.00	3.13	2.34^2	-

¹ For example, 0.12m by 0.15m, rectangular-shaped block cracks were observed (minor cracks), residing within 1.54 by 1.76 m rectangular-shaped block crack patterns (major cracks), see also Figure C-1.

C.4. Block crack dimension prediction using discrete element methods

C.4.1 Material properties and temperature input

The asphalt pavement surface was taken as viscoelastic in the discrete element modeling performed. Relaxation modulus parameters were obtained through interconversion of the creep compliance master curve at a reference temperature of -12°C . Fracture constitutive laws, i.e., load-displacement and fracture behavior in the connections between discrete elements, were input to the model based on the DC(T) fracture energy test results. Both the creep compliance and fracture properties were converted to local viscoelastic and fracture properties and used as material property inputs in the discrete element model (ref). A gradient material distribution was applied in the discrete element model, assuming that the relaxation modulus at the top of the surface layer was two times higher than that at the bottom, following an exponential grading distribution.

Aside from the vertical material viscoelasticity gradient, the temperature gradient with respect to depth from the surface is also a main factor contributing to the rate of block cracking in an asphalt pavement. As with the analytical solution, the temperature change per hour was taken as $1.5^{\circ}\text{C}/\text{h}$. The temperature change at the top of the pavement surface layer was also assumed to be two times faster than that at the bottom, following an exponential distribution.

C.4.2 Model description, results and discussion

A three-dimensional discrete element model was built via Particle Flow Code (PFC) software to predict the block crack patterns observed on US63 near La Plata. As shown in Figure C-4, a $1.99\text{m} \times 1.99\text{m} \times 0.073\text{m}$ pavement model with 199,900 elements and 1,129,979 contacts were constructed to simulate the top two layers of the US63 pavement system.

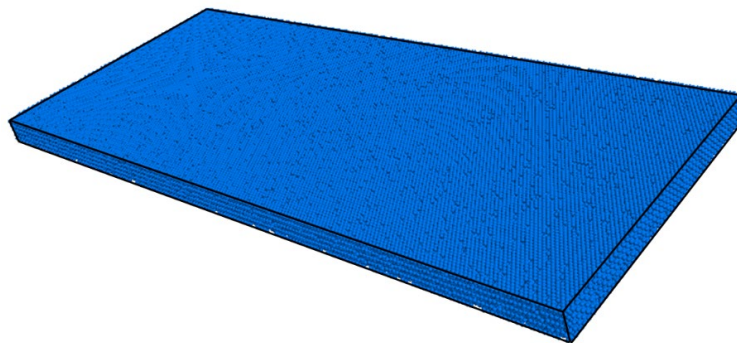


Figure C-4. Discrete element model of the pavement system of US 63 at La Plata, Missouri in PFC software

The location and extent of predicted microcracks were obtained from PFC and then plotted in AutoCAD. As shown in Figure C-5, the crack propagation process and final crack patterns can be clearly seen using this plotting scheme. The very first microcrack was initiated in the model in the analysis step ('loop') 4, and a denser block crack pattern becomes visible in loop 7. Next, the isolated cracks begin to channel across the pavement surface, and the transverse and longitudinal

cracks were predicted to develop (loop8). As more channeling occurred, cracks became interconnected, forming smaller, block-shaped crack patterns. Finally, the surface of the pavement was predicted to contain a highly saturated crack pattern at the end of loop 10. After the point of saturation was reached in the simulation, the crack widths grew larger, indicating that spalling and eventually potholes might develop (loop 16). The average crack size at the end of the simulation was about 0.13m*0.21m, which was similar to the smaller block crack size observed in the field (Figure C-1). Therefore, the three-dimensional discrete element model was shown to be capable of providing a reasonable prediction of the small block crack pattern observed in the chosen field section.

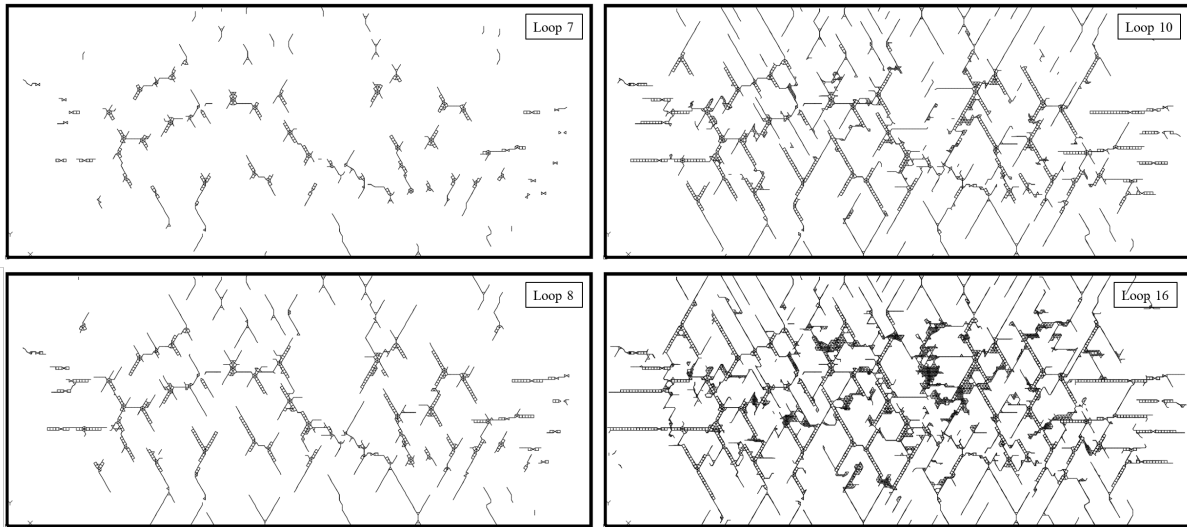


Figure C-5. Crack propagation patterns at various stages in the DEM simulation

C.5. Summary

Severe block cracks were observed on US63 near La Plata, MO, leading to an in-depth, integrated testing and modeling study. It was found that the average fracture energy of the tested samples was 244J/m^2 , which was far below the recommended fracture energy threshold of 400J/m^2 . Therefore, it was not surprising that a dense block crack pattern existed in the field. Several strategies might be taken to improve the fracture resistance of asphalt surfacing mixtures to mitigate block cracking, such as the use of softer binders, achieving higher field density, reducing recycled material content, or using stronger aggregates. The use of a balanced mix design, incorporating both cracking and rutting tests as part of mix design, is an attractive option to implement these concepts in an effective manner. Taking a closer look at binder chemistry, additives, and partial mixing of recycled binder content, is also recommended. The possible benefit of rejuvenators and antioxidants also deserves more study.

The modeling conducted herein helps to describe the mechanisms behind the formation of large (major) and small (minor) block cracks. With the validated 3D DEM model, simulation research into mitigation strategies for block cracking is now possible. This could be used to help steer mix design targets in a balanced mix design. The model could also be used to evaluate requirements for surface-applied rejuvenators, surface treatments, micro-surfacing, ultra-thin

bonded wearing courses, and strategies for mill-and-fill operations (depths of milling and thickness of the resurfacing layer).

C.6. References

- [1] Apegyei A.K. (2006). Development of Antioxidant Treatments for Asphalt Binders and Mixtures. University of Illinois at Urbana-Champaign.
- [2] ASTM D7313. Standard Test Method for Determining Fracture Energy of Asphalt-Aggregate Mixtures Using the Disk-Shaped Compact Tension Geometry. American Society of Testing and Materials, 2007.
- [3] ASTM E399 – 90(2002). Standard Test Method for Plane-Strain Fracture Toughness of Metallic Materials. DOI: 10.1520/E0399-90R97.
- [4] Braham, A.F., Buttlar, W.G., Clyne, T.R., Marasteanu M.O. and Turos, M.I. (2009). The Effect of Long-Term Laboratory Aging on Asphalt Concrete Fracture Energy, *Journal of Engineering Mechanics*, American Society of Civil Engineers, Vol. 78, 417-454.
- [5] Buttlar, W.G., Song, S.H., and G. H. Paulino (2006). “Application of Graded Finite Elements for Asphalt Pavement Analysis,” *Journal of Engineering Mechanics*, American Society of Civil Engineers, Vol. 132, No. 3, 240-249.
- [6] Dave, E.V., et al. (2013). ILLI-TC Low-temperature Cracking Model for Asphalt Pavements. *Road Materials and Pavement Design*, Vol 14, 57-78.
- [7] Marasteanu, M., Zofka, A., Turos, M., Li, X., Velasquez, R., Li, X., Williams, C., Bausano, J., Buttlar, W., Paulino, G., Braham, A., Dave, E., Ojo, J., Bahia, H., Gallistel, A., and McGraw, J. (2007). Investigation of Low Temperature Cracking in Asphalt Pavements (Report No. 776). Minnesota Department of Transportation, St. Paul, MN, 2007.
- [8] Wang, H., Buttlar, W.G. (2018). Three-dimensional Analytical Model for Exploration of the Block Cracking Phenomenon in Asphalt Pavements (submitted). *Road Materials and Pavement Design*, 2018.

Appendix D. Literature Review

Abstract

Sustainability is a cornerstone of today's engineering world. This ideal can be described as meeting the requirements of today's society without reducing the ability of future generations to meet their needs. Sustainability's broad arena stretches from economics to agriculture to construction. Specifically within construction, sustainability is met through the reduction of emissions, virgin material use, and energy consumption. In asphalt pavements, the sustainability movement was started in earnest with the steadily increasing use of reclaimed asphalt pavement (RAP) in asphalt mixtures over the past several decades. Other approaches, such as the use of recycled asphalt shingles (RAS), ground tire rubber (GTR), warm-mix asphalt (WMA), have seen initial usage decades ago, followed by a period of relative stagnation and then a resurgence in recent years. The introduction and increased availability and use of existing rejuvenator products has opened the door for the use of higher rates of RAP and RAS usage; however, the effectiveness and proper use of these materials in mix design are still open questions. In general, a proliferation of products, a lack of scientific test results, cost-benefit tradeoffs, and mixed reports in the literature makes it difficult to fully and effectively implement these sustainable approaches by state transportation agencies and hinders investment by asphalt producers. This review of the literature provides background information on RAP, RAS, GTR, and rejuvenators, with some emphasis on mixture performance tests due to their rising importance and increased usage in recent years. The review also contains information on WMA, since its usage in combination with the aforementioned asphalt recycling products is very prevalent in the literature.

This review is organized in three chapters, with a detailed reference list following each chapter. Detailed results are provided in this draft, mid-project report for selected studies conducted by the principle investigator, particularly to introduce the successful use of new recycled mix design and performance tests in recent studies to elevate the proper design and control of these materials. In general more details are also provided for project data from innovative studies that have not yet been reported extensively in the literature, such as hard-to-find thesis data and technical reports. Some of the longer sections will be consolidated upon insertion in the final report for this project; i.e., in cases where those results are available elsewhere in the literature at that time.

D.1. RAP and WMA

Two of the more mature topics in asphalt mixture sustainability are reclaimed asphalt pavement (RAP) and warm mix asphalt (WMA). The two are often used in conjunction with one another, as WMA can lower mixture production temperatures, resulting in less oxidation and damage to the recycled binder during the heating and mixing process at the production plant. However, issues such as incomplete mixing and its effect on mixture permanent deformation, moisture damage, and cracking resistance have been observed and reported on in research investigations. This chapter presents a review of the literature on RAP, WMA, and their combined usage, with an emphasis on modern mixture performance testing. A comprehensive review of the early

literature on these subjects can be found elsewhere, and is therefore not the emphasis of this review. However, some of the references provided herein are linked to studies that provide such reviews (and associated references). Detailed results from a recent RAP-WMA mixture performance study conducted by the principal investigator in Illinois are presented in Section 1.5.

D.1.1. Reclaimed Asphalt Pavement: an Introduction

Reclaimed asphalt pavement (RAP) is a product of asphalt pavement removal and is the primary recycled material used in asphalt concrete. Milling machines break down the bonded asphalt concrete into a multitude of particle sizes as shown in Figure D-1 to produce RAP. According to Collins and Ciesielski (1), more than 100 million tons of RAP is produced every year in the United States.



Figure D-1. Reclaimed asphalt pavement (RAP)

Producers generally fractionate RAP (FRAP) upon arrival to a plant location to properly manage the varying particle sizes. Specifically, the introduction of FRAP has allowed mix designers to meet Superpave mix design volumetric specifications more consistently (2).

The use of RAP in asphalt concrete adheres to the requirement of sustainable solutions in pavements because it is both environmentally friendly and cost effective. Chiu et al. (2008) found that adding RAP to mixtures reduces the environmental impact of production by 23%. Furthermore, RAP presents a significant material cost reduction (3). Quality virgin aggregate material is becoming increasingly difficult to find and purchase. Therefore, the use of RAP can offset costs and allow state and federal agencies to rehabilitate more roadways with similar budget capacities.

The addition of RAP to asphalt mixtures is generally limited to a 10-30% range. State agencies such as the Illinois Department of Transportation allow up to 30% RAP in binder and surface mixtures depending upon the traffic level present on a given roadway (4). As stated previously,

RAP is a sufficiently stiff material. This condition is caused by oxidative hardening and aging mechanisms present in nature. Consequently, the increased stiffness in RAP generally leads to brittle cracking failures that deter producers and state agencies from increasing RAP allowance (5).

D.1.2. Warm Mix Asphalt: An Introduction

Warm mix asphalt (WMA) is a new technological form of asphalt concrete. It differs from hot mix asphalt (HMA) only in the production temperatures required to meet appropriate standards of mixing and densification. Figure D-2 displays the various production temperatures required by the four common types of asphalt concrete (6). (Half-warm and cold mixtures will not be discussed in this document.) As shown, WMA is generally produced 35-55°F (20-30°C) less than HMA (7). However, several forms of WMA may allow an additional 20-40°F reduction in production temperatures.

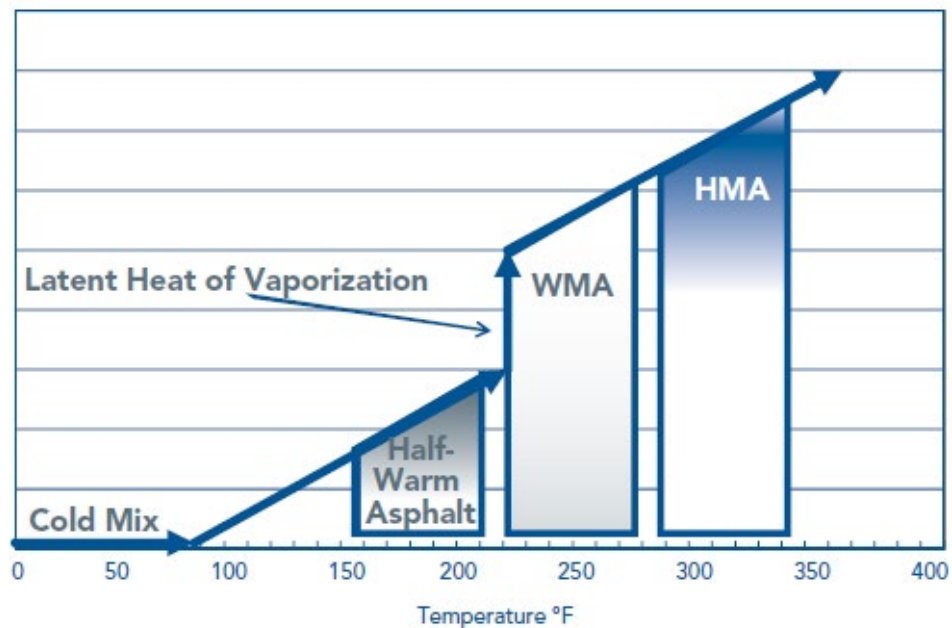


Figure D-2. Production temperatures of asphalt concrete

The production temperature changes generally lead to sustainability improvements via reduced fuel consumption and emissions production. In this era of rising fuel prices, the use of WMA has the ability to reduce plant fuel use 10-35% (6). In addition, as dangerous gaseous emissions such as sulfur dioxide, nitrogen oxide, and carbon dioxide have been significantly regulated in developed nations, WMA in locations such as European nations have found emissions reductions of approximately 15-70%.

Early WMA literature argued that the lessened production temperatures of WMA were caused by an altered binder viscosity-temperature relationship. The viscosity at the production temperatures was thought to be reduced in order to allow improved mixing and compaction (7). In fact, at many initial WMA demonstration locations mat densities increased significantly and

permeability was reduced. Therefore, moisture sensitivity distresses such as stripping were thought to be partially alleviated by the improved densities.

WMA additives and processes can be differentiated into three distinct groups. These groups include: organic additives, chemical additives, and foaming processes and additives. Organic additives involve the addition of wax materials which dissolve at temperatures below the mixing temperature. As a result, the material enhances mixing in its liquid state and hardens after compaction to provide stability. Organic additives tend to improve rutting resistance and reduce fracture resistance of asphalt mixtures. Chemical additives include a variety of chemical packages from surfactants to pastilles. These materials affect the surface bonding between the asphalt binder and aggregate and are most likely to improve fracture resistance and increase rutting potential. Foaming processes and additives use water to foam the asphalt binder and reduce its viscosity prior to or during the mixing period. This group contains the largest variety of WMA methods and tends to increase rutting potential and moisture sensitivity.

Finally, asphalt concrete users and producers consider the use of increased RAP percentages advantageous with WMA (6). The reduced production temperatures of WMA alleviate a considerable portion of the binder aging which occurs during the mixing process. Therefore, the addition of a significant percentage of oxidized RAP would not theoretically increase the potential for significant early age cracking. Research in this arena has been minimal to date and requires significant consideration to determine how WMA performance is affected by moderate to high percentages of RAP.

D.1.3. RAP – Black Rock vs. Total Blending

An important consideration in HMA and WMA mixture design is the interaction of RAP and virgin asphalt binder. RAP mixture designs require assumptions regarding the percentage of binder interaction, but there has been no definitive answer to this question. The black rock concept assumes that the RAP binder does not interact at all with the virgin asphalt binder (8). As a result, the asphalt mixture behaves similar to that of a completely virgin mixture and the full amount of virgin asphalt binder must be added to reach the chosen binder content. On the other hand, the total blending concept assumes that the RAP binder completely interacts with the virgin asphalt binder (8). Consequently, the asphalt mixture behaves as a hybrid between a completely virgin and completely recycled mixture. In addition, a percentage of the virgin asphalt binder can be subtracted from the total content because the binders interact 100%. NCHRP Report 9-12 determined that low percentages of RAP such as 15% did behave differently when either the black rock or total blending concepts were adopted (8). However, at 40% RAP, researchers found that the mixture behaves significantly different from both concepts. As a result, a certain percentage of the RAP binder must interact while the other does not. As stated above, the binder interaction is significant with the use of WMA technologies. WMA mixtures are generally less stiff initially due to the lessened aging effect of the reduced production temperatures. Consequently, as RAP percentages are increased, the percentage of binder interaction must be assumed. If the RAP binder does interact, rutting resistance becomes a significant issue and may require modified asphalt binder to reduce permanent deformation issues.

D.1.4. Warm Mix Asphalt Origin, Advantages, and Disadvantages

European asphalt producers launched WMA in 1995 using Aspha-min in anticipation of future greenhouse gas emissions restrictions. In 1997, the Kyoto Protocol set targets on greenhouse gases, such as CO₂, for the primary industrialized nations worldwide (2). As a result, the German Bitumen Forum proposed production temperature reductions to asphalt concrete mixtures. Over the next five years, products such as Sasobit and WAM Foam were introduced in Germany and Norway. United States asphalt officials began to take notice of these products and took a European WMA tour in 2002. In 2005, the WMA Technical Working Group was created to introduce these technologies to U.S. asphalt producers and develop preliminary specifications for the allowance of WMA (2). Finally, field trials were conducted over the next few years in many states, NCAT published laboratory results for a number of technologies, and the first WMA International Conference was conducted.

There are numerous advantages to the use of WMA. First, fuel consumption and emissions are reduced by WMA use. As stated previously, WMA projects have reported fuel savings between 10 and 35% because fuel usage has the ability to decrease 2-3% for every 10 °F drop in mixing temperature (9). However, these statistics require significant assumptions in issues such as moisture in the aggregate, type of fuel, and dryer exhaust temperature. Therefore, consideration must be given to these factors to significantly reduce fuel use. Emissions reductions are also significantly affected by the use of WMA technologies. Harmful gaseous emissions such as CO₂, SO₂, volatile organic compounds (VOCs), CO, and NO_x have been significantly decreased (15-70%) in locations such as Norway, Italy, Netherlands, France, and Canada (2). This is important because asphalt plants in areas which do not meet air quality standards have been generally shut down during daytime hours to avoid emissions production. The reductions in emissions would likely allow these plants to avoid closure during typical paving hours (10).

Late season paving, improved working conditions, and increased RAP usage are additional benefits presented by the use of WMA. The increase in paving season length occurs because WMA technologies have been found to be compacted at lower temperatures. Lower compaction temperatures are primarily caused by a reduced cooling rate because the temperature differential between compaction and ambient temperatures is reduced. In fact, locations in Europe were compacted properly at temperatures as low as -3 °F (7). Working conditions are improved by the use of WMA technologies. Figure D-3 displays the reduced amount of gaseous emissions at the placement location on a roadway. Several projects have shown that air quality was significantly improved by the use of WMA (4). Therefore, workers should have their quality of life enhanced. Finally, possible increases in RAP use may be available with WMA technologies. As stated previously, reduced production temperatures reduce asphalt binder aging. Therefore, the stiffening effects of the mixing process are likely reduced and the addition of RAP could improve the permanent deformation resistance of the mixtures during their early service lives.



Figure D-3. (a) HMA placement (b) WMA placement (11)

A number of possible disadvantages occur with the use of WMA as well. First, long-term pavement performance results are not available for WMA sections. As a result, predictive models are the only means to describe the performance of WMA over the long term and these models are not always accurate and require significant calibration. However, calibration cannot be completed successfully without some type of long-term results. Therefore, a cyclical loop is created and it produces questions regarding the true long-term performance of WMA sections. The large number of WMA technologies cause difficulty in creating specifications for WMA use in roadway and airfield pavements. To date, over 20 WMA technologies are in production worldwide and each one produces slightly different performance. Therefore, specifications regarding mixture volumetrics only may not provide enough assurance of quality and performance specifications may be necessary. Finally, laboratory performance tests of several WMA technologies have found significant issues with rutting resistance and moisture sensitivity (12, 13). Therefore, additional laboratory testing and correlation to field performance must occur.

D.1.5. Reclaimed Asphalt Pavement Origin, Advantages, and Disadvantages

RAP is a beneficial alternative to virgin aggregates economically and environmentally. This recycling product is created through the use of a milling machine similar to that shown in Figure D-4. Milling machines grind the aged and distressed asphalt pavement into virgin aggregate size particles through the use of system of blades that continuously cut the material. As shown in Figure D-4, RAP is dumped into a trailer via a conveyer belt on the milling machine. Once the trailer is filled, the material is taken back to an asphalt plant.



Figure D-4. Asphalt milling machine and dump trailer

Originally, RAP was left in an unfractionated state at the asphalt plant. However, as stated previously, the fractionation of RAP has become the acceptable practice in order to incorporate RAP without significantly affecting mix design volumetric properties (2). Figure D-5 displays the use of fractionation to produce two or more piles of RAP.



Figure D-5. Fractionated RAP stockpiles

RAP presents several advantages to the asphalt pavement community. First, as previously stated this material is generally cost effective and environmentally friendly. According to Kandhal and Mallick (14), the use of this recycled material can save up to 34% of the total cost with the use of 20-50% RAP. This reduction in cost is associated with a reduction in asphalt binder use, virgin material cost, and virgin material transportation. Furthermore, RAP is advantageous due to its environmental impact. As stated previously, Chiu et al. found a 23% reduction in eco-burden due to the reduced amount of asphalt binder required and the amount of energy required to heat

the materials. RAP generally supplies a significant amount of asphalt binder which can interact and coat the virgin aggregate material. Pavement performance has the potential to be improved by the use of RAP as well. The relative stiffness of the RAP material can improve performance in the area of permanent deformation. At locations such as intersections, PG binder grades are generally increased to avoid rutting issues. However, according to NCHRP Project Report 9-12 (8), the use of RAP may inherently increase the binder grade of the asphalt mixture. Therefore, the addition of RAP has the potential to create a rut resistant mixture.

Disadvantages arise with the use of RAP as well. RAP is an inherently stiff material due to the oxidizing effect of sunlight and the atmosphere. According to Xiao et al. (2007), the presence of as little as 15% RAP has the ability to significantly stiffen an asphalt mixture (5). Wagoner et al. (2005) found that the fracture resistance of asphalt mixtures was reduced through the use of an increased asphalt grade (15). Consequently, the addition of RAP, according to NCHRP 9-12, increases the PG grade of the asphalt binder. Therefore, the increased stiffness increases the brittle nature of the asphalt concrete and the probability of brittle failure at low temperatures. Variability among RAP stockpiles is also a significant issue. Dave (2003) studied the recovered asphalt binder of 16 different RAP stockpiles in Illinois through the use of the Dynamic Shear Rheometer (16). The complex modulus, G^* , of each RAP stockpile was calculated and they found that the complex moduli differed significantly. Therefore, RAP stockpiles must be considered on a case-by-case basis because the stiffness of a given RAP stockpile may require different considerations from a stockpile in a different location.

D.1.6. Recent WMA-RAP Research

This section of the literature review includes a review of past work on both WMA and RAP mixtures. Several WMA and RAP research papers have been produced to date. Two significant papers include: Mallick et al. (17) and Middleton and Forfylow (18). Mallick et al. examined the effects of using Sasobit, high RAP levels, and grade bumping (17). This research included HMA PG 64-28, HMA and RAP PG 52-28, WMA and RAP PG 52-28, and WMA and RAP PG 42-42 mixtures. Mixing temperatures were 125 and 150°C and all RAP mixtures were composed of 75% RAP. The research team chose to test the mixtures via indirect tension and asphalt pavement analyzer (APA) rut tests. The testing results produced several key findings. First, Sasobit had a significant stiffening effect upon the indirect tensile strength of the asphalt mixtures. This result validated the hypothesis that wax additives have a tendency to stiffen asphalt concrete mixtures at low temperatures. Next, the presence of 75% RAP did not offset the effect of adding a softer virgin asphalt binder in terms of indirect tensile strength. The HMA PG 64-28 mixture with no additional RAP was significantly stiffer than the HMA and RAP PG 52-28 mixture. Therefore, a total blending assumption is not a substantial claim with the presence of 75% RAP. Finally, due to the theorized stiffening effect of wax additives, Sasobit WMA mixtures would likely display lesser APA rut depths. However, the addition of Sasobit to the asphalt binder did not improve the rutting resistance of the WMA and RAP PG 52-28 mixture in comparison with the HMA and RAP PG 52-28 mixture.

Middleton and Forfylow (18) completed WMA and RAP mixture research using the Double Barrel Green foaming process (19). The asphalt binder, an 80/100A penetration grade, was kept constant throughout testing irrespective of the recycled material content. Researchers produced

foamed virgin, 15% RAP foamed, and 50% RAP foamed mixtures and tested them using the APA rut and AASHTO T-283 TSR tests among others. The APA rut depth results in dry and wet conditions did not determine significant rutting resistance issues in any of the mixtures. As a result, the softer WMA did not increase permanent deformation and the presence of RAP did not significantly stiffen the mixtures and improve rutting resistance. The moisture sensitivity test results provided several key conclusions. Middleton and Forfyflow determined that as RAP percentages increased, the TSR results increased as well. Consequently, the presence of RAP may have stiffened the material and lead to improved moisture resistance. Furthermore, the presence of RAP increased the TSR from a failing percentage to a passing percentage. (An 80% TSR rating indicates a passing result.) Therefore, RAP may be an integral part of WMA mixtures in order to produce satisfactory moisture sensitivity mixtures.

D.1.7. WMA Technologies

WMA technologies can be broken into three different categories. The first group includes organic additives and is comprised of technologies such as Sasobit, Asphaltan B, and Licomont BS 100. Sasobit is a synthetic paraffin wax material produced through via the Fischer-Tropsch method (20). This additive is generally supplied in a pellet, shown in Figure D-6, or flake form and is added at a rate of 0.8 to 3.0% by mass of the asphalt binder. Asphalt producers supply the Sasobit to the asphalt binder through a fan system or a RAP collar. Sasobit is considered a viscosity enhancer because it reduces the viscosity of asphalt binder at temperatures above the Sasobit melting temperature of 100°C (20). Temperature reductions of 20-30°C are found using this additive.



Figure D-6. Sasobit pellets

Asphaltan B and Licomont BS 100 are not significantly used in U.S. WMA applications. Asphaltan B is a montan (esterified) wax. It is also available in a pellet form and melts at a temperature slightly lower than Sasobit due to its lower molecular weight (21). Similar to Sasobit, Asphaltan B is generally blown into the asphalt binder and allows temperature reductions between 20 and 30°C. However, the dosage rate is slightly higher than Sasobit at a rate of 2-4% by weight of the asphalt binder. Licomont BS 100 is a fatty acid amide which is added at a rate of approximately 3.0% by weight of the binder (21). This organic additive acts as

a viscosity enhancer is available in a powder or granular form. Furthermore, the melting point of Licomont BS 100 differs significantly from the wax additives because it melts approximately 145°C. The U.S. performance of organic additives has largely been relegated to the discussion of Sasobit. Researchers in Texas and Alabama have found that Sasobit clearly reduces the viscosity of the asphalt binder at temperatures above the Sasobit melting point (22, 23). They have also found that rutting resistance is maintained or improved through the use of this organic additive. However, performance distress such as cracking may become a significant issue. This occurs because wax tends to stiffen the material at ambient temperatures which reduces the fracture resistance of the asphalt mixtures.

Chemical additives represent the second major group of WMA technologies. Additives such as Rediset WMX and Evothorm comprise this category in the United States. Rediset WMX, which is shown in Figure D-7, is an additive available in the pastille form which combines surfactants and organic matter (24). Generally, asphalt producers add 1 to 2% Rediset WMX by weight of the asphalt binder in order to reduce production temperatures by approximately 30°C.



Figure D-7. Rediset WMX pastilles

Evothorm chemical additives are the most significantly used WMA chemical additives and are delivered in three different forms (25). Evothorm ET and DAT are water-based additives while Evothorm 3G is a non-water based additive. The ET form completely replaces the asphalt binder at an asphalt plant because it contains 70% asphalt residue and reduces production temperatures by greater 55°C. Evothorm DAT requires an injection line in order to be added to the asphalt binder as it travels to the mixing drum. The DAT form reduces temperatures by approximately 10°C less than Evothorm ET, but allows the plant more flexibility in quickly switching from WMA to HMA production. The final form of Evothorm, 3G, is the newest type and reduces production temperatures by 33-45°C. Its lack of water has shown significant promise because residual moisture is not available to cause moisture damage. Performance of chemical additives in the United States has generally been completed on Evothorm. Research has found that Evothorm may be significantly susceptible to permanent deformation and moisture damage (25).

However, National Center for Asphalt Technology (NCAT) researchers determined that the Evotherm chemical package can be altered depending on the aggregate composition to avoid moisture damage distresses.

The final group of WMA technologies includes foaming additives and processes. This category has the largest variety of manufacturers and can be broken down into additive and process sub-categories. The additive sub-category includes Advera WMA and Aspha-min. Both of these additives are comprised synthetic zeolites. Zeolites are alumino-silicates of alkali metals which containing approximately 20% water by weight (17). At approximately 100°C, the outer membrane of the additive breaks down to release the water to foam the asphalt binder. Generally, Advera and Aspha-min, shown in Figure D-8, are added at a rate 0.2-0.3% by weight of the total mixture. Therefore, unlike the organic and chemical additives, the addition rate is dependent upon the total asphalt content of the mixture. NCAT researchers completed a laboratory study of Aspha-min in 2005. Researchers determined that Aspha-min displayed issues with moisture sensitivity in comparison with the control HMA mixtures (17). In addition, as production temperatures decreased, rutting resistance was reduced. Furthermore, a field trial section was placed in Orlando, FL to study the performance over a one year period. NCAT researchers determined that moisture sensitivity was not a significant problem for the Aspha-min during the year ending evaluation.



Figure D-8. Aspha-min Zeolite

Foaming processes include the Astec Double Barrel Green, Maxam Aquablack, Gencor Ultrafoam GX, and WAM Foam technologies. The Double Barrel Green, Ultrafoam GX, and Aquablack processes require use nozzle(s) to spray a chosen amount of water into the asphalt binder to foam it and sufficiently reduce its viscosity prior to mixing with the heated aggregates. The Double Barrel Green technology, shown in Figure D-9, requires a multi-nozzle attachment to inject approximately 1.0lbs of water per ton of mixture. According to the manufacturer (26), this system causes the asphalt binder to expand up to 18 times its original volume which transforms the viscosity-temperature relationship of the asphalt binder and provides 20-30°C

production temperature reductions. In terms of performance, Middleton and Forfyflow (2009) included up to 50% RAP in WMA mixtures produced via the Double Barrel Green and determined that both moisture sensitivity and rutting resistance were improved in comparison with a virgin Double Barrel Green WMA (18).



Figure D-9. Astec double barrel green foaming drum

The Aquablack and Ultrafoam GX systems require a single foaming nozzle. Similar to the Double Barrel Green technology, production temperatures are reduced by approximately 20-30°C. Water is introduced via the nozzle to foam the asphalt binder through micro-bubble technology (27). According to the producers, the reduced sizes of the bubbles allow entrainment throughout the mixture to enhance uniformity. These bubbles are subsequently released during the compaction process. NCAT researchers evaluated the Ultrafoam GX machine in 2010. They found that moisture sensitivity increased significantly and rutting resistance was reduced slightly through the use of this technology (19). The moisture introduced during the foaming process may not have been completely removed during compaction which produced unfavorable results in the AASHTO T-283 moisture susceptibility and AASHTO T-324 Hamburg Wheel Tracking tests. Consequently, NCAT researchers came to the conclusion that anti-stripping agent should be added to mixtures produced using the Ultrafoam GX. The WAM Foam technology requires several steps and two asphalt binders to produce WMA mixtures. The two asphalt binders include a softer grade (20-30% of total binder weight) and harder grade. The process begins when the aggregate fraction is heated to the chosen mixing temperature (7). Then, the softer asphalt is added to aggregate and the harder asphalt binder is foamed at a rate of 1.6 lbs of water per ton of mixture. Finally, the foamed asphalt binder is added to the softer binder and aggregate in the mixing drum. This process allows a significantly larger reduction in production temperatures as compared to the other foaming technologies. However, the process and requirement of two different asphalt binder grades causes additional asphalt lines and foaming compartments to be effective.

D.1.8. RAP-WMA Study at the University of Illinois at Urbana-Champaign

Hill (MS Thesis, 2011) conducted an extensive study on RAP/WMA mixtures. Because this is a recent study utilizing a very precise and controlled mixture design and some of the most prevalent and modern performance tests, detailed results are presented herein with permission of the author (28). The testing plan for this study was conducted in two phases. First, asphalt binder testing was completed to evaluate the viscosity-temperature profiles and the low temperature

behavior of the unmodified and WMA additive modified materials. Figure D-10 displays a schematic of the asphalt binder testing plan.

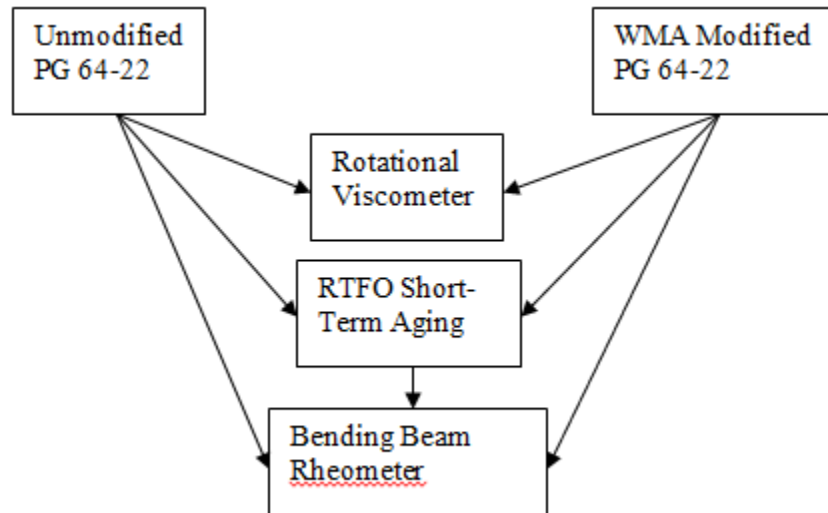


Figure D-10. Asphalt binder testing plan

Sasobit, Advera, and Evotherm M1 were selected as the three candidate WMA technologies. All percentages of WMA technologies were added at rates within the specified manufacturer tolerances. Two rates were selected for both Sasobit and Advera while one rate was chosen for Evotherm M1. The WMA technologies were chosen based upon the literature review of potential options. In the end, additives were preferred over other technologies such as foaming processes for several reasons. First, additives are significantly easier to mix and produce uniform modified asphalt binder. Next, laboratory foaming devices were not available at the onset of the study. Finally, additives are available in each WMA category in order to fully encompass the available technologies.

The second phase of the testing suite included mixture performance tests, including AASHTO T-283 TSR, AASHTO T-324 Hamburg Wheel Tracking, and ASTM D73713-07 DC(T) tests to evaluate the moisture sensitivity, rutting resistance, and fracture resistance of the asphalt mixtures. As shown in Figure D-11, virgin and 45% RAP mixtures were produced for the control HMA and each of the three WMA additive mixtures.

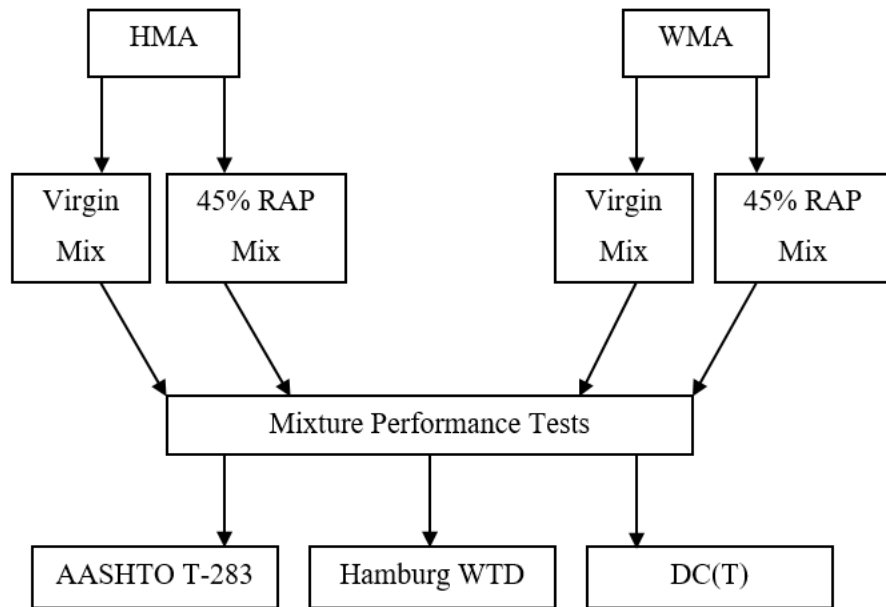


Figure D-11. Mixture testing suite

Mixing and compaction temperatures were chosen based upon the RV testing results. Mixing and compacting temperatures of 160°C and 150°C, respectively, were selected. The production temperature reduction chosen for the WMA technologies was 25°C. This value was selected because it was within the acceptable range for each of the WMA additives. The mixing and compaction temperatures of the WMA mixtures were 135 and 125°C, respectively. The RAP percentage was chosen as a multiple of the maximum RAP levels according to Illinois Department of Transportation (IDOT) RAP allowance table as of the year 2012. At that time, IDOT did not allow more than 30% RAP in a surface mixture. Based on this, a RAP content of 45% or 1.5 times the 30% maximum was selected.

The materials in this study included asphalt binder, RAP, and aggregate. The asphalt binder was supplied by Emulsicoat, LLC which is a local asphalt binder producer. PG 64-22 asphalt binder was chosen for this project because central Illinois environmental conditions require the use of this grade of binder. As stated previously, the percentage additions of the WMA additives were selected based upon the manufacturer’s recommendation. Consequently, 3.0% Sasobit and 0.5% Evotherm were added by weight of the asphalt binder while 0.25% Advera was supplied by weight of the total mixture.

The aggregate used in this study included CM16, FM20, FM02, and mineral filler. This aggregate combination was chosen in order to produce a 9.5mm NMA surface mixture. The CM16 and FM20 materials were limestone coarse and manufactured fine aggregates from Kankakee, IL, while the FM02 aggregate was a natural fine aggregate obtained locally from Material Services. The sands differed significantly from one another upon reaching the No. 200 sieve. This difference created volumetric issues within the mix design portion of this study and lead to increased dust-to-percent effective asphalt proportions.

The RAP material was collected from the Open Road Paving, LLC in Urbana, IL. This material was chosen over other RAP stockpiles because it originated from an unmodified IL Rte. 72 mixture. Open Road Paving fractionated the RAP into two stockpiles of 3/8" retained and passing material. The RAP used in this study included only the 3/8" passing material in order to produce a surface mixture. The apparent and actual RAP gradations are presented in Table D-1. Apparent RAP gradation represents the gradation of the material coated with asphalt binder and includes agglomerated particles. It was calculated by determining the total mass of RAP retained on the 3/8", #4, 8, and 30 sieves. Then, RAP extractions were completed on a representative sample of the RAP and were used to calculate the binder content of the 3/8" passing RAP and the true gradation of the material. Finally, the asphalt binder content was verified by IDOT. At the University of Illinois transportation research facility, the passing 3/8" RAP material was found to have 5.4% asphalt binder content while IDOT calculated 5.5% binder content in the same material.

Table D-1. RAP gradations

Sieve Sizes	True	Apparent
1" (25.0 mm)	100.0	100.0
3/4" (19.0 mm)	100.0	100.0
1/2" (12.5 mm)	100.0	100.0
3/8" (9.5 mm)	99.3	99.1
1/4" (6.25mm)	-	-
No. 4 (4.75 mm)	73.8	67.8
No. 8 (2.36 mm)	50.5	38.5
No. 16 (1.18 mm)	35.5	-
No. 30 (600 μm)	25.8	8.5
No. 50 (300 μm)	18.1	-
No. 100 (150 μm)	13.8	-
No. 200 (75 μm)	11.2	-

Each mixture design was completed according to the Superpave mix design method (29). In addition, the Bailey Method was used as an additional tool to evaluate the aggregate structure of the mix design. Mr. Robert Bailey developed the method during the 1980's and it allows users to adjust mixture designs to reach the volumetric requirements of Superpave (30). Properties such as gradation and unit weights are entered into an Excel VBA program and percentages of fine and coarse aggregate are toggled to produce acceptable sieve ratios. These ratios evaluate the percentages of aggregate passing specific sieves based upon the NMA S of the mixture and the gradation type. In this study, the mixture was chosen to be 9.5mm NMA S fine-graded mixture. According to the Bailey Method, a fine-graded mixture derives its strength and load capacity through the fine aggregate of the mixture. Therefore, the natural sand fraction of the mixture was minimized due to the rounded nature of the particles.

The Superpave requirements of a 9.5mm NMAS 70 gyration mixture were followed. The design gyration total of 70 gyrations was determined when considering a mid-to-low volume road with 20 year traffic levels between 3 and 10 million ESALs. This type of roadway was chosen because a high RAP WMA field trial would likely begin here instead of a major highway receiving greater than 10 million ESALs in a 20 year span.

Several assumptions were made in order to complete the mixture design process. First, all mixture designs occurred with unmodified PG 64-22 at the HMA mixing and compacting temperatures. Consequently, WMA additives were assumed to have no significant effects upon the volumetric properties of the asphalt mixtures. Research into this area has shown that this assumption may or may not be valid depending on several factors including production temperatures. Second, the true RAP gradation was assumed to be present at the time of mixing. In other words, all agglomerations were considered to be sufficiently broken down at the mixing temperatures. This assumption is difficult to confirm at WMA production temperatures because the agglomerated particles require sufficient heat to break apart. Next, the RAP binder content was assumed to remain constant. This assumption must be considered because virgin asphalt binder addition was calculated based upon the chosen percentage of RAP in the mixture. Finally, total blending of RAP and virgin asphalt binder was assumed to occur, at least from the standpoint of mixture compactability (lubricity and compressibility during compaction and its effect on mixture volumetrics). As a result, the percentage of virgin binder was reduced because the RAP binder supposedly had the ability contribute to aggregate coating and compactability.

The virgin mixture design did not include RAP material. Table D-2 and Figure D-12 (blue curve) display the chosen gradation and its subsequent combined plot.

Table D-2. Virgin mixture blend

Aggregate	Blend Percentage
CM16	36.4
FM20	42.2
FM02	20.0
MF	1.4

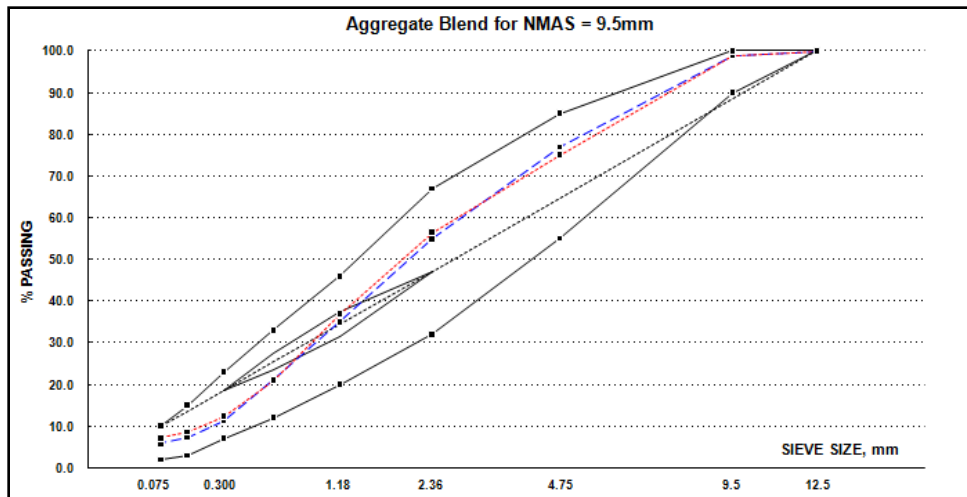


Figure D-12. Virgin and 45% RAP mixture design gradations

As shown in Table D-2, the sand fraction of the mixture equaled 62.2% of the total blend and the manufactured sand was added at a rate of 42.2%. This large percentage of manufactured sand led to a high percentage of material passing the #200 sieve and a high dust to percent effective binder ratio. However, this result was a consequence of limiting the amount of natural sand added to the blend. The natural sand's lack of angularity presents significant challenges in field placement and has the tendency to cause mixture tenderness (31). The chosen virgin blend passes through the restricted zone according to Superpave standards as shown in Figure D-12. Although this region was considered off limits in the past, research in the past decade has shown that mixtures passing through the restricted zone do not often display poor performance when higher proportions of manufactured sands are used relative to natural sands (30). Therefore, this mixture design was considered to be acceptable.

A three-point mixture verification procedure was completed to determine the target asphalt content for the virgin mixture. The target air void content of 4.0% was reached at 6.7% asphalt binder. Furthermore, the calculated VMA and VFA at 6.7% asphalt binder were found to be approximately 15.3% and 73.7%, respectively. Finally, the dust-to-percent effective binder was determined to be equal to 1.2. Therefore, although the sand fraction was significant in the virgin mixture, all Superpave requirements were met. The 45% RAP mixture design included the use of passing 3/8" RAP material and replacement aggregate for the manufactured sand. The gradation plot and blending percentages are provided in Table D-3.

Table D-3. 45% RAP blend

Aggregate	Blend Percentage
CM16	21.0
FM20*	15.1
FM02	17.7
MF	1.2
RAP	45.0

The manufactured sand was replaced in this mixture due to its high dust content. Dust and RAP have the propensity to reduce the VMA of mixtures so the FM20 material was adjusted in order to create an aggregate structure that satisfied VMA requirements. The adjustment to the FM20 sand occurred with the use of manufactured sand that passed the #8 sieve and was retained on the #30 sieve. The adjusted FM20 gradation is shown in the Appendix of Hill (MS Thesis, 2011, reference 28). The percentage of natural sand was kept relatively constant with the addition of 45% recycled material as well. The use of 20% or less natural sand reduces the effect of the rounded nature of these sand particles. Finally, the RAP mixture had to approach the volumetric quantities of the virgin asphalt concrete mixture. Therefore, the gradation of the 45% RAP mixture was chosen to be approximately equal to the virgin gradation (within several tenths of a percent) at each sieve.

A three-point mixture verification procedure was completed to determine the target asphalt content for the 45% RAP mixture. A total asphalt content of 6.2% was originally used to produce satisfactory voids in the mineral aggregate, VMA, and air void contents. This asphalt content was approximately 0.5% less than the virgin asphalt mixture content. However, due to the reduction of dust present in the manufactured sand, the total asphalt binder required to sufficiently coat the aggregate was reduced in the RAP mixture. The assumption of total blending had an effect upon the total virgin asphalt content. As stated previously, this assumption leads to a reduction in the virgin asphalt binder fraction required. Approximately 3.9% virgin asphalt binder was added to the aggregate and RAP particles within this mixture due to the total RAP binder content available. A three-point verification occurred at total asphalt contents of 5.7, 6.2, and 6.7%. The target air void content of 4.0% was reached at 6.2% asphalt binder. In addition, the calculated VMA and VFA at 6.2% asphalt binder were found to be approximately 15.3% and 73.3%, respectively. Finally, the dust-to-percent-effective-binder was determined to be equal to 1.4 which was slightly higher than the Superpave maximum value. However, the effective asphalt content of the 45% RAP mixture was equal to that of the virgin mixture. Therefore, the dust-to-effective asphalt binder ratio was considered acceptable in this case.

The full suite of Superpave binder tests were conducted on virgin binder and extracted RAS binder. In addition, AASHTO T-283 moisture sensitivity testing (following the IDOT modified AASHTO procedure) along with Hamburg wheel track and disk-shaped compact tension fracture

energy (DC(T)) testing were performed. The latter two mixture tests are evolving mixture performance tests, and thus, details regarding their use in this study are provided in detail.

Hamburg Wheel Tracking Test

The Hamburg Wheel Tracking test (Hamburg test) measures the rutting resistance of asphalt mixtures. The test device is shown in Figure D-13 and occurs according to AASHTO T-324. Hamburg testing is generally conducted in water at 50°C to induce both rutting and moisture damage. The number of passes run during a test is dependent upon the high temperature asphalt binder grade. For example, PG 64-22 mixtures are generally run for 10,000 passes. The load applied by the steel wheel is approximately 158lbs. External LVDT's are used to determine the maximum rut depths at regular pass intervals. Finally, several parameters are calculated upon completion of the test and include: the creep slope, stripping slope, stripping inflection point, and maximum rut depth. The creep and stripping slopes represent the slopes of the rut depth profile before and after reaching the stripping inflection point. The stripping inflection point is the point at which the rut depth begins to increase at an increasing rate with respect to the number of passes applied. Finally, the maximum rut depth is the rut depth present at the end of the test.

Hamburg testing in this study was conducted on each of the eight WMA and HMA mixtures. Gyrotory specimens which were 130mm in height were cut in half and given flat faces to produce a geometry as shown in Figure D-14 (32). Finally, the heights of the two sides of the gyrotory specimen were adjusted in to reach equal heights and avoid dynamic loading. All Hamburg tests were conducted for a duration of 20,000 passes to examine the full rutting resistance capabilities of RAP mixtures. Furthermore, all specimens were compacted to approximately 7.0% air voids to comply with AASHTO T-324 standards and four replicates were completed for each mixture.



Figure D-13. Hamburg Wheel Tracking device

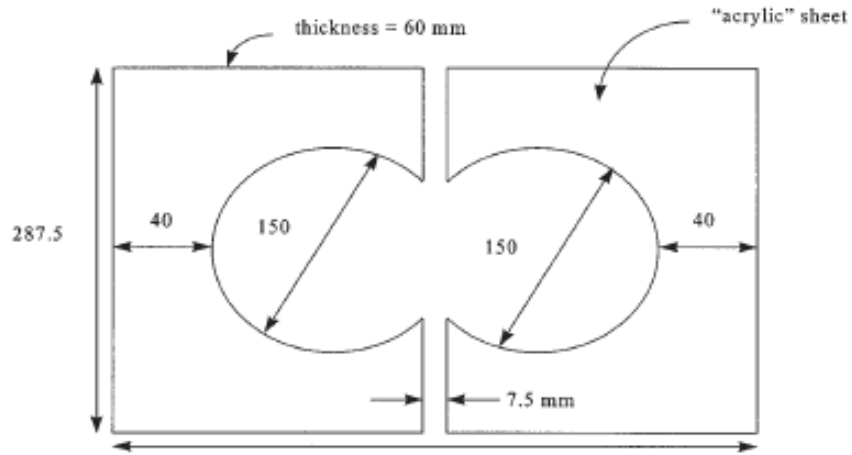


Figure D-14. Hamburg gyratory specimen molds

Disk-Shaped Compact Tension (DC(T)) Test

The DC(T) test is a low temperature mixture test conducted in accordance with ASTM D7313-07. This test measures the fracture resistance of asphalt mixtures by characterizing the pre-peak and post-peak load-CMOD behavior. The primary testing result is a measure of fracture energy which is calculated by determining the area under the load-CMOD plot. (An example plot is shown in Figure D-15.) The test is conducted using a servo-hydraulic system that allows it to be run under strain control at a CMOD opening rate of 1.0mm/min. A conditioning chamber surrounds the testing set-up in order to maintain constant temperatures. Furthermore, a LabVIEW program is generally used to collect data from the servo-hydraulic system. In addition to a CMOD gauge, δ -25 gauges are generally attached to the sides of specimens at the crack tip to differentiate the total fracture energy from the creep opening of the specimen arms. An example of the DC(T) testing arrangement equipped with CMOD and δ -25 gauges is provided in

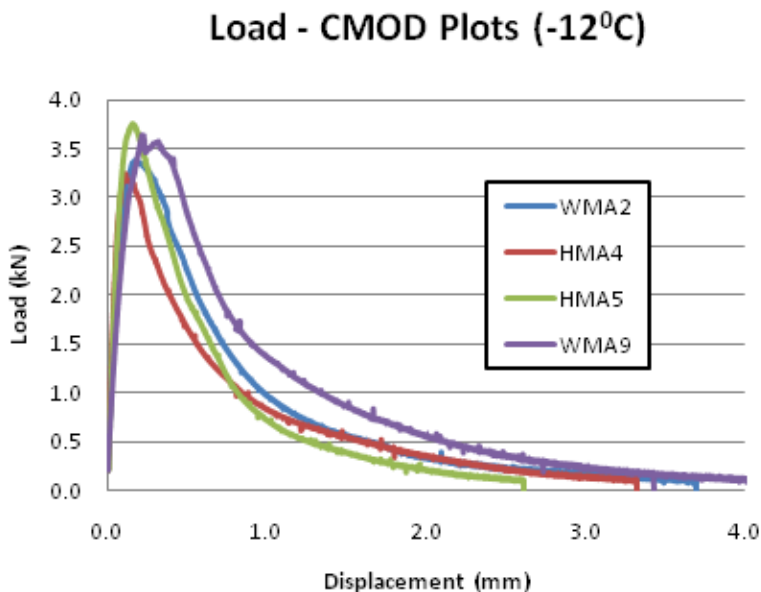


Figure D-15. Typical DC(T) load-CMOD plots

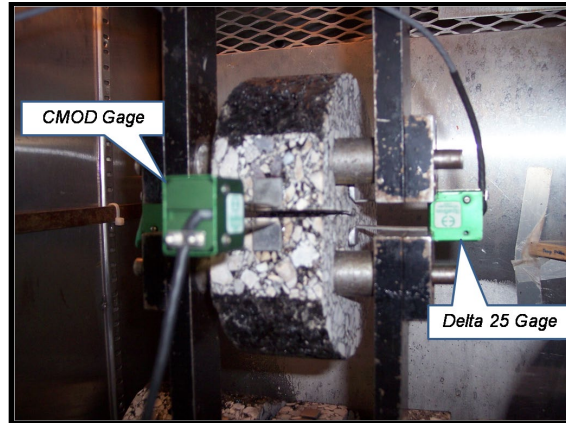


Figure D-16. DC(T) testing arrangement

DC(T) specimens are produced through cutting gyratory specimens. These specimens are cut such that 50mm thick specimens with smooth top and bottom faces are produced. In order to create precise cuts, a water-cooled carbide-tipped masonry saw was used. Then, a straight edge was cut using a tile saw to allow placement of the crack mouth opening displacement (CMOD) gage points. Afterward, core holes were inserted using a coring machine to place connections for the loading fixtures. Finally, the notch was cut using the straight edge tile saw.

All mixtures in this study were tested using this fracture test. Four replicates of each mixture with approximately 7.0% air voids were tested at -12°C in order to characterize the average fracture resistance and the variability associated with each mixture set. In this case, an Instron 8500 with a 10kN Instron load cell was used to complete the testing. The 10kN load cell was chosen due to its increased accuracy with loads below 4kN.

D.1.9. Asphalt Binder Performance Test Results and Analysis

Several observations were made from RV testing results. First, the assumption that WMA technologies reduce production temperatures by reducing the asphalt binder viscosity is not valid in all cases. Some technologies, such as Advera and Evotherm, do significantly alter the viscosity-temperature relationship of the asphalt binder. Therefore, other properties such as the ionic nature of the modified asphalt binder and its effect on lubricity and mixing characteristics at a given temperature relative to non-WMA binder may be the more significant factor behind improved workability and reduced production temperatures.

The Bending Beam Rheometer (BBR) apparatus was used in this study to examine the low temperature cracking susceptibility of the modified and unmodified asphalt binders. The results are plotted in Figures D-17 through D-20. As shown in Figures D-17 and D-18, an increased concentration of Advera increased the stiffness, decreased the m -value of the asphalt binder, and lead to increased low temperature susceptibility. RTFO short-term aging further reduced the m -value and increased bending beam stiffness. This result was anticipated because RTFO conditioning simulates the aging which occurs during the early service life of the asphalt concrete. As stated previously, 0.25% Advera by weight of the mixture, the chosen for mixture performance testing, displayed slightly higher stiffness in comparison with the unmodified

binder. Therefore, the Advera DC(T) fracture resistance may be slightly less than the control HMA mixture.

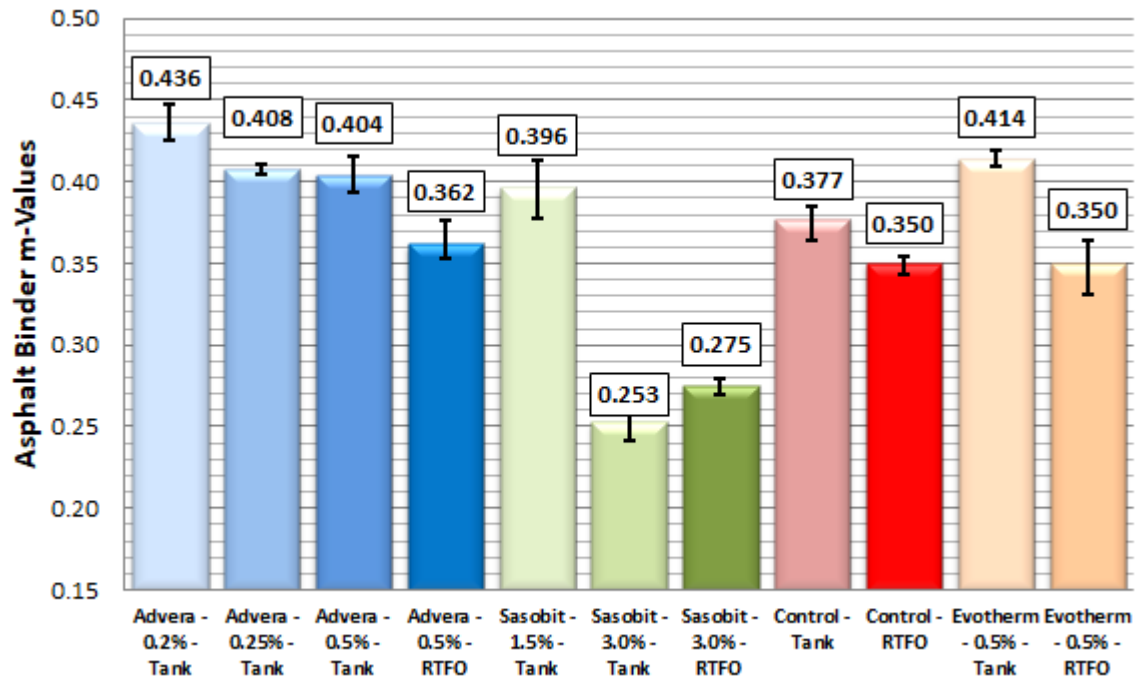


Figure D-17. Tank and RTFO binder M-Values

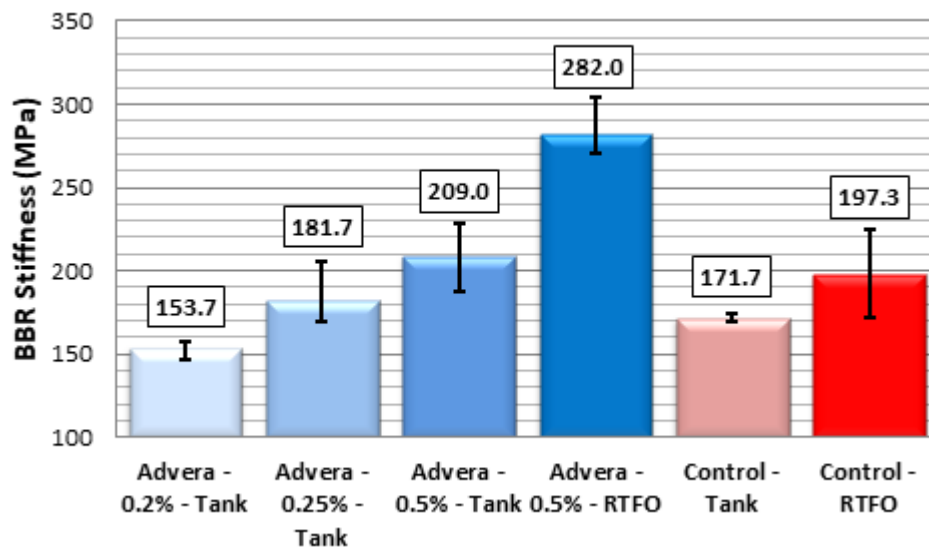


Figure D-18. Advera tank and RTFO binder stiffness

The Evotherm modified asphalt binder displayed similar results in comparison to the Advera binder. First, RTFO short-term aging reduced m-values and increased the stiffness relative to the unmodified control binder. Next, as shown in Figure D-19, the tank and RTFO aged Evotherm samples were not significantly stiffer than the control binder and the tank m-value was significantly higher than the unmodified binder. Consequently, the asphalt concrete mixture's fracture resistance is likely improved by the use of Evotherm as compared to the control HMA.

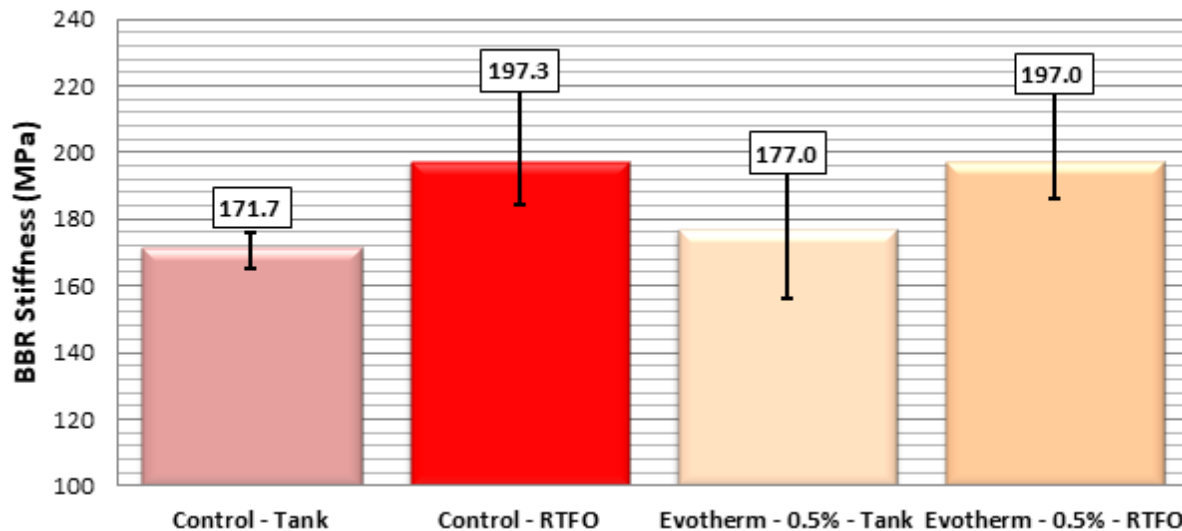


Figure D-19. Evotherm tank and RTFO binder stiffness

Sasobit modified asphalt binder deviated significantly from the other modified and unmodified binders at low temperatures. First, as shown in Figure D-20, the m-value of the RTFO aged binder increased after the conditioning process. This was not anticipated because all other asphalt binders displayed reduced m-values after the RTFO aging period. Next, Sasobit tank and RTFO asphalt binders exhibited significantly greater stiffness than the unmodified control binder. This result should have occurred because the RV results displayed the increased stiffness of the Sasobit binder below 90°C so the wax present at low temperatures should significantly increase stiffness at low temperatures as well. Finally, due to the stiffening effect of this wax additive, the DC(T) fracture resistance of Sasobit modified asphalt mixtures should be significantly less than the control HMA mixture.

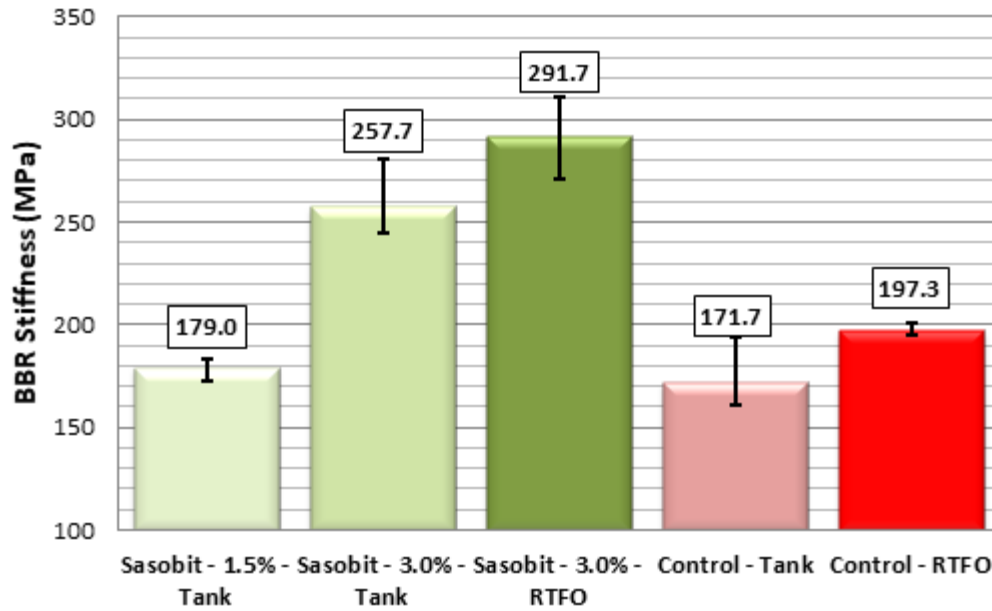


Figure D-20. Sasobit tank and RTFO binder stiffness

Three conclusions can be made with respect to the BBR results for WMA additive modified and unmodified asphalt binders. First, increasing the percentages of WMA additives does not improve the low temperature binder properties of asphalt binders. Consequently, manufacturer recommendations must be adhered to in order to improve fracture resistance. Next, RTFO aging of modified asphalt binders produces expected results in which stiffness increases and m-values decrease. As a result, the RTFO and Pressure Aging Vessel can continue to be used to condition the asphalt binder similar to general PG grade binders. Finally, Sasobit stiffens the asphalt binder considerably more than the other WMA additives at low temperatures. Therefore, this type of modified binder will likely display considerably lower fracture resistance than the other asphalt binders presented in this study.

D.1.10. Asphalt Mixture Performance Test Results and Analysis

The Hamburg Wheel Tracking device was employed to examine the rutting resistance WMA and HMA mixtures in this study. Several assumptions and conditions were chosen with the use of the Hamburg test. First, although other studies have presented 4 hour aging periods for WMA mixtures, a 2 hour oven aging period was chosen in this experiment to examine the worst case scenario in which the asphalt binder is aged to a minimal degree. Furthermore, the 2 hour aging period matched the DC(T) aging period in order to effectively discuss fracture and rutting resistance. A 12.5mm rut depth was also considered a maximum for the Hamburg test. This value was chosen to match the maximum rut depth considered by many state agencies including the Texas Department of Transportation.

The virgin mixture Hamburg test results are shown in Table D-4 and Figures D-21 and D-22. Several observations can be made from these results. First, all mixtures reached a 12.5mm rut depth prior to reaching 10,000 wheel passes. Consequently, each mixture could be rutting

susceptible with the use of virgin aggregate. Moisture sensitivity was also present in each of the virgin mixtures. As shown in Figure D-23, asphalt binder was stripped from the aggregate throughout the test and lead to increased permanent deformation after the stripping inflection point.

Table D-4. Sasobit tank and RTFO binder stiffness

<i>Specimen</i>	<i>Inverse Creep Slope (p/mm)</i>	<i>Stripping Inflection Point</i>	<i>Inverse Stripping Slope (p/mm)</i>
Control	1181.1	3320	313.8
Evotherm	370.5	1800	157.8
Sasobit	1517.9	4040	288.1
Advera	494.1	2390	169.5

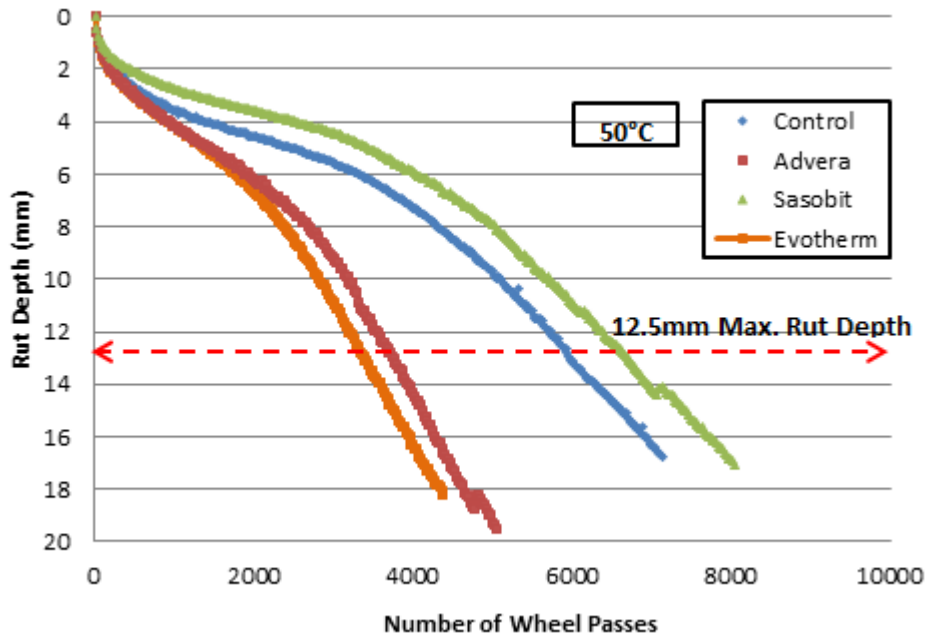


Figure D-21. Virgin Mixture rut depth profiles

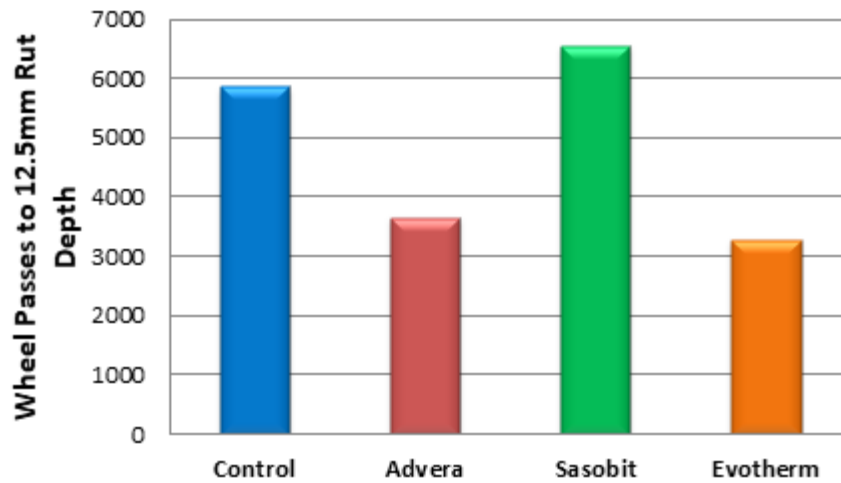


Figure D-22. Virgin mixture wheel passes to maximum rut depth



Figure D-23. Moisture sensitivity of virgin mixture specimen

The results display that WMA additives had significant effects upon the rutting resistance of the virgin asphalt mixtures. As shown in Figure D-22, the Sasobit and control HMA mixtures behaved similarly while the Evotherm and Advera mixtures failed at a considerably lower number of wheel passes. The Sasobit mixture performed better than all other mixtures in terms of the number of passes required to meet the failure depth and the associated inverse creep and stripping slopes. This result was anticipated due to the stiffening effect of the wax additive. The Evotherm and Advera mixtures displayed reduced rutting resistance in comparison with the virgin control HMA. These results were also foreseen due to the contents of these WMA additives. Evotherm M1 acts as an emulsifying agent so the asphalt binder and aggregate interface bond was softened and lead to increased rutting. Also, the presence of residual water in the Advera mixture leads to increased stripping potential which reduced the asphalt mixture's ability to resist permanent deformation.

The 45% RAP mixtures exhibited significantly different results in terms of Hamburg rutting resistance. The results are presented in Figures D-24 and D-25 and Table D-5. As shown in Figure D-24, all mixtures met the 10,000 pass requirement prior to reaching a rut depth of 12.5mm. The mixtures displayed significantly rutting profiles with the presence of 45% RAP. In this case, the control HMA exhibited the best rutting resistance followed by the Sasobit, Evotherm, and Advera WMA mixtures. Evotherm and Advera reached the 12.5mm rut depth limit after 10,000 wheel passes. In addition, each of these mixtures exhibited a stripping inflection point and displayed stripped aggregate similar to Figure D-26. The Sasobit and control HMA mixtures did not exhibit true stripping inflection points. This result is validated by Figure D-25 in which little to no asphalt binder was stripped from the aggregate during the testing period. The Sasobit and control HMA mixtures switched rankings when comparing 45% RAP and virgin mixtures. This change was likely due to variability within the RAP material because the percentage of Sasobit added to the total asphalt binder remained constant for each mixture design.

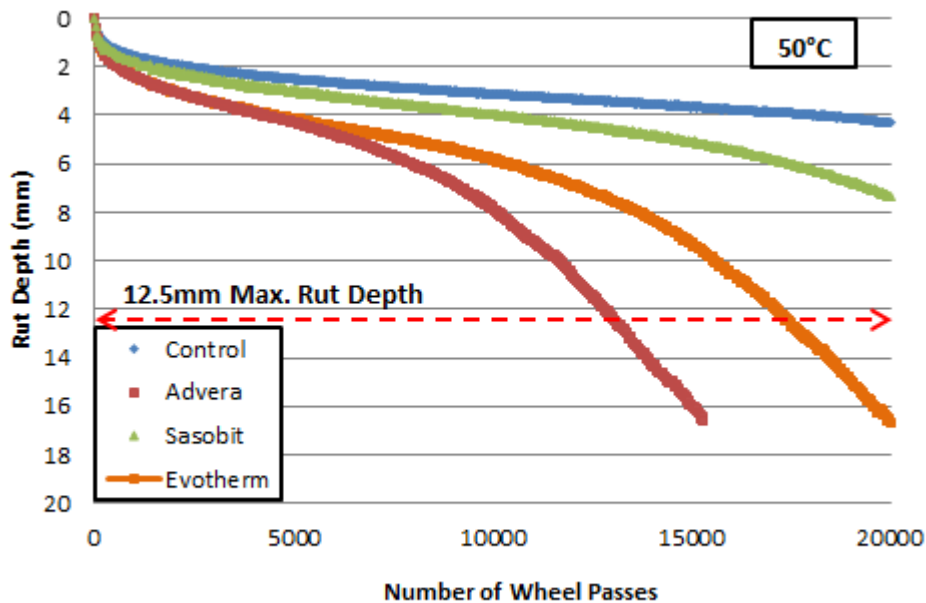


Figure D-24. 45% RAP mixture rut depth profiles

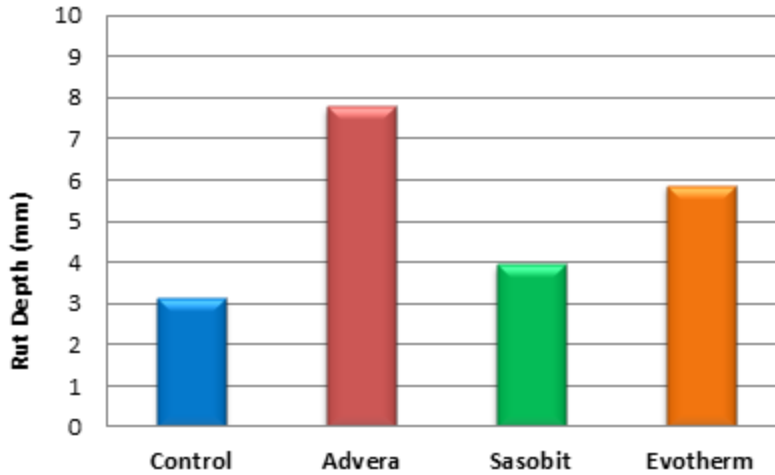


Figure D-25. 45% RAP mixture rut Depths at 10,000 wheel passes

Table D-5. 45% RAP Hamburg WTD results

<i>Specimen</i>	<i>Inverse Creep Slope (p/mm)</i>	<i>Stripping Inflection Point</i>	<i>Inverse Stripping Slope (p/mm)</i>
Control	5813.0	-	-
Evotherm	2839.8	10340	690.7
Sasobit	4218.2	-	-
Advera	1657.7	8000	513.5



Figure D-26. RAP Sasobit Hamburg Specimen

Several general observations can be made with regard to the Hamburg results for virgin and RAP mixtures in this study. First, RAP significantly improved the rut resistance of each WMA and HMA mixture. As a result, binder blending must occur to some degree to behave differently from virgin mixtures. Second, the potential reduction in aging due to reduced production

temperatures for the WMA modified mixtures did not have considerable effects upon the results. The additives' individual attributes had a much more appreciable effect upon the rutting resistance of the virgin mixtures. The potential residual moisture in the Advera mixtures and the emulsifying effect of the Evotherm additive lead these mixtures to display the least rutting resistance. Furthermore, the Sasobit mixture exhibited the closest performance to the control HMA. This effect was likely caused by the stiffening effect of the wax present in Sasobit additives.

Moisture sensitivity testing was completed using the AASHTO T-283 TSR procedure. The virgin mixture results are presented in Table D-6 and Figure D-27. As shown in Table D-6, strengths are not shown as indirect tensile strengths because of the types of failure present were not of the indirect tensile variety in all cases. The most common type of failure in these mixture sets occurred due to punching so material strengths may not be true measures of indirect tensile strength at intermediate temperatures. The results in Figure D-27 display that Evotherm M1 was the only mixture that passed the 80% minimum TSR rating. However, this mixture stripped a considerable amount in the fine and coarse aggregate as shown in Figure D-28. Therefore, this mixture should also be considered a potentially moisture susceptible asphalt concrete. The strength retention in the Evotherm mixtures was likely caused by the ionic nature of this additive because Evotherm additives can be engineered to improve bonding based upon the aggregate present in the mixture. As stated previously, the other WMA and HMA mixtures failed by considerable margins. These failed results were likely caused by the moisture sensitivity of limestone aggregates. Furthermore, Advera mixtures exhibited the greatest moisture sensitivity among all mixtures. This result was caused by a combination of poor quality aggregate and the residual moisture present in the Advera additives. Due to the poor moisture sensitivity results, anti-stripping agents may be a requirement for WMA additives such as Advera.

Table D-6. Virgin mixture TSR results

<i>Mix Type</i>	<i>Conditioned Str. (kPa)</i>	<i>Unconditioned Str. (kPa)</i>	<i>TSR</i>	<i>Visual Rating</i>
Control	483.3	726.0	67%	5
Advera	443.3	859.8	52%	5
Sasobit	519.9	857.0	61%	5
Evotherm	635.7	743.9	86%	3

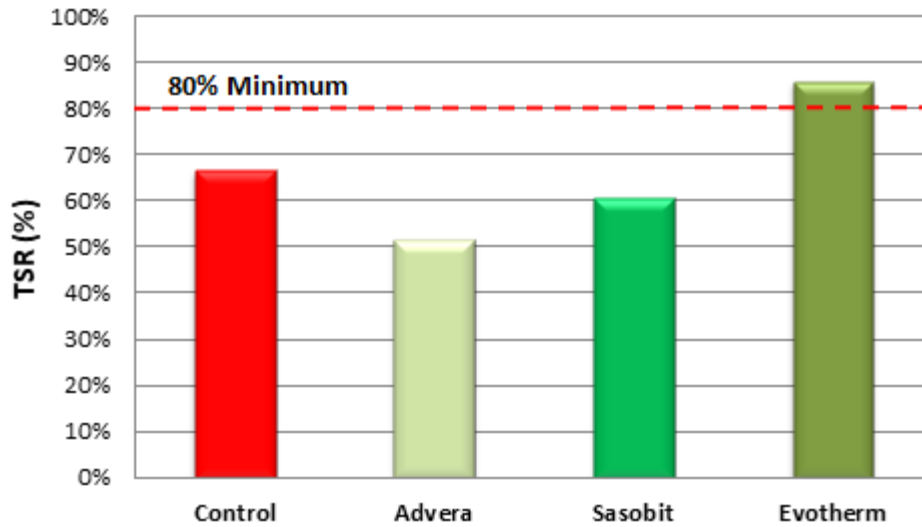


Figure D-27. TSR results for virgin HMA and WMA mixtures

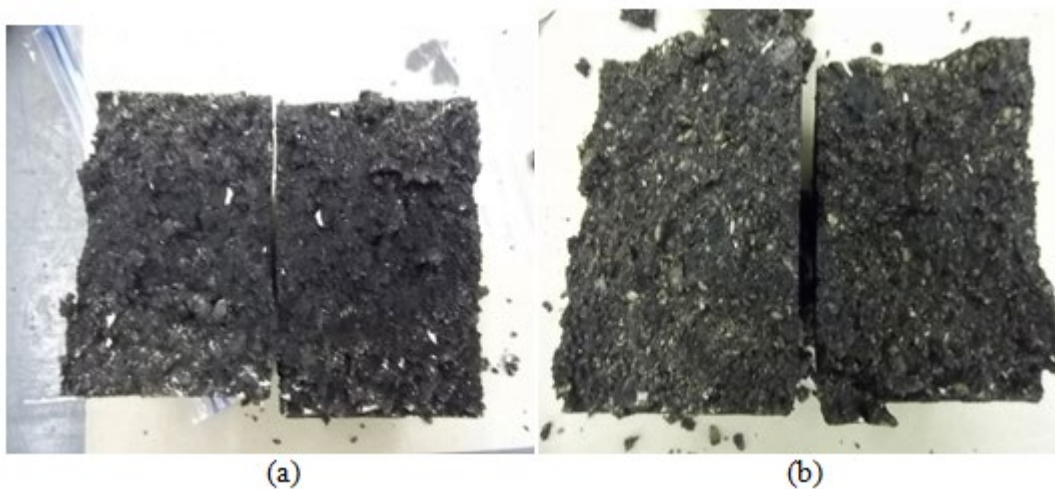


Figure D-28. (a) Unconditioned Evotherm TSR sample and (b) Conditioned Evotherm TSR sample

Similar to the Hamburg results, the WMA and HMA mixtures exhibited improved performance with the presence of 45% RAP. These results agreed with the Middleton and Forfylow (18) results for Double Barrel Green mixtures containing recycled materials. The 45% RAP TSR results are presented in Figure D-29 and Table D-7. In all cases except Evotherm M1, TSR values increased considerably with RAP included in the mix design. However, Evotherm remained the only mixture that passed the TSR requirement. The average strengths of the conditioned and unconditioned TSR specimens increased as well. In several cases, mixture strengths increased by as much as 600kPa. Overall, the 45% RAP mixtures displayed less moisture sensitivity than the virgin mixtures. This occurred because the RAP particles have a stiffer asphalt coating that is less likely to be stripped. Finally, the rankings of moisture

sensitivity remained the same with respect to the virgin and 45% RAP mixtures. Consequently, the WMA technologies' properties had significant effects upon performance because ranking consistency would not have occurred in the case that production temperatures affected results more than additive properties.

Table D-7. 45% RAP mixture TSR results

<i>Mix Type</i>	<i>Conditioned Str. (kPa)</i>	<i>Unconditioned Str. (kPa)</i>	<i>TSR</i>	<i>Visual Rating</i>
Control	1030.1	1354.8	76%	4
Advera	812.2	1152.1	70%	4
Sasobit	917.0	1232.1	74%	4
Evotherm	1052.1	1218.3	86%	3

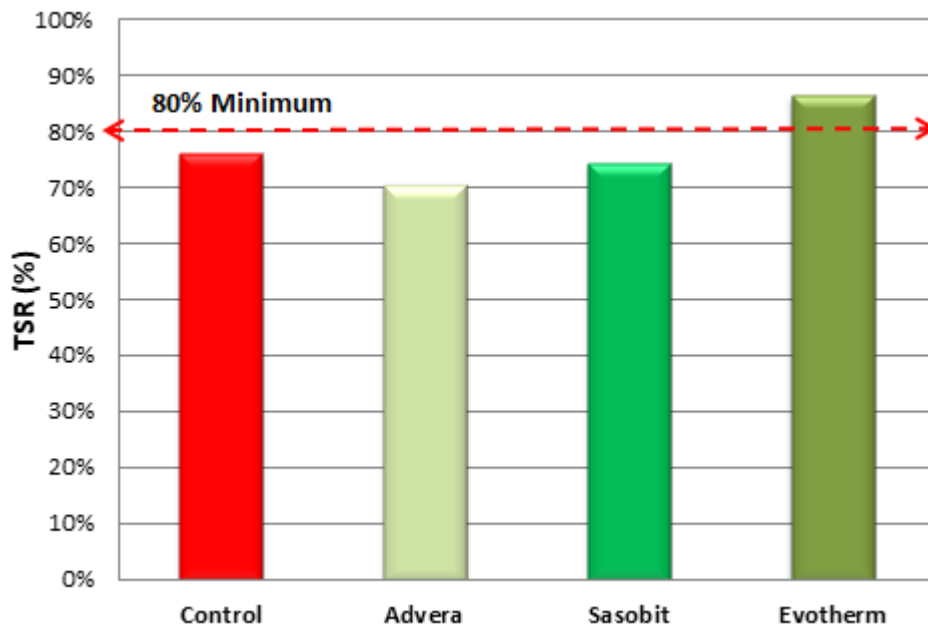


Figure D-29. 45% RAP HMA and WMA mixture TSR results

The disk-shaped compact tension (DC(T)) test results describe the low temperature cracking susceptibility and are shown in Figures D-30 and D-31. The error bars represent the high and low values within each data set. Furthermore, tabular results which include peak loads and δ_{25} fracture energies are presented in the Appendix. The virgin mixtures displayed the greatest variation in CMOD fracture energies. Consequently, WMA additive properties have a more significant effect upon low temperature performance than lessened aging due to production temperatures. The virgin HMA mixture will likely exhibit slight to moderate transverse cracking because the fracture energy is approximately 25 J/m^2 less than the 400 J/m^2 optimum for asphalt mixtures as reported by Buttlar et al. (2010) (33). The Advera WMA mixture displayed a reduced fracture resistance when compared to the control HMA. As a result, the foaming

process' residual moisture may cause damage due to the phase transformation of water to ice at approximately 0°C and lead to lessened fracture energy. The Sasobit WMA mixtures exhibited the worst fracture performance of all virgin mixtures. The stiffening effect of the Sasobit wax additives leads to mixtures that are unable to undergo toughening mechanisms. Consequently, this mixture will likely produce the most thermal cracking in comparison with the other virgin mixtures. Finally, the emulsifying effect of the Evotherm additive improved the fracture resistance this WMA mixture in comparison with the control HMA. This asphalt binder displayed the least stiffness in terms of the BBR results so the softening caused by Evotherm M1 was anticipated.

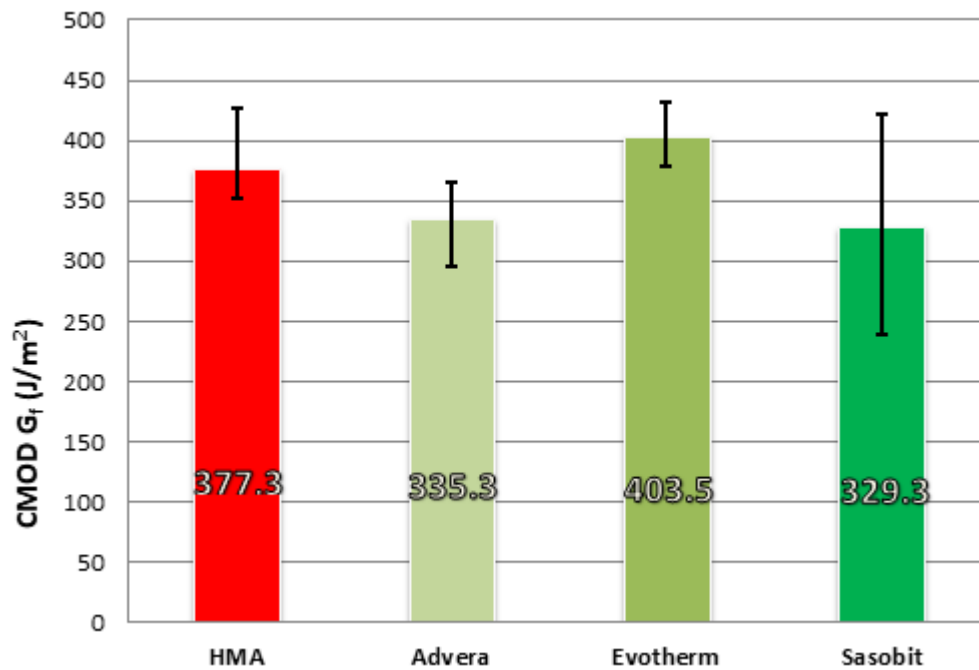


Figure D-30. DC(T) results for virgin HMA and WMA mixtures

The presence of 45% RAP reduced fracture resistance by a significant amount as shown in Figure 31. In several cases, the average CMOD fracture energy decreased by as much as 100 J/m² with addition of 45% RAP. This result was anticipated due to the aged stiffness of the RAP particles and will likely lead to significant transverse cracking. As stated in the Hamburg results section, asphalt binder blending must have occurred to some degree in this study. That particular observation agrees with the DC(T) results because RAP had a significant effect upon the fracture resistance of each mixture. The differences in CMOD fracture energy were lessened by the presence of 45% RAP. This large amount of recycled material may have more of an effect upon fracture resistance than the addition of WMA additives. Further research would be required to determine how WMA and low RAP contents interact in terms of low temperature fracture testing. Finally, Advera and Evotherm WMA mixtures switched in terms of the highest ranking material. This result was not anticipated because WMA additive percentages remained constant. Additional testing is required in this instance to determine if this trend remains the same or if RAP variability was the underlying cause.

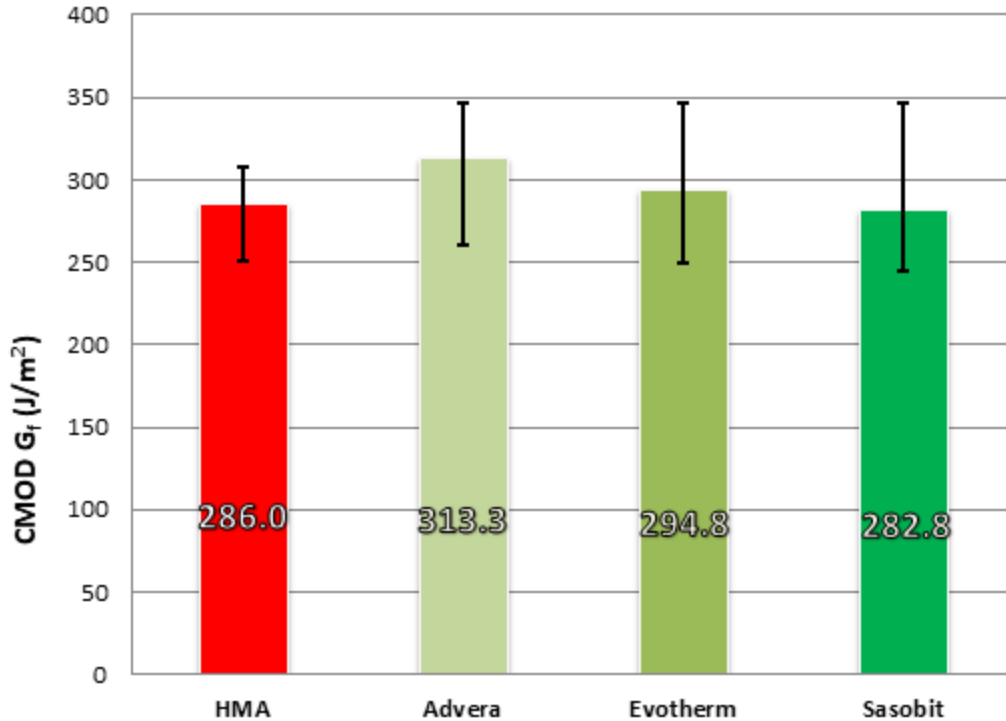


Figure D-31. DC(T) results for 45% RAP HMA and WMA mixtures

The key findings identified through the RAP-WMA study are:

1. WMA additives do not necessarily reduce the viscosity of the asphalt binder at production temperatures in all cases. In two out of three cases in this study, modified asphalt binder viscosity was not significantly different from unmodified binder viscosity throughout the test temperatures (Hill, 2011).
2. WMA additives produced increased BBR stiffness in comparison with unmodified asphalt binder. Consequently, the addition of WMA additives must be optimized to avoid potential distresses such as thermal cracking.
3. Rutting resistance may be problematic for non-wax modified WMA mixtures. Chemical and foaming additive displayed reduced rutting resistance when compared with control HMA and Sasobit WMA mixtures.
4. Moisture sensitivity is a significant issue for the majority of WMA additives. As a result, anti-stripping agents or hydrated lime may be required to address this performance distress.

5. Fracture resistance differed significantly among the WMA additives. Therefore, reduced production temperature does not have an appreciable effect on DC(T) fracture energy.
6. Finally, RAP may in some circumstances lead to reduce rutting and moisture susceptibility of WMA mixtures as characterized by the Hamburg and TSR tests, respectively. However, the reduced fracture resistance of RAP mixtures must be considered in order to produce quality asphalt concrete mixtures, and WMA additives and reduced mixing temperatures alone were not sufficient to reduce the embrittlement of the study mixtures upon inclusion of 45% RAP

The following conclusions can be drawn from the study findings:

1. Reduced viscosities at production temperatures are not the primary cause for the lessened production temperatures available in all WMA technologies. Other factors such as chemical composition must be considered as well.
2. The properties of WMA technologies have a significant effect upon the fracture, moisture, and rutting resistance of asphalt concrete mixtures. Therefore, the proper technology must be chosen to produce the desired performance, and performance testing appears to be a necessary component in the design of sustainable mixtures containing WMA and RAP.
3. The addition of RAP to WMA has the potential to improve the performance of these mixtures at intermediate to high temperatures. However, sufficient care must be taken in terms of virgin binder grade adjustments and virgin aggregate type to ensure adequate cracking resistance.

D.1.11. References

- [1] Collins, R.J. and Ciesielski, S.K. Recycling and Use of Waste Materials and By-Products in Highway Construction. NCHRP Synthesis 199. National Cooperative Highway Research Program (NCHRP), TRB, Washington, D.C., 1994.
- [2] Brown, D.C. Asphalt Recycling Gains Momentum. Public Works Magazine. March 1, 2005. <http://www.pwmag.com/industry-news>. Accessed March 5, 2011.
- [3] Chiu, C., Hsu, T., Yang, W. Life Cycle Assessment on using Recycled Materials for Rehabilitating Asphalt Pavements. Resources Conservation and Recycling 52(3), 2008, pgs. 545-556.
- [4] Illinois Department of Transportation. Hot Mix Asphalt Level III Technician Course. Lakeland College. February 2011, Chapter 2, pg. 56.
- [5] Xiao, F., Amirhanian, S., Juang, C. H. Rutting Resistance of Rubberized Asphalt Concrete Pavements Containing Reclaimed Asphalt Pavement Mixtures. *Journal of Materials in Civil Engineering* 19(6), 2007, pgs. 475-483.
- [6] Prowell, B. and Hurley, G.C. Warm-Mix Asphalt: Best Practices. National Asphalt Pavement Association Quality Improvement Series 125. Lanham, MD, December 2007.
- [7] D'Angelo, J., Harm, E., Bartoszek, J., Baumgardner, G., Corrigan, M., Cowser, J., Harman, T., Jamshidi, M., Jones, W., Newcomb, D., Prowell, B., Sines, R., and Yeaton, B. Warm-Mix Asphalt: European Practice. FHWA Report No. FHWA-PL-08-007, February 2008.
- [8] McDaniel, R.S., Soleymani, H., Anderson, R.M., Turner, P., and Peterson, R. Recommended Use of Reclaimed Asphalt Pavement in the Superpave Mixture Design Method. NCHRP Final Report (9-12), TRB, Washington, D.C., 2000.
- [9] Young, T.J. Energy Conservation in Hot-Mix Asphalt Production. National Asphalt Pavement Association. Quality Improvement Series 126. Lanham, MD, December 2007.
- [10] Anderson, R.M., Baumgardner, G., May, R., and Reinke, G. Engineering Properties, Emissions, and Field Performance of Warm Mix Asphalt Technologies. NCHRP 9-47. National Cooperative Highway Research Program (NCHRP), TRB, Washington, D.C., October 2008.
- [11] Graniterock. HMA and WMA mix was dumped from truck. http://www.graniterock.com/technical_notes/warm_mix_asphalt.html. Accessed December 13, 2009.
- [12] Prowell, B. and Hurley, G.C. Evaluation of Evotherm for Use in Warm Mix Asphalt. NCAT Report 06-02, June 2006.
- [13] Prowell, B. and Hurley, G.C. Evaluation of Aspha-min Zeolite for Use in Warm Mix Asphalt. NCAT Report 05-04, June 2005.

- [14] Kandhal, P.S. and Mallick, R.B. Pavement Recycling Guidelines for State and Local Government. National Center for Asphalt Technology, 1997.
- [15] Wagoner, M.P., W.G. Buttlar, G.H. Paulino, and P. Blankenship. Investigation of the Fracture Resistance of Hot-Mix Asphalt Concrete Using a Disk-Shaped Compact Tension Test. *Transportation Research Record*. No. 1929, 2005, pgs. 183-192.
- [16] Dave, E. Determination of Presence and Amount of Recycled Asphalt Pavement in Asphalt Mixtures. University of Illinois Urbana-Champaign. Master's Thesis. 2003.
- [17] Mallick, R.B., Kandhal, P.S., Bradbury, R.L. Using WMA Technology to Incorporate High Percentage of RAP Material in Asphalt Mixtures. *Transportation Research Record*, No. 2051, 2008, pgs. 71-79.
- [18] Middleton, B. and Forfylyow, R.W. Evaluation of Warm-Mix Asphalt Produced with the Double Barrel Green Process. *Transportation Research Record* No. 2126. 2009, pgs. 19-26.
- [19] Kvasnak, A., Taylor, A., Signore, J.M., and Bukhari, S.A. Evaluation of Gencor Green Machine Ultrafoam GX. NCAT Report 10-03, July 2010.
- [20] Sasol International. What is Sasobit®?. <http://www.sasolwax.us.com/sasobit.html>. Accessed January 20, 2010.
- [21] U.S. Department of Transportation – Federal Highway Administration. Warm-Mix Asphalt: European Practice. http://international.fhwa.dot.gov/pubs/pl08007/wma_08_d.cfm. Accessed June 20, 2010.
- [22] Prowell, B. and Hurley, G.C. Evaluation of Sasobit for Use in Warm Mix Asphalt. NCAT Report 05-06, June 2005.
- [23] Estakhri, C., Button, J., and Alvarez, A.E. Field and Laboratory Investigation of Warm Mix Asphalt in Texas. FHWA Report No. FHWA/TX-10/0-5597-2, July 2010.
- [24] Akzo Nobel. Rediset WMX. www.surfactants.akzonobel.com/asphalt/newwarmmixsystem.cfm. Accessed June 21, 2010.
- [25] Meadwestvaco. Evotherm. www.meadwestvaco.com/products/mwv002106. Accessed June 21, 2010.
- [26] Astec, Inc. Double Barrel Green. www.astecinc.com/products/drying_mixing/db_mixers/default_green.htm. Accessed June 20, 2010.
- [27] Gencor. Ultrafoam GX. <http://gencorgreenmachine.com/index.html>. Accessed June 23, 2010.

[28] Hill, B. C., “Performance Evaluation of Warm Mix Asphalt Mixtures Incorporating Reclaimed Asphalt Pavement,” Master’s Thesis, University of Illinois at Urbana-Champaign, 2011.

[29] Roberts, F.L., Kandhal, P.S., Brown, E.R., Lee, D.Y., and Kennedy, T.W. Hot Mix Asphalt Materials, Mixture Design, and Construction. National Asphalt Pavement Association 2nd Edition. Lanham, MD, 1996.

[30]. Pine, W.J. The Bailey Method: Achieving Volumetrics and HMA Compactability. Heritage Research Group. Bailey Method Mix Design Course, 2009, Urbana, IL.

[31] Kandhal, P.S. and Cooley, L.A. The Restricted Zone in the Superpave Aggregate Gradation Specification. NCHRP Final Report (9-14), TRB, Washington, D.C., 2001.

[32] Izzo, R.P. and Tahmoressi, M. Use of the Hamburg Wheel-Tracking Device for Evaluating Moisture Susceptibility of Hot-Mix Asphalt. *Transportation Research Record*. No. 1681, 1999, pgs. 76-85.

[33] Marasteanu et al., (2012). Investigation of Low Temperature Cracking in Asphalt Pavements National Pooled Fund Study #776 - Phase II. Final Report to the Federal Highway Administration.

D.2. Recycled Asphalt Shingles (RAS) and Rejuvenators

Another source for secondary materials is recycled asphalt shingles (RAS). Asphalt shingles, like RAP, also contain mineral aggregates and asphalt cement, making RAS a candidate for product replacement in HMA. This chapter summarizes the past and recent literature on RAS and its usage in asphalt paving mixtures, and provides detailed data from recent studies involving advanced mixture performance testing on RAS mixtures.

D.2.1. Reclaimed Asphalt Shingles: an Introduction

High asphalt demand and the large amount of shingles waste in landfills have led to the increased use of asphalt shingles in asphalt paving mixtures. RAS comes from two different sources, post-manufactured shingles and post-consumer shingles. Figure D-32 displays the composition of typical roofing shingles. Post-manufactured shingles are the waste products of the shingle manufacturing process, which include factory rejects and tab cut-outs, while post-consumer shingles are shingles that come directly from roofs of commercial and residential buildings after their service life including damage from severe weather. Historically, the vast majority of research on RAS has focused on post-manufactured shingles since government engineers and regulators have traditionally accepted post-manufactured shingles over post-consumer shingles in the development of construction materials specifications and environmental regulations. With more recent technological advances in processing asphalt shingles, research efforts are trending towards the utilization of post-consumer shingles (Figure D-33). A major factor driving this interest is that ten million tons of post-consumer shingles are placed in landfills in the United States each year, while only one million tons of post-manufactured shingles are placed in landfills each year (FHWA and EPA 1993). With this large pool of post-consumer shingle resource, there is significant potential for cost savings in mix constituents and landfill space.

Recycling manufactured shingle scrap has been occurring for the last 25 years due to the many applications of RAS as a construction material (McGraw et al., 2007). RAS has been used mostly as a secondary material for HMA in commercial and private pavements. Recently, it has become more widely used in highway pavements by transportation agencies. Specifically, the asphalt content of RAS lies between 20 and 40% and approximately 11 million annual tons of shingle waste are produced in the United States (CIWMB (2005) and CMRA (2007)). According to a well-known calculation, it would save 1 billion dollars annually if 11 million tons of asphalt shingles would be used in the asphalt pavement (Brock (1998)). Therefore, responsible use of RAS in asphalt pavement materials may yield significant environmental and economic benefits. RAS has been used in asphalt mixtures in Missouri for years. According to a specific project, \$135,000 was saved compared to conventional asphalt mixture. The field performance of these sections was observed a period up to 5 years and no cracking was reported for any of the RAS sections (Schroer et al. 2013).

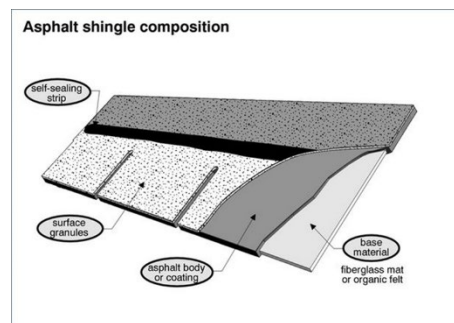


Figure D-32. Asphalt shingle composition



Figure D-33. Post-consumer RAS

Asphalt shingles are composed of 20-40% asphalt, 40-70% aggregate granules, and 1-25% base materials (Arnold (2014)). In roofing applications, asphalt affords weather resistance, high temperature stability and water-proofing. Before being manufactured to asphalt shingles, refined asphalt is oxidized by an air blowing process to increase its viscosity to prevent high temperature flow. Air-blown shingle asphalt is typically much stiffer than the asphalt used in traditional asphalt pavement. For example, the performance grade of shingle asphalt obtained from a

shingle manufacturer may be on the order of PG 112+2, which is much stiffer than a typical asphalt paving grade such as PG 62-22. Aggregate granules protect asphalt from sun damage and provide a desired surface color for shingles. Ceramic granular, headlap granules, backsurfacer sand and stabilizer are typical constituents of aggregate granules, which are designed to a similar quality level as aggregates in paving materials, i.e., hard, angular and neither flat nor elongated. Thus, their presence in a recycled mixture tends to help build voids in the mineral aggregate (VMA). Base materials, categorized as organic base and fiberglass base, provide a matrix to support all the other materials. These materials, when used in recycled asphalt mixtures, tend to help prevent draindown and provide needed fines in stone-mastic asphalt (SMA) mixes. As shown, the asphaltic and aggregate portions of the asphalt shingle have some similarities with respect to asphalt concrete, and can provide significant benefits in designing SMA mixtures in particular. However, careful attention must be paid to the large stiffness disparity between RAS and virgin asphalt binders when designing with RAS.

D.2.2. RAS Research in the Literature

Early RAS studies showed that the addition of RAS did not have an evident effect on volumetric properties and improved compactability (Watson et al. (1998), Foo et al. (1999), Mallick et al. (2000)). Watson et al. (1998) and Mallick et al. (2000) showed that the gradation and volumetric properties of RAS-modified mixtures did not change appreciably in reference to the control mixtures. Foo et al. (1999) confirmed that voids in the total mixture (VTM), VMA, and VFA of RAS-modified HMA mixtures are similar with conventional HMA mixtures. Newcomb et al. (1993) and Sengoz et al. (2003) found that the optimum total asphalt content for RAS mixtures dropped, which implied that a certain amount of shingle asphalt comes off of the shingles and participates as a binder in blending with aggregates. All in all, no significant changes of volumetric properties encourage researchers and asphalt engineers to investigate the application of RAS in the asphalt paving materials.

Binder characterization studies have been completed to investigate RAS participation in the asphalt binder and to characterize the effect of RAS on virgin binders. Newcomb et al. (1993) pointed out the inclusion of RAS reduced the required amount of virgin asphalt which indicated that the RAS binder indeed participated the mixture blending. Mallick et al. (2000) confirmed this viewpoint by comparing the asphalt content of the extracted binders from RAS mixtures and control mixtures and found results which showed that the asphalt content of all mixtures are similar. However, those two research results only demonstrated that almost all of the RAS binder still exists in the asphalt mixture after mixing and a certain amount of RAS asphalt participated in mixture blending. The quantity of effective RAS asphalt in the mixtures is still unknown. Paulsen et al. (1986) evaluated roofing waste from five different states. Binder test results showed that the inclusion of RAS generally increased the penetration and decreased the viscosity of virgin asphalt, and the amount of change due to the additional RAS for each parameter was different from source to source. Maupin et al. (2010) studied the performance grade changes after adding 25% tear-off shingle binder into PG 64-22 asphalt by testing the performance grade of binders after extraction and recovery. It was found that the inclusion of stiffer RAS asphalt bumps up the overall grade 2-3 high temperature grades, and one higher low temperature grade (i.e. PG 82-16). This demonstrates that the inclusion of RAS makes the virgin binder stiffer, and a softer virgin binder is an option to counterbalance the stiffer RAS binder in this case. You et al.

(2010) investigated the influence of 5% and 10% RAS on the PG 52-34 binder. The Bending Beam Rheometer test results showed that the net creep stiffness of binder increased with the increase of RAS content. In summary, research results have shown that RAS makes binder much stiffer which is beneficial in terms of rutting resistance, but it could be an issue for low temperature performance if complete blending of the asphalt binders occurs.

In order to verify the influence of RAS on the pavement performance, various mixture performance studies were completed. Testing in these studies characterized temperature susceptibility, moisture susceptibility, permanent deformation performance, low temperature behavior and fatigue cracking resistance. Resilient modulus tests was conducted by Newcomb et al. (1993) to investigate the temperature susceptibility and moisture susceptibility properties by comparing the resilient modulus of mixtures with 0%, 5%, 7.5% RAS. Results showed that 5.0% of felt-backed or fiberglass shingles eliminated temperature susceptibility of asphalt mixture at 0°C and 25°C, and mixture containing 5.0% RAS were stiffer than mixture containing 7.5% at both and 25°C and 40°C. By comparing resilient moduli and tensile strengths of control mixture and RAS-modified mixtures under unconditional (dry) and conditional (wet) cases, it was found that the ratio of conditional to unconditional moduli and strength did not change significantly as the percentage of RAS increased. Therefore, RAS had no distinct effect on the moisture susceptibility of asphalt mixture. Wu et al. (2014) conducted the Hamburg wheel tracking test to characterize the rutting resistance of RAS modified asphalt. The results showed that the rut depths of RAS modified asphalt mixtures were smaller than control mixture due to the stiffer RAS binder, which is consistent with the binder test results. Many other researchers also concluded that RAS is beneficial for resist permanent deformation of asphalt material based on mixture testing (Foo et al. (1999), (2000), (2003), Maupin (2010)). However, improved high temperature performance brought by RAS could lead to the degradation on the low temperature performance of asphalt mixture. The DC(T) test and acoustic emission technique were utilized by Arnold (2014) to examining low temperature behavior. Test results showed that the inclusion of RAS decreased the fracture energy and increased embrittlement temperature of mixtures, which means RAS-modified asphalt materials were more susceptible at low temperatures without a grade bump. A softer asphalt binder was recommended if a RAS-modified asphalt mixture failed specifications of low temperature performance test, such as the DC(T) test.

D.2.3. Chicagoland RAS Forensic Study

A comprehensive investigation was carried out by Buttlar (2014) to investigate the mechanisms behind asphalt pavement surface cracking observed on state roads in IDOT Districts 1 and 2. More specifically, the study investigated whether or not the District 1 Special Provision for RAP/RAS caused or contributed to cause premature pavement failures on certain asphalt overlay projects constructed in 2012 and 2013. A comparison of the District 1 (D-1) and statewide specification for RAP/RAS is shown in Table D-8, where the statewide specification is more conservative in asphalt binder replacement (ABR) levels for mixtures con

Table D-8. (a) D-1 RAP/RAS specification, (b) Statewide RAP/RAS specification

HMA Mixtures ^{1/2/4}	Maximum % ABR		
	Ndesign	Binder/Leveling Binder	Polymer Modified ^{3/}
30L	50	40	30
50	40	35	30
70	40	30	30
90	40	30	30
4.75 mm N-50			40
SMA N-80			30

(a)

HMA Mixtures ^{1/2/}	Maximum % ABR		
	Ndesign	Binder/Leveling Binder	Polymer Modified ^{3/}
30L	50	40	10
50	40	35	10
70	40	30	10
90	40	30	10 ⁴
4.75 mm N-50			30
SMA N-80			20

(b)

The study involved on-site pavement investigation in District 1 and 2, evaluation of selected projects using a state-of-the-art data collection vehicle, fracture testing and density assessment of cores obtained from projects in D1, and evaluation of associated plans and specifications. A summary of sections investigated is shown in Figure D-34.

Investigated Projects in District 1	Mix Type	Asphalt Binder Replacement (ABR) (%)	Allowed by Statewide BDE spec	Max. Allowable ABR (%) (Current D-1 spec)	Max. Allowable ABR (%) (Current Statewide BDE)	Difference between maximum allowable ABR of D-1 and Statewide BDE
Edens Expressway - Let 8/3/2007 (Virgin Mix)	N80 SMA	0	Yes	30	20	10
Interstate 55 between Jefferson St. and Plainfield Rd. - Let 6/15/2007 (Virgin Mix)	N80 SMA	0	Yes	30	20	10
Bishop-Ford Expy-Let 4/1/09 (5% RAS)	N80 SMA	16.7	Yes	30	20	10
IL Route 83 from Il 64 to IL 19 - let 4/26/13 (14.2% FRAP, 3.1% RAS)	N80 SMA	27.6	No	30	20	10
US 6/159th St. in Oak Forest - let 4/26/13 - (8% FRAP, 5% RAS)	N90	29.1	No	30	10	20
US 52/Jefferson St. - let 4/26/13 (N50 Binder: 30.5% FRAP, N90 surface: 2.4% RAS, 14% FRAP)	N50	23.7	Yes	40	40	0
	N90	30.0	No	30	10	20
Illinois Route 58 - Dempster st. -Let 5/15/2009 (10% FRAP)	N90	10.0	Yes	30	10	20
Green Bay Road south of Tower Rd. in Winnetka- Let 23/4/2010 (20% FRAP)	N70	14.5	Yes	30	30	0
Wolf Rd. north of Roosevelt Rd. -Let 4/26/2013 (30% FRAP)	N70	20.0	Yes	30	30	0
Harrison Rd. north of Roosevelt Rd. - Let 4/26/2013 (TRA mix, 53% FRAP, 5% RAS)	N50	57.0	No	60	-	-
Jefferson St. downtown - let 4/3/09 -(20% FRAP)	N70	18.9	Yes	30	30	0
State St. in Thornton -4/26/13 -(2.5% RAS, 17.5% recycled agg)	N70	29.8	Yes	30	30	0

Figure D-34. Summary of sections investigated in Chicago area

From field investigations, the predominant mode of pavement deterioration (distress) observed was determined to be reflective cracking, caused by traffic-induced movement of underlying Portland Cement concrete (PCC) slabs, which constituted the main pavement structure in all sections investigated. This finding was supported by a number of identifying factors, including the observance of eight well-known symptoms/markers associated with reflective cracking. Although low temperatures can accelerate this form of distress, research has shown vehicular traffic to be the primary driver of this cracking form. In comparison to reflective cracking, other distresses observed were relatively minor and infrequent, including: slippage cracking, bleeding, and segregation/raveling. Common distresses that were not observed on pavements investigated were traditional thermal cracking, block cracking, or rutting. Similar reflective cracking patterns and amounts were observed in both District 1 and District 2, which included a number of projects designed according to the statewide specification for RAP/RAS, which calls for lower levels of asphalt binder replacement through the use of RAP and/or RAS as compared to the District 1 special provision for RAP/RAS.

Fracture tests were conducted to determine the fracture resistance of pavement surfaces following the D1 Special Provision for RAP/RAS, selected control sections following the statewide specification for RAP/RAS, and selected control sections using only virgin materials (no recycled asphalt binder replacement). Fracture testing and specification levels used were those developed over the past 12 years by the University of Illinois and partnering universities, particularly under a FHWA Pooled Fund study involving a number of Midwest states including Illinois. The recommended cracking performance tests have been recently implemented by the Minnesota DOT and the Chicago Department of Transportation. Combining all mixture types and comparing ABR specifications, for the Statewide specification, 5-of-8 sections met cracking criteria (62.5%), while for the D1 Special provision, 3-of-4 sections met cracking criteria (75%). Additionally, in each traffic category considered, mixtures following the D1 special provision for RAP/RAS had a higher percentage of compliance with recommended fracture energy levels than mixtures following the Statewide specification. A sample result (high traffic level) is shown in Figure D-35.

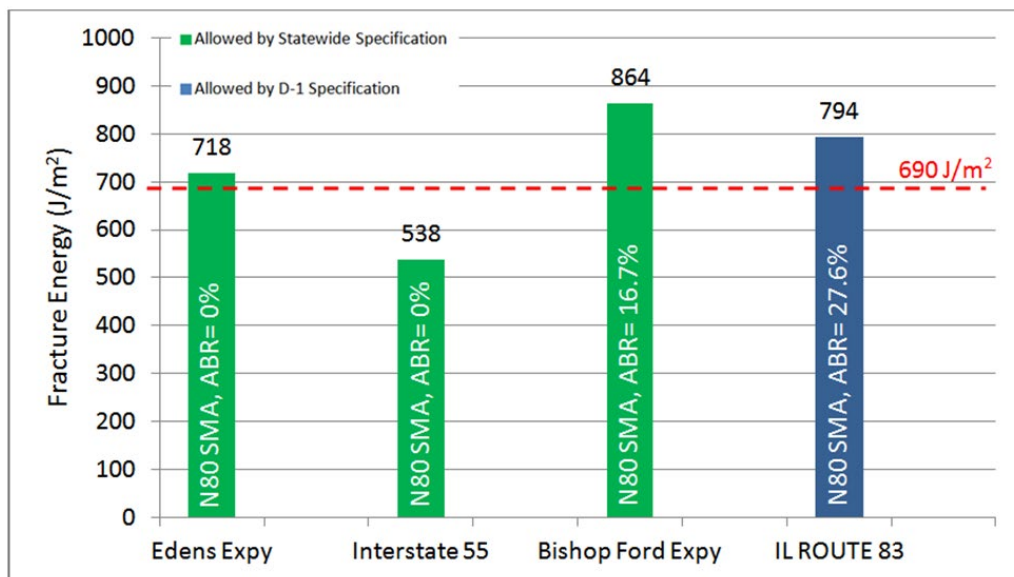


Figure D-35. Sample fracture energy results from cores tested in DC(T): High traffic SMA mixes

The lowest fracture energy of all sections tested was in fact one that adhered to the Statewide specification (lower recycling rate). Fracture testing results demonstrated that mixtures following the D1 Special Provision can be designed to exceed recommended fracture energy thresholds for thermal cracking resistance, having similar fracture energy levels as mixtures produced under the statewide specification and a better overall percentage of compliance with recommended levels when viewed in aggregate. Thus, the main driving force behind lowering ABR levels for mixes containing polymer, i.e., the dilution of the virgin polymer benefit by replacing some with recycled binder, was not supported by this investigation. Rather, the study suggested the merit of designing high ABR mixtures containing RAS using a balanced approach, i.e., supplementing volumetric design with Hamburg plus DC(T) performance testing.

D.2.4. Binder Availability Study for RAS Mixtures

Research in RAS has led to industry questions revolving around the amount of available RAS binder and the effect of RAS modification on laboratory measured performance properties. Current documentation, AASHTO PP78, developed by the Federal Highway Administration (FHWA) brings the amount of available binder into question without sufficient scientific vetting. This document states that 70 to 85 percent of the RAS asphalt binder is considered available to the mixture. As a result, the remaining percentage of RAS asphalt binder is considered aggregate without a specified gradation or specific gravity. Research conducted in academia prior to 2015 considered the asphalt binder availability from RAS in the presence of rejuvenators. For instance, research by Cooper et al. (2014) determined that up to 100% may be available with rejuvenators in a polymer modified stone matrix asphalt (SMA) mixture. However, early research did not address asphalt binder availability in dense-graded asphalt mixtures with a grade-bumped neat asphalt binder, leading to a comprehensive investigation by Buttlar (2015) as described below.

Early research begged the question: *what exactly is 'binder availability' from a mix design and performance standpoint?* Buttlar (2015) study sought to determine this through rigorous laboratory mix design and performance testing. The study carefully separated the issues of binder blending and binder availability, which are not the same. The first portion of the study investigated RAS binder availability for a dense-graded mixture with neat binder and two commonly used levels of RAS (2.5% and 5% by weight of mixture). The second part of the study evaluated RAS asphalt mixtures via low and high temperature performance tests. Although available asphalt binder is an interesting concept to debate, field performance is ultimately what mix design and associated performance testing needs to ensure. Therefore, a bracketed performance methodology was used in this study to examine high and low temperature properties of RAS modified asphalt mixtures. The only two tests with full standards from either AASHTO or ASTM to study the rutting resistance and low temperature fracture resistance of asphalt mixtures are the Hamburg wheel tracking (AASHTO T-324) and disk-shaped compact tension (DC(T)) (ASTM D-7313) tests. Therefore, they were used in this bracketed performance scheme to evaluate the suitability of the RAS mixtures, and effect of virgin and recycled binder on mixture performance.

Several implications such as asphalt gradation, volumetric property changes, and performance effects occur with the employment of a RAS availability factor. First, as stated previously, the asphalt binder which is considered as unavailable is designated as aggregate. This designation should require an asphalt gradation which could affect gradation control point requirements and dust-to-asphalt ratios. Furthermore, this unavailable RAS binder would need specific gravity definitions affecting volumetric properties. Thus, the designation of unavailable RAS as aggregate leads to mixture gradation ambiguity.

Volumetric property changes occur with the use of a RAS binder availability factor as well. Specifically, VMA decreases with the use of an availability factor which could lead to recycled mixtures falling below the VMA minimum, or stated otherwise, having a higher bar to pass. Furthermore, dust-to-binder ratios would increase leading to failing values. In order to modify the volumetric properties, additional aggregate stockpiles may be required and increase mixture

cost. These modifications may be unnecessary if performance testing can be used in addition to volumetric evaluation without an availability factor. Tests such as the Hamburg wheel tracking and DC(T) tests provide indicators of good performing mixtures in the field. Although appropriate volumetric properties are a necessity, they do not ensure performance. Laboratory tests at high and low temperatures coupled with time-tested volumetric mixture analysis form the basis for a rational, performance-based approach to the design of modern, sustainable asphalt mixtures.

The development of asphalt mixture designs in the study followed Superpave and IDOT design standards. Mixing and compaction temperatures met the IDOT standards for laboratory production for PG 58-28 asphalt binder. Bulk and maximum specific gravity measurements for compacted asphalt mixtures followed ASTM D2726 and ASTM D4021, respectively. The aggregate stockpiles used in the study were evaluated in terms of specific gravity, absorption, etc. by IDOT. The effective asphalt cement associated with binder from RAS was determined by holding all other mixture variables constant, and calculating any additional virgin asphalt binder required to meet 4% air voids in RAS mixtures as compared to virgin asphalt mixtures, if any.

To characterize the cracking behavior of the asphalt mixtures, DC(T) fracture and acoustic emission (AE) tests were performed. Generally, temperature-induced transverse (or thermal cracking) in asphalt pavements is thought to predominantly occur in a Mode I opening manner. This is supported by field observations, where evidence of fracture mode-mixity (curvilinear crack trajectory) is fairly minimal. In other words, thermal cracks are generally found to propagate perpendicular to the direction of traffic and vertically through the pavement depth. Since thermal cracks are easier to handle from an experimental and theoretical standpoint as compared to traffic-induced fatigue cracks or reflective cracks, they are directly addressed with the mode-I-type low-temperature tests selected for this study. However, it is likely that the mixture characteristics that promote higher resistance to thermal cracking will also tend to reduce other forms of pavement cracking. Wagoner et al. (2005) determined that the most viable test configuration available for asphalt mixture Mode I fracture was the DC(T) geometry. This configuration, adjusted from ASTM E-399 for metals, contains a sufficiently large fractured surface area to reduce test variation and is easily fabricated from field cores or laboratory-produced gyratory specimens

Furthermore, studies such as Dave et al. (2008) demonstrated that the DC(T) test can accurately capture the thermal cracking potential of asphalt concrete mixtures. In 2006, ASTM specified the DC(T) test as ASTM D7313. An FHWA national pooled fund study on low temperature cracking involving the participation of 10 states and over \$1M of funding to 4 universities (led by the university of Minnesota) investigated several mixture cracking performance tests (DC(T), hollow cylinder, SCB, and notched beam) and selected the DC(T) as the most effective and practical cracking performance test (Marasteanu et al., 2007, 2012). The other finalist, the SCB, was not found to relate to field cracking in the blind testing stage of the investigation (Marasteanu et al., 2012).

The Hamburg Wheel Tracking test was used to evaluate the permanent deformation characteristics of the asphalt mixtures investigated. The Hamburg test, specified in AASHTO T-

324, is conducted in a water immersed state at 50°C to induce both permanent deformation and moisture damage. A steel wheel applies a load of approximately 158 lbs. to each specimen and external linear variable differential transducers (LVDT) measure the rut depths at regular intervals during each pass of the wheel. PG 58-28 mixtures are considered satisfactory in terms of permanent deformation resistance if they can withstand 5,000 wheel passes prior to reaching a 12.5mm rut depth in order to conform with IDOT standards in central Illinois. The presence of stripping can be validated by visually examining the tested material. Finally, the maximum rut depth is defined as the rut depth present at the end of the test.

Gyratory specimens, 130 mm in height, were cut in half, and sawn along one edge to produce a flat face to produce a geometry suitable for the Hamburg test (using a the cylindrical geometry option). The heights of the two sides of each gyratory specimen were adjusted to reach equal heights to avoid dynamic loading. All Hamburg tests were conducted until either 20,000 passes was reached or 20.0 mm of rut depth was induced. Finally, all specimens were compacted to approximately 7.0% air voids to comply with AASHTO T-324 standards and four replicates per mixture were tested.

This study also employed the acoustic emission (AE) technique to obtain a relative comparison of the expected low temperature cracking threshold of RAS asphalt mixtures. This test was included as a supplement to the DC(T) testing. Mixture specimens of 150 mm diameter semicircular shape with 50 mm thickness were prepared for AE testing. This geometry was selected in order to be able to reuse specimens previously tested in the DC(T) test. AE tests were conducted in a polystyrene box containing dry ice as the coolant. Wideband AE sensors (Digital Wave, Model B1025) with a nominal frequency range of 20 kHz to 1.5 MHz were utilized to monitor and record acoustic activities of the sample during the test. High-vacuum grease was used to couple the AE sensors to the test sample. AE Signals were pre-amplified 20 dB using broad-band pre-amplifiers to reduce extraneous noise. The signals were then further amplified 21 dB (for a total of 41 dB) and filtered using a 20 kHz high-pass double-pole filter using the Fracture Wave Detector (FWD) signal condition unit. The signals were then digitized using a 16-bit analog to digital converter (ICS 645B-8) using a sampling frequency of 2 MHz and a length of 2048 points per channel per acquisition trigger. The outputs were stored for later processing using Digital Wave software (Wave-Explorer TM V7.2.6). Sample temperature was continuously recorded through using K-type thermocouple placed on the specimen surface. Typical temperature versus time cooling plot is shown in Figure 5. The average cooling rate was around 0.8°C/min.

D.2.5. Mixture Designs

The components of the asphalt mixtures included: PG 58-28 asphalt cement, RAS provided by Southwind RAS, LLC, CM16 (crushed dolomitic limestone coarse aggregate), FM20 (crushed dolomitic limestone sand), and FM02 (natural sand). The aggregates were sampled from Open Road Paving in Champaign, IL. The RAS product used in the study did not contain any reclaimed asphalt pavement (RAP) material in order to evaluate the availability of the asphalt binder provided by the RAS only. The mixture design portion of the study was separated into two parts. First, traditional shingle mixture designs were developed in order to control volumetric properties such as VMA, VFA, and air voids. In this section, the RAS asphalt binder

which is active in mixing can be estimated, as RAS mixtures are compared to the virgin asphalt mixture with respect to total asphalt content. In the second portion of the study, extracted RAS pulp and virgin asphalt binder were substituted in the RAS asphalt mixtures in lieu of non-extracted RAS. This substitution allows the amount of available asphalt binder to be determined which in turn allows a calculation of the RAS availability factor.

Traditional Shingle Mixture Designs

Mixing and compacting of asphalt mixture specimens occurred at a temperature of 150°C in accordance with IDOT specifications. All aggregate and asphalt cement samples were heated for approximately 4 hours prior to mixing to ensure temperature consistency. The RAS present in each mixture sample was thoroughly mixed with virgin aggregate prior to placement in the oven to avoid RAS clumping in the mixture. In order to develop comparable mixtures, the VMA, VFA, and P_{be} were held approximately equal. The final mixture design gradations are shown below in Table D-9.

Table D-9. Mixture design gradations

Sieve	Virgin Mix	2.5% RAS Mix	5.0% RAS Mix
25.0 mm	100.0	100.0	100.0
19.0 mm	100.0	100.0	100.0
12.5 mm	100.0	100.0	100.0
9.5 mm	99.2	99.3	99.4
4.75 mm	72.9	74.6	76.3
2.36 mm	45.9	47.9	50.3
1.18 mm	27.7	29.2	31.5
0.60 mm	16.7	17.9	20.1
0.30 mm	9.4	10.9	13.4
0.15 mm	6.2	7.6	10.1
0.075 mm	5.3	6.4	8.5

The mixture designs in this study met the 3 million equivalent single axle loads requirement with 90 design gyrations. The mixtures contained 0.0, 2.5, and 5.0% RAS to evaluate those with approximately 0, 10, and 20% asphalt binder replacement (ABR). The volumetric properties of the asphalt mixtures (assuming 100% blending of the RAS asphalt binder) are shown in Table D-10. These results demonstrate that the total asphalt content at 4.0% air voids remains equal while holding the VMA, VFA, and P_{be} approximately constant. Therefore, the asphalt binder provided by the RAS was approximately 100% active in this case. Complete activity of this binder demonstrates that the material may be completely available to act as an asphalt binder in mixing and material performance. In order to evaluate availability, extracted RAS pulp and 100% virgin asphalt binder were substituted for the non-extracted RAS product. The discussion of the availability of RAS asphalt binder is provided in the substitution portion of the study.

The primary issue found in the volumetric results is the dust (percent passing the #200 sieve) to asphalt ratio. In particular, this value slightly exceeds the Superpave and IDOT criteria. However, in order to maintain VMA, the dust to effective asphalt ratio was allowed to reach above the maximum limit of 1.6. According to AASHTO, dust-to-effective binder ratio specifications are normally 0.6 – 1.2, but a ratio of up to 1.6 may be used at an agency’s discretion. Illinois uses a max dust-to-total-binder ratio of 1.0 in design and a range of 0.6 – 1.2 during mix production. This particular issue with dust to effective asphalt is not believed to be a significant issue with 5.0% RAS mixtures. The high percentage of dust existing in this research study tended to reduce VMA such that it stayed approximately equal to 15.3%. In practice, future applications of 5.0% RAS mixtures in the field would allow VMA to increase and hold the ratio of dust to effective asphalt below the maximum threshold.

Table D-10. Mixture volumetrics in RAS availability study

Volumetric Property	Virgin Mixture	2.5% RAS Mixture	5.0% RAS Mixture
Total Asphalt Content (%)	6.6	6.6	6.6
ABR (%)	0.0	10.6	21.2
Air Voids (%)	4.0	4.0	4.0
VMA (%)	15.2	15.3	15.2
VFA (%)	74.0	73.8	73.7
Effective Asphalt Content (%)	4.9	4.9	4.9
Dust/Total AC	0.8	1.0	1.3
Dust/Effective AC	1.1	1.3	1.7

Pulp Substitution Mixture Designs

This portion of the study substituted RAS pulp and PG 58-28 virgin asphalt binder for non-extracted RAS to evaluate RAS binder availability. Mixture proportions of virgin aggregate remained constant in comparison with the traditional RAS mixture designs. This consistency in aggregate proportioning allowed for appropriate volumetric comparisons between all mixtures. The total asphalt content was optimized with the RAS pulp substitution. The difference between the total asphalt contents for the pulp substitution and traditional RAS mixtures indicate the availability of the RAS asphalt binder. The volumetric properties of the mixtures are shown below in Tables D-11 and D-12.

Results indicate the RAS availability factor of the mixtures in this study is approximately 100%.

In Tables D-11 and D-12, the total asphalt contents for the RAS and RAS pulp mixtures remained equal or adjusted by 0.1% asphalt binder. Thus, all RAS binder was active and available to act as an asphalt binder in the mixtures. As shown in Table D-12, the RAS pulp mixture total asphalt content was 0.1% higher than the traditional RAS mixture. However, the VMA in the RAS pulp mixture increased slightly in this case which likely led to increase in asphalt content from 6.6 to 6.7%. Therefore, if the VMA had remained unchanged, the total asphalt content would likely fall to 6.6% which would yield equal asphalt contents for the 5.0% RAS and 5.0% RAS pulp mixtures.

Table D-11. 2.5% RAS pulp mixture design

Volumetric Property	Virgin Mixture	2.5% RAS Mixture	2.5% RAS Pulp Mixture
Total Asphalt Content (%)	6.6	6.6	6.6
Air Voids (%)	4.0	4.0	4.0
VMA (%)	15.2	15.3	15.3
VFA (%)	74.0	73.8	73.7
Effective Asphalt Content (%)	4.9	4.9	4.9
Dust/Total AC	0.8	1.0	1.0
Dust/Effective AC	1.1	1.3	1.3

Table D-12. 5.0% RAS pulp mixture design

Volumetric Property	Virgin Mixture	5.0% RAS Mixture	5.0% RAS Pulp Mixture
Total Asphalt Content (%)	6.6	6.6	6.7
Air Voids (%)	4.0	4.0	4.0
VMA (%)	15.2	15.2	15.4
VFA (%)	74.0	73.7	73.2
Effective Asphalt Content (%)	4.9	4.9	4.9
Dust/Total AC	0.8	1.3	1.3
Dust/Effective AC	1.1	1.7	1.7

It was clearly found that the 100% RAS availability factor demonstrated in this study does not agree with the range of 70-85% recommended in AASHTO PP78-14. This value is also higher than that presented in the research findings of Cooper et al. (2014). The current study considers a dense graded asphalt mixture with a softer virgin asphalt grade. The results found by Cooper et al. (2014) considered a polymer modified SMA and a different RAS sample which may lead to differing results. That notwithstanding, the results in this case demonstrate that 100% RAS availability is possible and the adjusted availability value used AASHTO PP78 may not be appropriate. Quality design practices can lead to mixtures with very high recycled binder availability. However, performance testing is needed to determine if a mixture, when designed with standard volumetric design procedures, can withstand mechanical and environmental loads.

It should also be noted that binder availability is not the same as binder blending. A number of previous studies have shown that incomplete blending of virgin and recycled binder may occur in both RAP and RAS mixtures. However, that finding alone does not guarantee that recycled binder is ‘unavailable’ from the standpoint of both mixture volumetric design and mixture performance. After all, a key contribution of binder from a compaction and mixture volumetric standpoint is its lubricating effect, which is responsible for the concave upward VMA versus asphalt content curve. Although aggregate mass remains constant, additional binder (up to a point) leads to additional densification of the aggregate structure via lubrication. Thus, even if

incompletely blended, the recycled and virgin binder may in fact work together to lead to the same mixing and volumetric characteristics in the mixture (and thus, 100% available). Thus, binder availability is a mixture volumetric issue, not a binder blending issue, and should be evaluated accordingly.

So far, the current study has demonstrated that 100% RAS binder availability is possible, when a properly designed and carefully controlled laboratory study is carried out...even when incomplete binder blending is likely present in the mixture. Next, the study sets out to investigate the performance side of the equation. In other words, can recycled mixtures, even with incomplete blending, be designed assuming 100% binder availability (and therefore using the time-tested mixture volumetric approach and not PP78-14) and still lead to good mixture performance?

D.2.6. Performance Testing of RAS-Availability Study Mixes

Performance testing of the mixtures in this study evaluated the high and low temperature performance of RAS mixtures with respect to reference asphalt mixtures. As stated previously, the mixtures were evaluated at high and low temperatures to consider bracketed performance. The mixtures in this portion of the study included PG 64-22 and PG 58-28 reference mixtures, 2.5% and 5.0% RAS mixtures, and 2.5% and 5.0% RAS pulp mixtures. Unlike the mixture design portion of the study, the 2.5 and 5.0% RAS pulp mixtures contained a mixed virgin and extracted RAS asphalt binder with 10.6 and 21.2% ABR, respectively. The two reference mixtures were used in this study to examine the effects of binder grade bumping. The three asphalt mixtures containing PG 58-28 and a volumetrically similar PG 64-22 virgin asphalt mixture were compared using the Hamburg wheel tracking, DC(T), and AE tests. Additionally, the mixed asphalt binder mixtures were tested using the Hamburg and DC(T) tests only.

Hamburg Rut Test Results

The Hamburg test results (Table D-13) determined that the virgin asphalt mixtures did not meet the Hamburg testing requirement developed by IDOT. On the other hand, the RAS mixtures both exceeded the minimum requirement of 5,000 wheel passes prior to reaching 12.5 mm (1/2") rut depth. This result demonstrated that aggregates with lacking strength coupled with a softer virgin asphalt binder benefited from the inclusion of RAS. The improvement in Hamburg wheel tracking performance from 2.5% RAS to 5.0% RAS showed that an increase in ABR from 10.6% to 21.2% significantly improved the bulk stiffness properties of the mixture at high testing temperatures. The 2.5% and 5.0% RAS mixed binder Hamburg results demonstrate the increased stiffness created by mixing virgin and extracted RAS binder. Research by Mogawer et al. (2013) found that complex modulus of traditional RAP-RAS mixtures yielded a lesser modulus as compared to a fully mixed RAP-RAS binder mixture. This result would likely manifest itself in less Hamburg rut depth for fully mixed binder mixtures which agreed with the findings of the current study. Although mixed asphalt binders yielded improved rutting performance, low temperature fracture properties may be negatively affected.

Table D-13. Hamburg test results

Mixture	No. of Passes to Failure (12.5mm)	Required Passes	Pass/Fail
<i>Virgin PG 58-28</i>	3030	5000	Fail
<i>Virgin PG 64-22</i>	5860	7500	Fail
<i>2.5% RAS PG 58-28</i>	5110	5000	Pass
<i>5.0% RAS PG 58-28</i>	14430	5000	Pass
<i>2.5% RAS Mixed Binder</i>	7370	5000	Pass
<i>5.0% RAS Mixed Binder</i>	15850	5000	Pass

DC(T) Fracture Test Results

The DC(T) results are shown in Figure D-36. The PG 58-28 virgin asphalt binder was used in this study to offset the potential stiffening provided by the RAS. The stiffening effect of RAS helped improve Hamburg performance, but an overly stiff asphalt mixture will yield poor DC(T) and AE performance. In this study, it was found that the use of PG 58-28 and two levels of RAS did not lead to poor performance in either low temperature test. As shown, all three PG 58-28 mixtures met the 460 J/m² threshold developed during the FHWA Pooled Fund Low Temperature Cracking study partially completed at the University of Illinois. Furthermore, the RAS mixtures outperformed the PG 64-22 virgin asphalt mixture. Therefore, the presence of RAS did not lead to low temperature cracking susceptible mixtures. In fact, the only mixtures that met the bracketed performance requirements were the 2.5% and 5.0% RAS mixtures.

Acoustic Emission Asphalt Mixture Embrittlement Test Results

The AE mixture embrittlement temperature test results are plotted in Figure D-37. The AE test results demonstrate similar trends to the DC(T) test results. Mixture embrittlement temperatures provide an indication of the temperature at which micro-cracking in the mixture begins. In this study, all PG 58-28 mixtures with and without RAS outperformed the PG 64-22 mixture. Therefore, the use of grade bumping in concert with 2.5 and 5.0% RAS led to improved low temperature micro-cracking performance.

Additional DC(T) Tests Performed on Manually Mixed, Fully-Blended RAS Mixtures

Additional DC(T) tests (shown with red bars) were completed on mixtures containing RAS pulp and mixed virgin and extracted RAS binders. In both RAS mixtures, the binder mixing led to decreases in fracture energy, but said fracture energies did not fall outside the statistical range of the DC(T) results for the traditionally mixed samples. Furthermore, the mixed binder mixtures exhibited improved DC(T) fracture energy as compared to the reference PG 64-22 mixture. Thus, in the worst case scenario in which the asphalt binders complete mix, grade bumping in this case allowed the mixtures to meet the bracketed performance requirements.

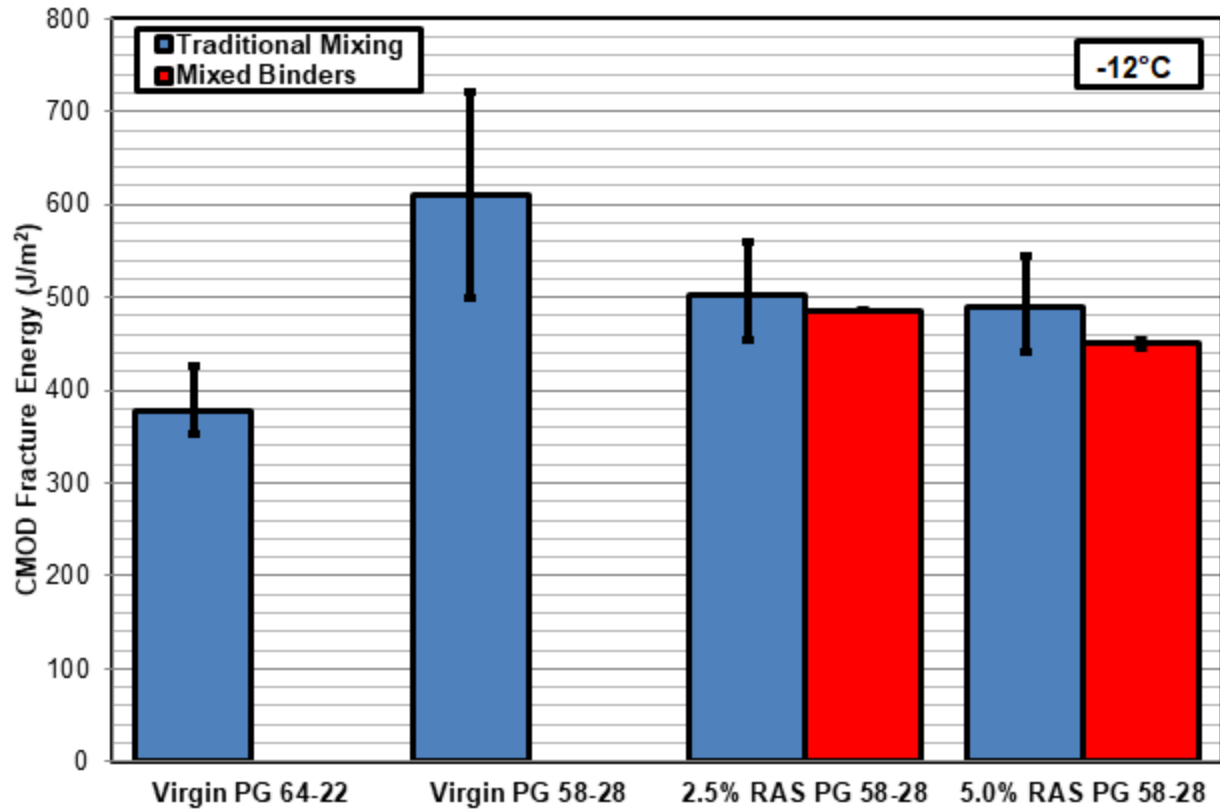


Figure D-36. DC(T) test results at -12°C

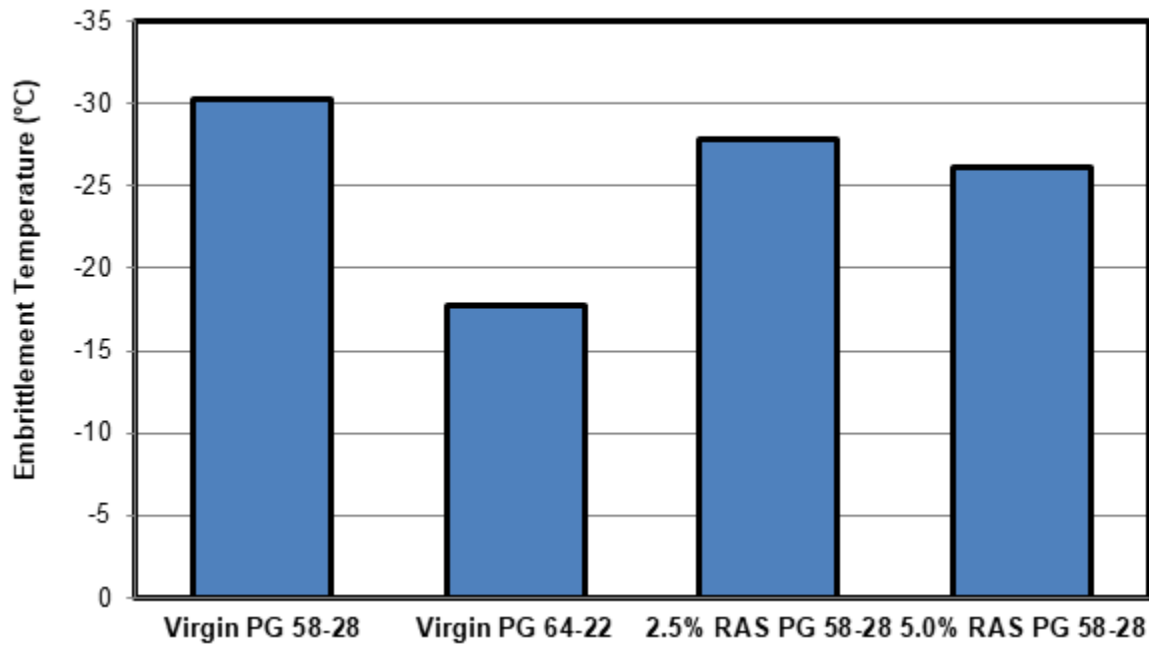


Figure D-37. Acoustic emission embrittlement temperature test results

Hamburg-DC(T) Plot and Findings

Very recently, the concept of plotting performance data in a ‘performance space’ diagram was introduced (ICAT, FHWA Mixtures ETG, Buttlar, April 2015). When plotting Hamburg rut depths (on a reverse, arithmetic scale, y-axis) versus DC(T) fracture energy (arithmetic scale, x-axis), a two-dimensional view of high/low temperature mixture performance can be conveniently viewed. Moreover, adjustments/change to mix composition and design can be readily observed in the context of change in high/low temperature performance using this plot. Figures D-38 through D-40 present the ‘Hamburg-DC(T)’ plots, both conceptually, and for mixtures evaluated in this study. As shown in Figure D-38, conceptually, there are 4 corners to the plot with performance implications:

- Lower-Right: High Rutting Potential, High Cracking Potential – not recommended
- Upper-Left: Low Rutting Potential, High Cracking Potential – not recommended for pavement surfaces
- Lower-Right: High Rutting Potential, Low Cracking Potential – not recommended for pavement surfaces
- Upper-Right: Good Performance Zone, suitable for all mixtures, especially surface mixtures

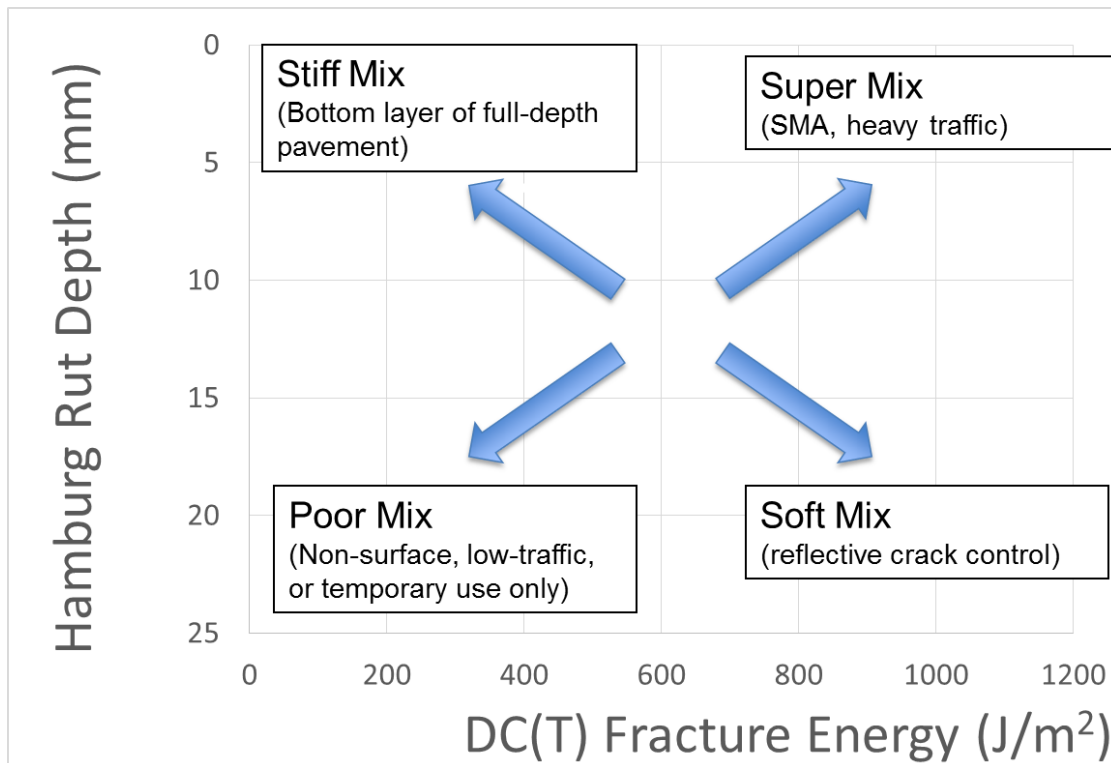


Figure D-38. Hamburg-DC(T) plot concept and Performance zones

Figure D-39 adds typical Hamburg and DC(T) performance limits to the plot, along with convenient gradient shading (deeper red for more rutting potential, deeper blue for more cracking potential). Since the DC(T) cracking test is usually accompanied with three levels of fracture energy thresholds based on traffic (400, 460, and 690 J/m² for low, med, and high traffic, respectively), these three zones are identified on the plot. For low traffic, data plotting in all three upper-right zones are acceptable. For medium traffic, a higher DC(T) fracture energy threshold is required; thus, only the two upper-right-most zones are allowable. For high traffic, only the upper-right-most zone is acceptable.

The current understanding of the effect of binder grade change on mixture performance in the Hamburg-DC(T) space (Buttlar et al., AAPT 2016) suggests that the swapping of straight-run binder grades does not always give the designer much mixture improvement, as the movement of the mix is along a ‘performance-tradeoff’ axis (upper-left to lower-right, or vice-versa). For a weak aggregate system, this might mean that a soft mix failing the Hamburg (in the lower-right region of the plot), will be difficult to ‘save’ by simply substituting a harder virgin binder grade. Instead, a combination of recycled materials and polymer-modified binder may be a better solution. Polymer modified binder tends to rotate the arrows on the plot away from the performance tradeoff axis, and toward the desired upper-right portion of the Hamburg-DC(T) space.

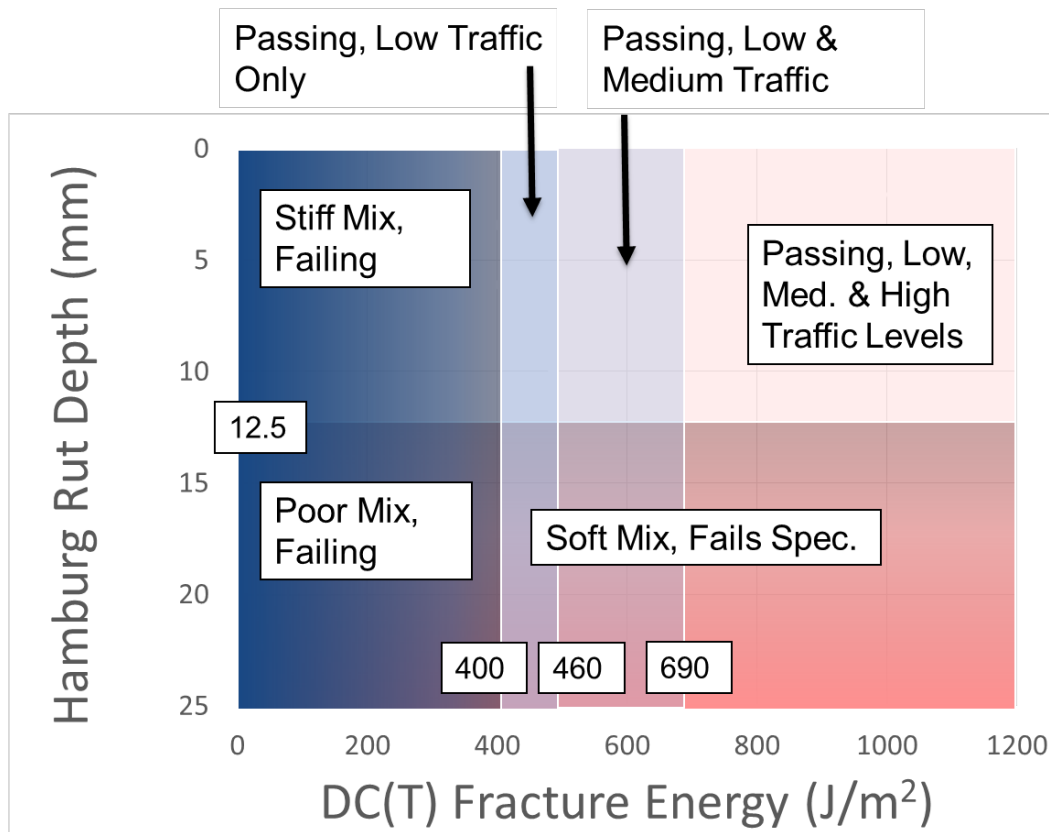


Figure D-39. Hamburg-DC(T) plot with typical specification limits superimposed

Figure D-40 presents four of the study mixtures as plotted in the Hamburg-DC(T) space. For the purposes of uniform comparison, the rutting depth plotted for all Hamburg results was taken at 5000 cycles, when in fact, the Hamburg criterion in Illinois is based on binder grade (thus, the PG 64-22 could have been plotted using the 7500 cycles data point, which would have shifted that data point to the lower-left corner of the plot). But for the purposes of evaluating relative movement in the Hamburg-DC(T) space as a function of change in binder and RAS level, the 5000-pass result was used. In addition, the DC(T) test temperature was selected to be -12°C for all data points plotted; again, for the purposes of a uniform comparison. Based on this analysis, the following observations were made:

- Swapping PG 58-28 binder for PG 64-22 binder results in a movement of the mixture along the ‘performance tradeoff’ diagonal, or axis. In this case, where a fairly soft limestone mixture was used, the mixture moves from the ‘failing in rutting’ region to the ‘failing in cracking’ region.

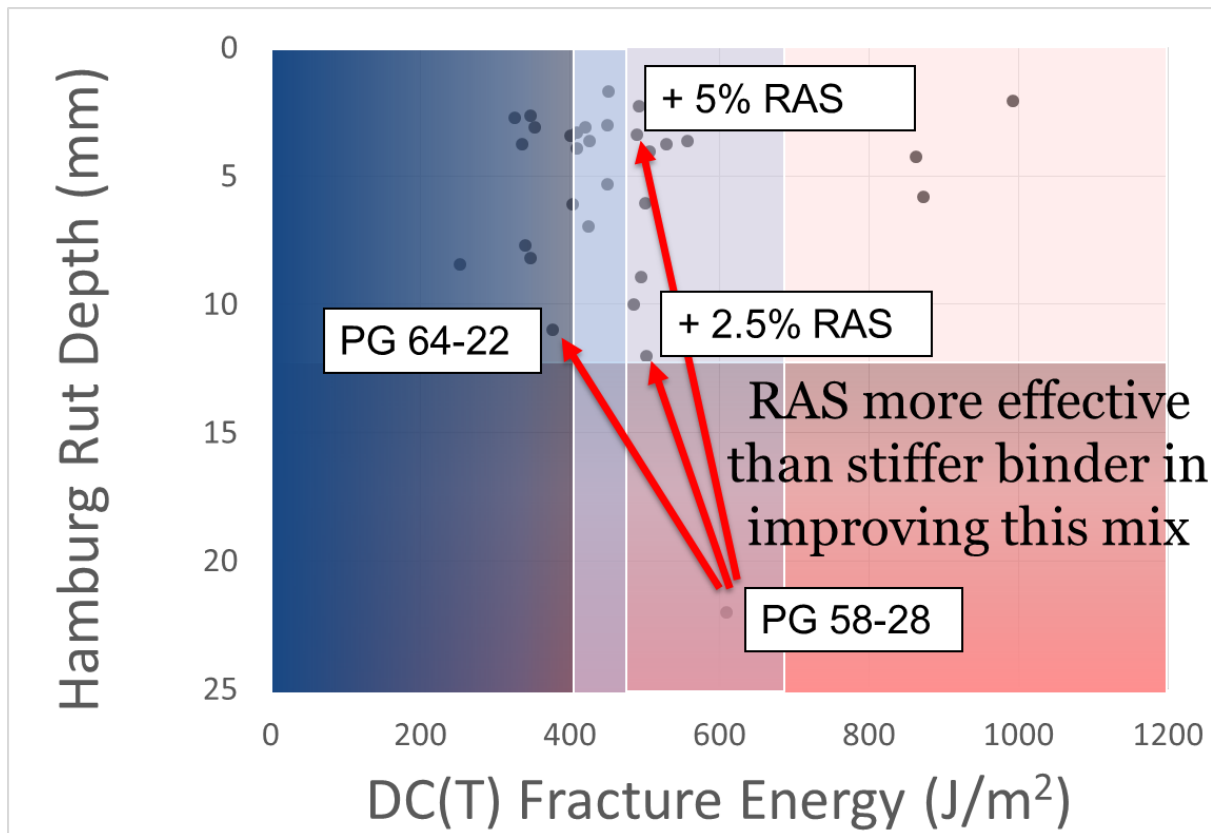


Figure D-40. Hamburg DC(T) Plot showing typically Illinois’ mixture data, along with 4 data points collected in this study (located at the beginning and ends of red arrows)

Note: for a uniform comparison in the Hamburg-DC(T) space, Hamburg rut depths plotted for all 4 mixtures at 5000 passes on this plot.

- For the 2.5% RAS mixture, the mixture shifts just inside the passing region for Low and Medium traffic levels, for both Hamburg and DC(T) specifications. Thus, the 2.5% RAS mix has better overall performance than either the PG 58-28 or PG 64-22 mix.
- For the 5.0% RAS mixture, the mixture easily passes the Hamburg spec, and is still passing the DC(T) low and medium traffic level specs. Thus, the 5.0% RAS mix has better overall performance than either the PG 58-28 or PG 64-22 mix.
- The trajectory of mixture alteration in the Hamburg-DC(T) space relative to the trajectory associated with virgin binder swapping is slightly off the performance-tradeoff axis. This suggests that the RAS is acting as a slightly modified material, perhaps due to the heterogeneity of the resulting mix (composite materials are known for their strength), and perhaps due to the presence of fibers in the pulp material or the hard aggregate added).
- In reality, the designer would not stop here. There would be an opportunity to continue to push the mixture further into the upper-right corner of the Hamburg-DC(T) space if more performance was desired. This could be done by using a polymer-modified binder grade, and likely using RAP in combination with RAS to maximize sustainability potential. Also, starting with a stronger aggregate system would likewise improve the mix's position in the Hamburg-DC(T) space.

D.2.5. Higher ABR Mixes and use of Rejuvenators in Balanced Mix Design

Recent studies have, through careful mixture analysis and performance design, demonstrated the ability of higher asphalt binder replacement (ABR) mixtures to meet design and performance requirements. In particular, mixtures with proper combinations of reclaimed asphalt pavement (RAP) and recycled asphalt shingles (RAS), along with a suitably soft and often modified binder, have shown great promise in promoting high mixture sustainability, while meeting stringent rutting and cracking performance tests. A study by Buttlar (2005b) was conducted to a) to demonstrate the ability to produce high ABR mixes that can perform as well or better than mixes that are currently allowed by IDOT and CDOT specifications, and; b) to promote a balanced, performance-testing-guided mix design approach in Illinois as an option to contractors who are willing to go the extra mile to design mixtures with higher ABR levels using stringent high *and* low temperature performance tests. The main hypothesis of the study can be summarized as follows. With the equipment, test methods, and technology that are available today, it is feasible for IDOT or other agencies to allow contractors to produce higher ABR mixes, provided that they can demonstrate through balanced performance testing (rutting and cracking tests), that their mixtures can perform well in the field?

The study also considered the performance effects of soft base binders, warm-mix agents, *rejuvenating agents*, and combinations thereof. High temperature mixture performance was evaluated using the Hamburg wheel track device, while low temperature and cracking

performance was evaluated using fracture energy results obtained from the disk-shaped compact tension test (DC(T)) and flexibility index results from the new protocols developed by the Illinois Center for Transportation for the semi-circular bend test (SCB).

Experimental Design and Field Test Sections

Two mixture designs, an N30 LC surface mix (reference low ESAL mix, currently allowed by CDOT) and N70 CHI surface mix (higher ABR mix designed with proposed balanced performance testing approach), were investigated. Each mixture was produced with two different binder systems: PG 46-34 binder with MWV Evotherm additive, and PG 58-28 binder with MWV Evoflex additive. The two binders and their respective additives were selected to evaluate two methods to arrive at higher ABR mixes with a suitably soft virgin binder. In the case of the first binder system, a soft base binder grade (PG 46-34) along with a warm-mix additive (Evotherm - to reduce mixture production temperature and hence to limit short-term aging) was used. In the second system, a slightly harder base binder grade (PG 58-28) was used along with a rejuvenating additive (Evoflex). The Evoflex rejuvenator is designed to be used with recycled materials as a means to soften the base binder grade and to promote blending of the recycled binder with the virgin binder. This comparison was deemed useful, since having more virgin binder system options might provide additional leeway to the designer and help improve mixture economy and/or durability.

Mixtures were paved at a materials recycling facility operated by Reliable Asphalt Corporation, located at 4613 W Grand Ave Chicago, Illinois. The approximate lengths of the test sections were:

- N30 LC (with Evotherm) = 450 LF
- N70 CHI (with Evotherm) = 610 LF
- N30 LC (with Evoflex) = 710 LF
- N70 CHI (with Evoflex) = 590 LF

The lifts placed during paving in May of 2015 (Figure D-41) consisted of a 3 inch surface course (this study) placed on 3 inch binder course (not tested herein). Cores of 150-mm diameter were taken and used for mixture performance tests, as outlined in this report. Mix designs were carried out by S.T.A.T.E. Testing, LLC, with results presented in Appendix A of the report by Buttlar (2015b). The N30 LC mixture was designed at 3.0% air voids at the design gyration level, with an optimum binder content of 6.8% and an ABR level of 66.5%. The N70 CHI mixture, designed as a new, higher ABR alternative for medium-traffic routes in the Chicagoland area, was designed at 3.5% air voids, with a total asphalt content of 5.9% and an ABR level of 50%.



Figure D-41. Paving of the Grand Avenue test sections in May, 2015

Testing Methods

To characterize the cracking behavior of the asphalt mixtures, DC(T) fracture and semi-circular bend (IL-SCB) tests were performed. For high temperature performance characterization, Hamburg wheel track testing was conducted. Extraction, recovery and Superpave PG binder testing and grading of the recovered binder was also performed.

Generally, temperature-induced transverse cracking (or thermal cracking) in asphalt pavements is thought to predominantly occur in a Mode I opening manner. This is supported by field observations, where evidence of fracture mode-mixity (curvilinear crack trajectory) is fairly minimal. In other words, thermal cracks are generally found to propagate perpendicular to the direction of traffic and vertically through the pavement depth. Since thermal cracks are easier to handle from an experimental and theoretical standpoint as compared to traffic-induced fatigue cracks or reflective cracks, they are directly addressed with the mode-I-type low-temperature tests selected for this study. However, it is likely that the mixture characteristics that promote higher resistance to thermal cracking will also tend to reduce other forms of pavement cracking. Wagoner et al. (2005) determined that the most viable test configuration available for asphalt mixture Mode I fracture was the DC(T) geometry. This configuration, adjusted from ASTM E-399 for metals, contains a sufficiently large fractured surface area to reduce test variation and is easily fabricated from field cores or laboratory-produced gyratory specimens. Furthermore, studies such as Dave et al. (2008) demonstrated that the DC(T) test can accurately capture the thermal cracking potential of asphalt concrete mixtures. In 2006, ASTM specified the DC(T) test as ASTM D7313. An FHWA national pooled fund study on low temperature cracking involving the participation of 10 states and over \$1M of funding to 4 universities (led by the university of Minnesota) investigated several mixture cracking performance tests (DC(T), hollow

cylinder, SCB, and notched beam) and selected the DC(T) as the most effective and practical cracking performance test (Marasteanu et al., 2007, 2012). The other finalist, the SCB, was not found to relate to field thermal cracking in the blind testing stage of the investigation (Marasteanu et al., 2012).

Since the mid 1980's, the semi-circular bend test (SCB) has been developed by several research groups, primarily in an attempt to achieve a very low-cost performance test on a very compact specimen geometry. Despite its lack of correlation to low temperature cracking when evaluating the fracture energy obtained from the test, the test has been recently reconsidered as a low-cost test method to evaluate other forms of pavement distress. Research is still in progress with the Illinois modified IL-SCB, with significant correlation to field performance and test standardization yet to occur. In this test, a 150mm diameter puck-shaped specimen is halved and notched, to create semicircular, notched test specimens. The specimen is placed in a standard, 3-point bending loading fixture (roller supports at specimen ends, blunted loading head applied at center span). Testing was conducted using an Instron closed-loop, servohydraulic test frame with a 10 kN load cell. Recent adaptations of the test developed at the Illinois Center for Transportation call for a further simplification of the test, requiring only a constant rate of ram displacement for loading and testing at room temperature. Although the test has never been standardized in the US, a draft standard was recently submitted to AASHTO as TP105-XX (2015). The new parameter proposed from the IL-SCB test is a flexibility index; an empirical index involving the quotient of the fracture energy at room temperature obtained at a very fast loading rate (specimen fails in ~5 seconds) and the slope of a selected portion of the post-peak response curve. See Appendix B of Buttlar (2015b) for more details.

The Hamburg Wheel Tracking test was used to evaluate the permanent deformation characteristics of the asphalt mixtures investigated. PG 58-28 mixtures were considered satisfactory in terms of permanent deformation resistance if they can withstand 10,000 wheel passes prior to reaching a 12.5mm rut depth in order to conform with IDOT standards in medium traffic designs (such as the N70 mixture). The presence of stripping can be validated by visually examining the tested material. Field core specimens were sawn to produce a flat face and thickness suitable for the Hamburg test (using the cylindrical geometry option). All Hamburg tests were conducted until either 20,000 passes was reached or 20.0 mm of rut depth was induced.

Extraction, recovery, and Superpave PG binder testing was also conducted to determine the binder performance grades of the binder systems used in the study. ASTM D2172 was followed for the extraction of binders from field cores, and ASTM D7906 was followed for the recovery of binders from the extracted solvent/asphalt blend. The requisite Superpave PG binder tests were performed for grading purposes (ASTM D6373), including the dynamic shear rheometer (DSR), as specified in ASTM D7175, and bending beam rheometer (BBR), as specified in ASTM D6648. Although imperfect blending is thought to occur in practice, the fully-blended binder rheology and PG grade of the recycled mixtures provides a useful baseline to determine the grade of the binder in the recycled mixture if perfect blending were to occur. Some believe that it is a conservative approach to require the PG grade of the extracted and recovered, perfectly blended binder to be equivalent or superior to the plan PG grade for the designed mixture.

D.2.6. Performance Testing Results

Hamburg Rut Test Results

The Hamburg test results are provided in Figure D-42. As can be seen, all mixtures exceeded 10,000 passes to a rut depth of 12.5mm. In general, the 'Flex' mixtures, that is, the mixes with the harder base binder (PG 58-28) plus rejuvenator, performed better in the Hamburg than the softer PG 46-34 binder with Evothem, or 'Evo' mixtures. The lower rut depths in the N30 LC mixtures is probably due to the use of the same virgin binder systems, along with the higher ABR levels in the N30 mixes (66.5% vs. 50%).

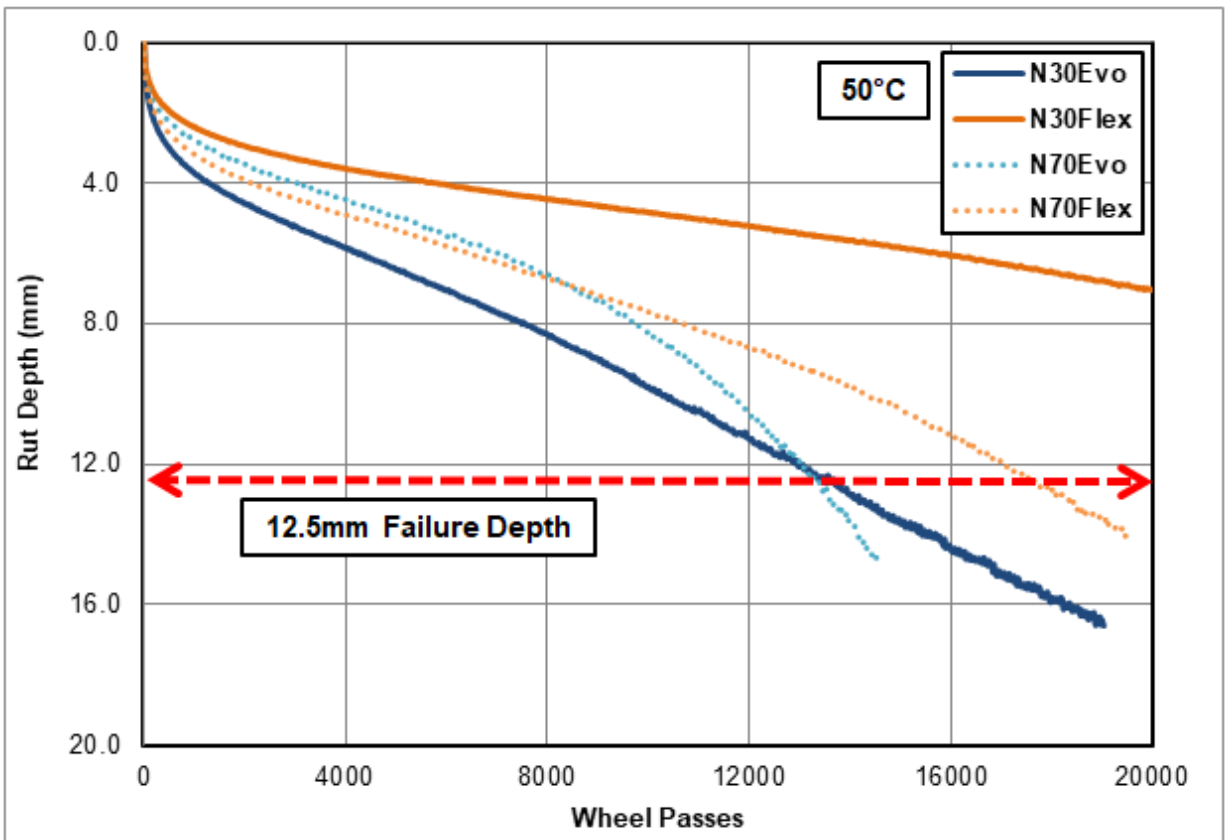


Figure D-42. Hamburg test results

DC(T) Fracture Test Results

The DC(T) results are shown in Table D-38 and Figure D-43. As can be seen, all four mixtures passed DC(T) specification requirements for CDOT. Each of the four mixtures possessed a fracture energy, G_f , of greater than 400 J/m^2 , which is the minimum CDOT requirement for medium traffic routes. Consistent with the Hamburg results, the N70 mixtures were slightly more ductile as compared to the higher ABR N30 mixes. This resulted in higher fracture energies for the N70 mixtures. If the higher DC(T) requirement were imposed for the N70 mixtures (typically 460 J/m^2 is used by other agencies for medium traffic), then the N70EVO mix would easily pass the specification, while the N70FLEX mix would require a slight mix

design or material adjustment to meet the requirement (softer base binder, higher dosage rate of rejuvenator, etc.).

Table D-14. DC(T) Grand Ave. mixture results

Specimen ID	Peak Load (kN)	Avg. Peak Load (kN)	Fracture Energy, G_f (J/m ²)	Average Fracture Energy, G_f (J/m ²)	COV (%)
N30EVO	2.577	2.701	385.6	412.8	9.8
N30EVO	2.587	2.701	393.6	412.8	9.8
N30EVO	2.938	2.701	459.1	412.8	9.8
N30FLEX	2.827	2.986	361.5	404.1	9.1
N30FLEX	3.090	2.986	427.0	404.1	9.1
N30FLEX	3.040	2.986	423.9	404.1	9.1
N70EVO	2.711	2.523	538.3	521.8	9.6
N70EVO	2.516	2.523	561.8	521.8	9.6
N70EVO	2.341	2.523	465.4	521.8	9.6
N70FLEX	2.313	2.471	368.6	442.2	16.7
N70FLEX	2.510	2.471	516.3	442.2	16.7
N70FLEX	2.589	2.471	441.7	442.2	16.7

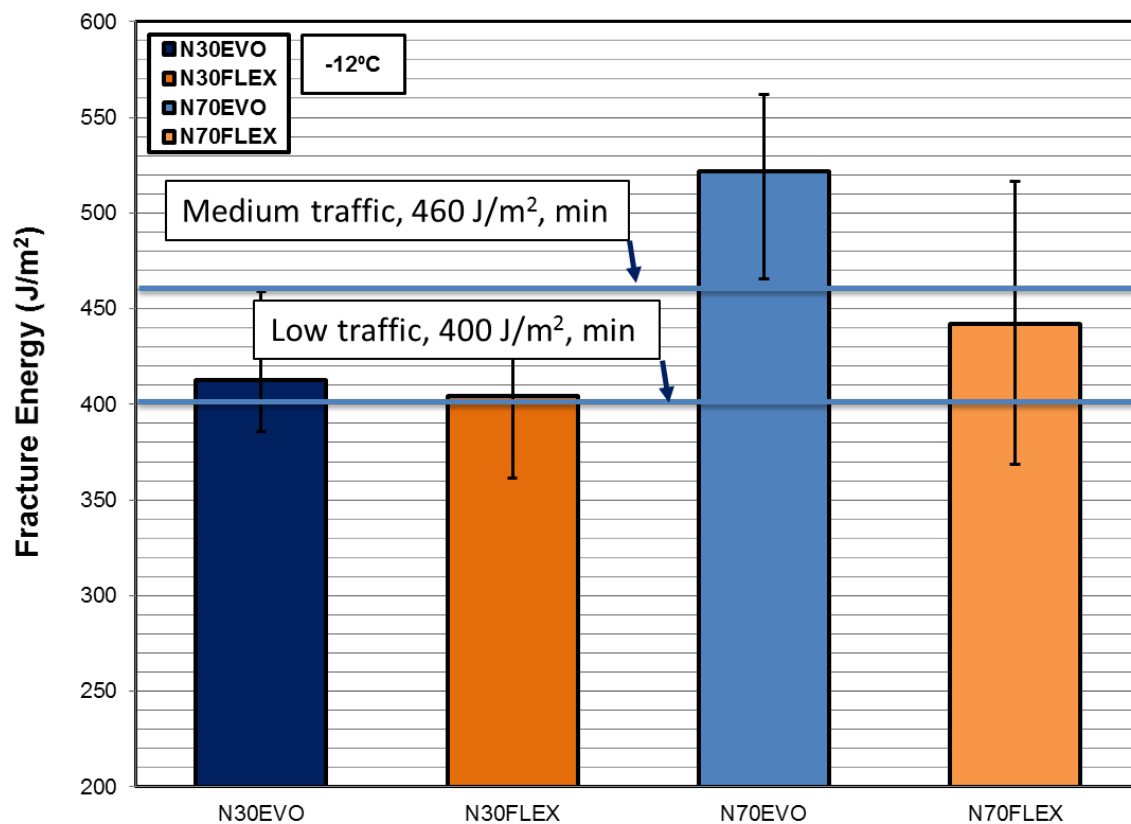


Figure D-43. DC(T) test results

I-FIT SCB Results and Comparison to DC(T)

The main parameter obtained from this test is the ‘flexibility index,’ which was designed to be linked to pavement cracking susceptibility. Preliminary research has suggested values of greater than 4 for passing, between 2 and 4 for borderline, and lower than 2 for failing. As this is not a low temperature test (it is run at room temperature, thus, at an intermediate temperature), the meaning of pavement cracking can be inferred as being potentially related to fatigue cracking or reflective cracking, pending confirmation in future research.

A comparison of the DC(T) and SCB results are shown in Tables D-15 and D-16. While the DC(T) qualifies the four study mixtures as passing in thermal crack resistance, the SCB test produced only a single passing result. This might suggest that while the four study mixtures are resistant to thermal and block cracking (as per the DC(T) results), they may be questionable from the standpoint of traditional fatigue if used in a conventional flexible pavement structure or full-depth pavement. The results may also suggest the mixes are susceptible to reflective cracking. The highest result, easily passing the suggested flexibility index requirement, was obtained for the N70 EVO mix. This mixture also displayed the best repeatability. The other N70FLEX mixture, was characterized in the ‘borderline’ range.

Table D-15. Summary DC(T) and SCB results

Specimen ID	DC(T) Fracture Energy (J/m²)	DC(T) Thermal Cracking Interpretation	SCB Flexibility Index Result	SCB Cracking Intermediate Temperature Interpretation
N30EVO	413	Passing	3.4	Borderline
N30FLEX	404	Passing	1.2	Failing
N70EVO	522	Passing	6.2	Passing
N70FLEX	442	Passing	2.8	Borderline

Additional SCB results are shown in Table D-17 and Figure D-44. Based on these results, the following observations are made:

- The DC(T), which has been extensively correlated to low temperature cracking field performance, showed all four sections to be thermal cracking resistant. For the N70 mixtures, the ‘Flex’ mixture could be considered as either passing or borderline, since some agencies use a threshold value of 400, while others use 460 J/m² for the intermediate traffic level.
- The SCB predicted only one passing mixture, two borderline, and one failing.
- The test repeatability for the two SCB tests associated with the N30 mixtures were in an unacceptable range of COV, 30% and 56% for the EVO and FLEX mixtures (33% COV on average), respectively. Generally, COV values 20% or lower are considered to be acceptable.
- The average COV for all 4 SCB tests was 26.3%, while the DC(T) average COV was 11.8%.
- In general, it is difficult to assess the meaning of the SCB results. The lack of existing correlation to field cracking, the difficulty in assessing the cause of reflective cracking (with field data sets containing the potential for reflective cracking), and the high COV render it difficult to interpret at the present time.
- Ignoring SCB COV’s and focusing on average values, the SCB results seem to suggest that three of these mixes may be prone to fatigue and reflective cracking. The DC(T) results can also be used to assess reflective cracking potential. Generally, values above 690 J/m² and preferably over 1000 J/m² are desirable to slow down (but typically not prevent) reflective cracking. So in that sense, the two tests are in general agreement on

that point. However, the design objective for asphalt overlays placed on concrete typically does not realistically include reflective crack prevention, as it is often difficult and expensive to adequately address reflective cracking.

- Because reflective cracking is difficult and expensive to prevent in most applications, and since fatigue cracking is generally only relevant in new, full-depth asphalt pavements (which represent a relatively small fraction of paved miles each year), it can be argued that the SCB test is not nearly as critical for implementation as compared to the DC(T). And for applications where it is desirable to control reflective cracking, the DC(T) can also be employed (using higher target fracture energy levels).

Table D-16. Detailed DC(T) and SCB comparison

Specimen ID	DC(T) Results (-12°C) CMOD G_f (J/m²)	DC(T) Results (-12°C) Avg. CMOD G_f (J/m²)	DC(T) Results (-12°C) CMOD G_f COV (%)	Flexibility Index	SCB Results (25°C) Avg. FI	SCB Results (25°C) FI COV (%)
N30EVO	385.6	412.8	9.8	4.6	3.4	29.7
N30EVO	393.6	412.8	9.8	2.7	3.4	29.7
N30EVO	459.1	412.8	9.8	3.0	3.4	29.7
N30FLEX	361.5	404.1	9.1	1.4	1.2	56.4
N30FLEX	427.0	404.1	9.1	1.7	1.2	56.4
N30FLEX	423.9	404.1	9.1	0.4	1.2	56.4
N70EVO	538.3	521.8	9.6	6.4	6.2	4.3
N70EVO	561.8	521.8	9.6	6.2	6.2	4.3
N70EVO	465.4	521.8	9.6	5.9	6.2	4.3
N70FLEX	368.6	442.2	16.7	2.9	2.8	14.9
N70FLEX	516.3	442.2	16.7	3.2	2.8	14.9
N70FLEX	441.7	442.2	16.7	2.4	2.8	14.9
N70FLEX		Average	11.8		Average	26.3

Table D-17. Detailed SCB results

Specimen ID	Avg. Peak Load (kN)	Avg. FI	FI COV (%)	Avg. G_f (J/m²)	G_f COV (%)
N30EVO	4.367	3.4	29.7	1886.0	16.5
N30FLEX	5.430	1.2	56.4	1115.7	9.5
N70EVO	3.436	6.2	4.3	1865.3	6.6
N70FLEX	4.424	2.8	14.9	1669.7	17.2

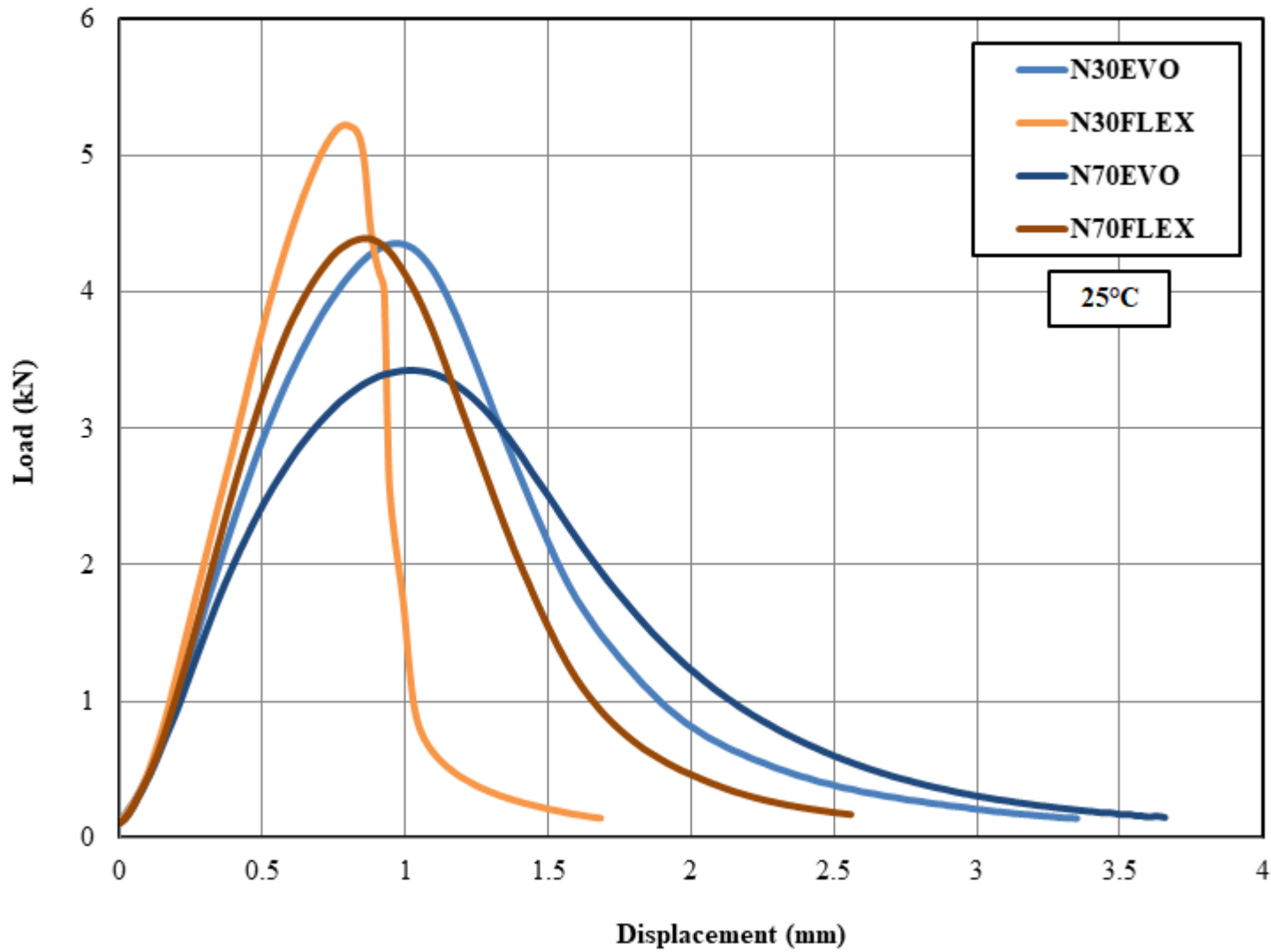


Figure D-44. SCB load-displacement plots

Hamburg-DC(T) Plot and Findings

Very recently, the concept of plotting performance data in a ‘performance-space diagram’ was introduced (ICAT, FHWA Mixtures ETG, Buttlar, April 2015). When plotting Hamburg rut depths (on a reverse, arithmetic scale, y-axis) versus DC(T) fracture energy (arithmetic scale, x-axis), a two-dimensional view of high/low temperature mixture performance can be conveniently viewed. Moreover, adjustments/change to mix composition and design can be readily observed in the context of change in high/low temperature performance using this plot. Figure D-45 shows typical Hamburg and DC(T) performance limits along with convenient gradient shading (deeper red for more rutting potential, deeper blue for more cracking potential). Since the DC(T) cracking test is usually accompanied with three levels of fracture energy thresholds based on traffic (400, 460, and 690 J/m² for low, med, and high traffic, respectively), these three zones are identified on the plot. For low traffic, data plotting in all three upper-right zones are acceptable. For medium traffic, a higher DC(T) fracture energy threshold is required; thus, only the two upper-right-most zones are allowable. For high traffic, only the upper-right-most zone is acceptable.

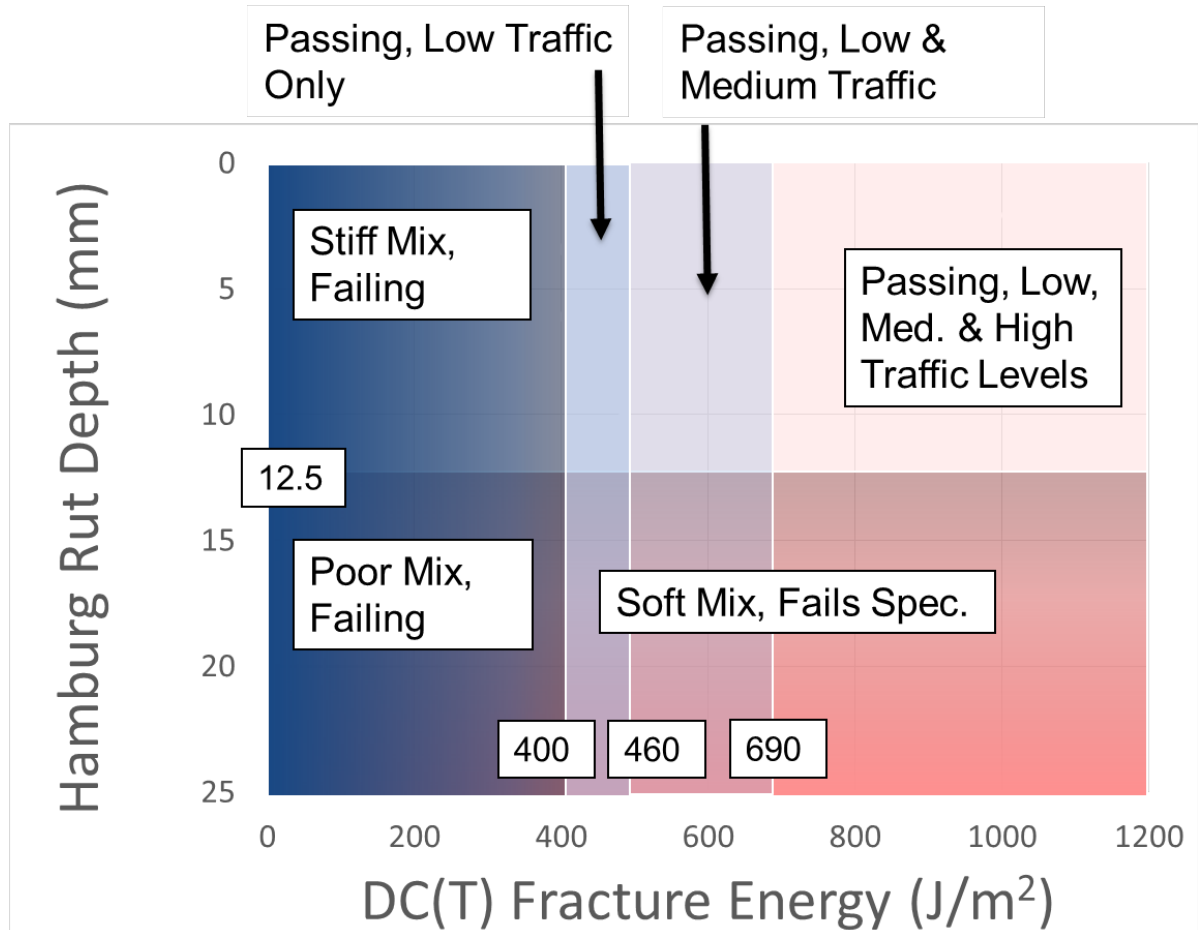


Figure D-45. Hamburg-DC(T) plot with typical specification limits superimposed

Figure D-46 presents the four study mixtures as plotted in the Hamburg-DC(T) space. All four N70 CHI mixtures are found to reside in the passing zones for low traffic, and

the N70 CHI mixtures also fall in the medium traffic passing zone for CDOT. The N70 Evo mix appears to be the best overall performer, as it is closest to the upper-right corner of the plot. The N70 Flex mix has some room for adjustment if a slightly higher fracture energy is desired. A straight tradeoff towards a softer binder might achieve this goal (shifting the data point downward and to the right), although the Hamburg rut limit will eventually be encountered. A similar adjustment may also benefit the N30 Flex mix. The combination of a softer binder and/or more rejuvenator, along with a slightly higher RAS/RAP ratio might also shift these two mixtures more toward the position of the N70 Evo mix.

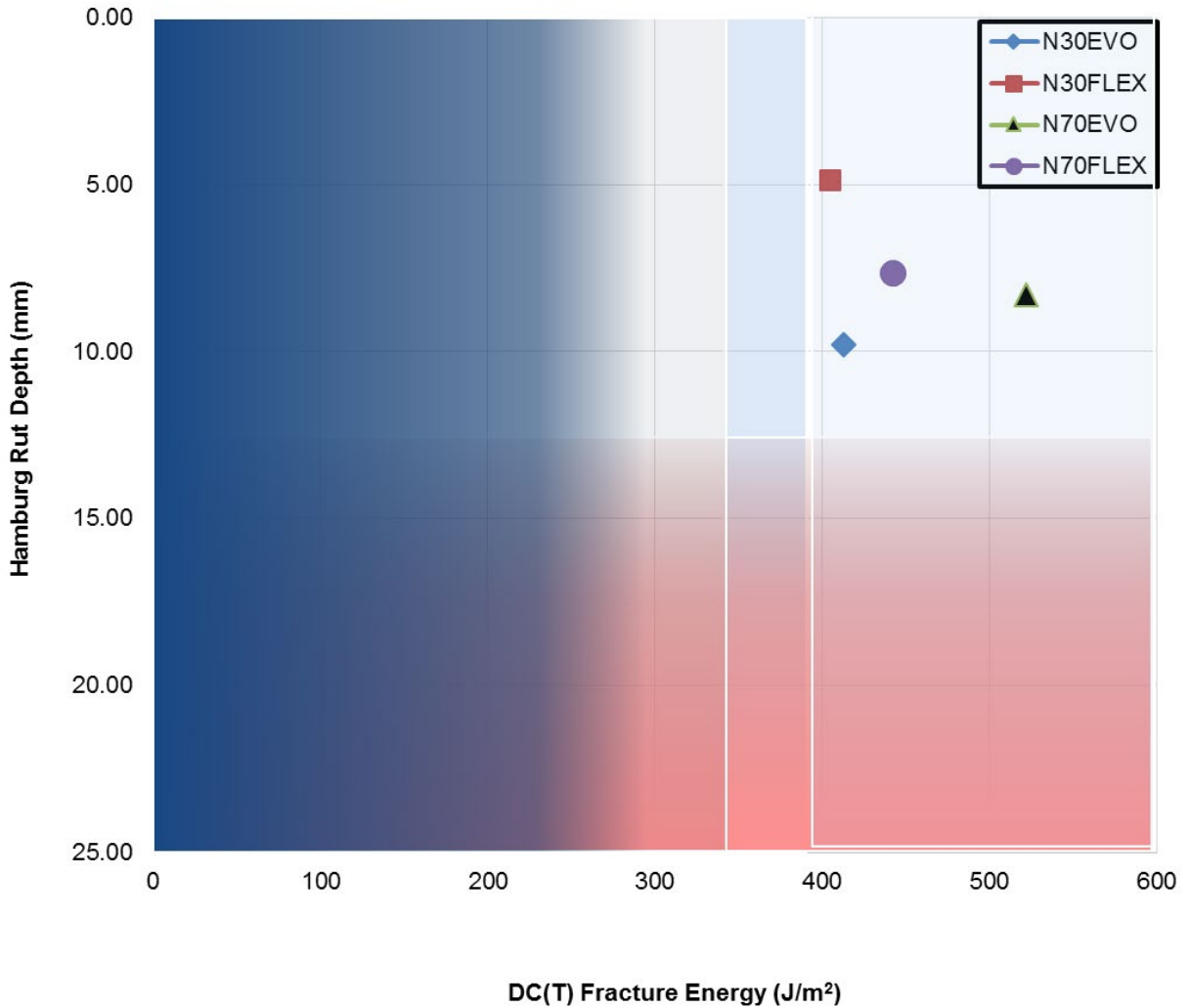


Figure D-46. Hamburg-DC(T) plot for N70 CHI mixes and N30 reference mixes

Extraction, Recovery, and Binder Testing Results

Table D-18 presents the results of the PG binder grading of the N70 CHI study mixtures. Both N70 mixtures easily passed the PG XX-22 requirements on the low temperature grade side; in fact, they both almost reached the PG XX-28 grade. Although one would naturally expect the high temperature PG grade to be met for these higher ABR mixes,

both of the recovered, blended binder systems actually met the Superpave PG 82-22 grade, which has a PG-spread (or UTR, Useful Temperature Range) resembling that of a highly modified binder. The actual spread between the high and low temperature grades were 109 and 110 C for the N70Flex and N70 Evo, respectively.

The UTR for the recovered binders can be compared to that of a PG 64-22 binder, which has a UTR of 84C. The N70 mixtures possess a much higher UTR in comparison. One can also compare the UTR to the most highly modified grade generally available, PG 76-28, which has a UTR of 104. The N70 CHI materials both possessed a UTR of approximately one grade (6 C) wider than that of even the highly modified PG 76-28 grade (109 and 110 C for the N70Flex and N70 Evo, respectively). This is consistent with the fact that the mixtures passed both the Hamburg wheel tracking test and the DC(T) low temperature test. Thus, the N70 CHI mixtures with 50% ABR were shown to be able to meet and exceed Superpave binder requirements when extracted, recovered and tested according to ASTM standards.

Table D-18. Superpave binder grade determination results for N70 CHI mixtures

High Temperature Testing

Mixture	Temperature (°C)	G* (kPa)	Phase Angle	G*/sinδ (kPa)
N70Flex	70	4.81	76.9	4.94
N70Flex	76	2.33	80	2.36
N70Flex	82	1.13	82.7	1.14
N70Evo	76	2.68	76.8	2.76
N70Evo	82	1.33	79.8	1.35
N70Evo	88	0.67	82.5	0.68

Low Temperature Testing

Mixture	Temperature (°C)	S (MPa)	m
N70Flex	-12	122	0.31
N70Flex	-18	319	0.301
N70Evo	-12	99	0.351
N70Evo	-18	235	0.278

True Grade

Mixture	HT (°C)	LT (°C)
N70Flex	82	-27
N70Evo	85	-26

Final Grade

Mixture	HT (°C)	LT (°C)
N70Flex	82	-22
N70Evo	82	-22

D.2.7. Summary and Conclusions of High ABR-Balanced Mix Design Study

This aforementioned findings presented details for mixture designs and performance results for a new, eco-friendly N70 CHI mixture with 50% asphalt binder replacement (ABR). Moreover, the study investigated the following hypothesis: ‘With the equipment, test methods, and technology that are available today, it is feasible for IDOT or other agencies to allow contractors to produce higher ABR mixes, provided that they can demonstrate through balanced performance testing (rutting and cracking tests), that their mixtures can perform well in the field?’ For reference, two N30 mixtures were also placed in accompanying field sections and tested in the laboratory. Several conclusions can be drawn from the findings produced in this study:

1. The N70 CHI mixtures met Hamburg and DC(T) performance test requirements for CDOT, and in general, slightly outperformed the N30 reference mixtures when viewed in the Hamburg-DC(T) space diagram.
2. The N70 CHI mixture with the slightly softer base binder grade (PG 46-34) plus Evotherm was found to meet Hamburg requirements, plus the more stringent DC(T) requirements for the medium traffic level imposed by most agencies (460 J/m² minimum fracture energy). Thus, this mixture is recommended for use in medium traffic areas in its current design configuration.
3. The N70 CHI mixture with the slightly harder base binder grade (PG 58-28) plus Evoflex was found to meet Hamburg requirements and CDOT DC(T) requirement, but the more stringent DC(T) requirement for the medium traffic level imposed by most agencies (460 J/m² minimum fracture energy) was missed by a small margin. However, the Hamburg-DC(T) plot shows that this mix has room for simple adjustment of the binder system to meet both requirements.
4. The extraction, recovery, and Superpave PG binder testing results showed that the binders in the N70 CHI mixtures easily met the plan grade requirements. Both binders met the PG 82-22 specification, and although masked by grade rounding, nearly met the next grade lower on the low temperature side. PG 82-27 and PG 85-26 were the continuous grades obtained for the N70 CHI-Flex and N70 CHI-Evo mixture, respectively. This suggests that the combination of virgin binder, RAP binder, RAS Binder, and additives, when fully blended, combine to produce the equivalent of a highly modified PG binder grade when tested and graded according to Superpave.

5. The binder test results concurred with the Hamburg and DC(T) performance test results. Thus, good performance at both high and low temperatures should be expected from the N70 CHI mixtures, for medium traffic and the Chicagoland climate.
6. The SCB results produced high variability (COV average of 26.3% and as high as 56%, as compared to an 11.8% average and a maximum COV of 16.7% in the DC(T)). In addition, the SCB results did not correlate well to DC(T) or Superpave binder test results. However, from the standpoint of reflective crack abatement, a general correspondence in DC(T) and SCB rankings was found.
7. With the current technology and available test methods it is possible to produce more sustainable mixes with higher ABR levels that can perform as well or better than the mixes that are currently being produced and used in Illinois.
8. Performance testing should be considered as a promising option for the contractors who chose to go to higher ABR levels than the ABR levels that are currently allowed in IDOT and CDOT specifications.
9. The flexibility index parameter, as obtained from the SCB test, appears to have higher-than-desired variability and its link to field cracking behavior is presently unclear. It does not appear to be appropriate or necessary to introduce the flexibility index as a second cracking performance indicator at the present time.
10. The mixtures investigated herein utilized design air void levels below 4% (3.0% and 3.5% air void targets were used herein), which provides enhanced asphalt film thickness. The use of standard volumetric mix design procedures along with a lower design air void level appears to be an effective mix design strategy for high ABR mixtures, especially when coupled with a balanced performance testing approach.

D.2.8. References

- [1] Arnold, J.W. (2014). Quantitative Evaluation of Low-Temperature Performance of Sustainable Asphalt Mixtures and Binders Containing Recycled Asphalt Shingles (RAS) and Rejuvenators. University of Illinois at Urbana-Champaign.
- [2] Brock, J.D. (1998). "From Roofing Shingles to Roads," Astec Industries, Technical Paper T-120.
- [3] CIWMB (2007). "Asphalt Roofing Shingles Recycling: Introduction." <<http://www.ciwmb.ca.gov/ConDemo/Shingles/>> (Accessed April 14th, 2015).
- [4] CMRA (2007). <<http://www.shinglerecycling.org>> (Accessed April 14th, 2015).
- [5] Cooper, S.B., Mohammad, L.N., Elseifi, M.A. (2014) "Infrastructure Sustainability: The Use of Recycled Asphalt Shingles in Flexible Pavements," Proceedings of the ASCE Geo-Shanghai 2014 Conference, Pavement Materials, Structures, and Performance, pp. 69-78.
- [6] Foo, K.Y., Hanson, D.I. and Lynn, T.A. (1999). "Evaluation of Roofing Shingles in Hot Mix Asphalt," Journal of Materials in Civil Engineering, vol. 11, no. 1, pp. 15-20.
- [7] Lippert, D. and Brownlee, M. (2012). "Use of Reclaimed Asphalt Shingles in Illinois," Illinois Department of Transportation: Bureau of Materials and Physical Research, Springfield, IL.
- [8] Marasteanu, M., Zofka, A., Turos, M., Li, X., Velasquez, R., Li, X., Williams, C., Bausano, J., Buttlar, W., Paulino, G., Braham, A., Dave, E., Ojo, J., Bahia, H., Gallistel, A., and McGraw, J., "Investigation of Low Temperature Cracking in Asphalt Pavements", Report No. 776, Minnesota Department of Transportation, Research Services MS 330, St. Paul, MN 55155, 2007.
- [9] Marasteanu, M, Moon, K.H., Teshale, E.Z., Falchetto, A.C., Turos, M., Buttlar, W., Dave, E., Paulino, G., Ahmed, S., Leon, S., Bahia, H., Arshadi, A., Tabatabaee, H., Ojo, J., Velasquez, R., Mangiafico, S., Williams, C., Buss, A., "Investigation of Low Temperature Cracking in Asphalt Pavements National Pooled Fund Study -Phase II", Final Report, Minnesota Department of Transportation, St. Paul MN, 2012.
- [10] Mallick, R.B., Teto, M.R. and Mogawer W.S. (2000). "Evaluation of Use of Manufactured Waste Asphalt Shingles in Hot Mix Asphalt," Chelsea CENTER FOR Recycling and Economic Development, Chelsea, MA.
- [11] Maupin, G.W. (2010). "Investigation of the Use of Tear-Off Shingles in Asphalt Concrete," Virginia Department of Transportation, Richmond, VA.
- [12] Newcomb, D., Stoup-Gardiner, M., Weikle, B., and Drescher, A. (1993). "Influence of Roofing Shingles on Asphalt Concrete Mixture Properties," Minnesota Department of Transportation, St. Paul, MN.

- [13] Paulsen, G., Stroup-Gardiner, M. and Epps, J. (1986). "Roofing Waste in Asphalt Mixtures," University of Nevada, Reno, NV.
- [14] Sengoz, B. and Topal, A. (2005). "Use of asphalt roofing shingle waste in HMA," *Construction and Building Materials*, vol. 19, pp. 337-346.
- [15] Watson, D.E., Johnson, A. and Sharma, H.R. (1998). "Georgia's Experience with Recycled Roofing Shingles in Asphaltic Concrete," *Transportation Research Record: Journal of the Transportation Research Board*, vol. 1638, no. 0361-1981, pp. 129-133.
- [16] Wu, S., Zhang, K., Wen, H., DeVol, J. and Kelsey, K. (2014). "Performance Evaluation of Hot Mix Asphalt Containing Recycled Asphalt Shingles in Washington State," *Transportation Research Board*.
- [17] You, Z., Mills-Beale, J., Fini, E., Goh, S.W. and Colbert, B. (2011). "Evaluation of Low-Temp Binder Properties of Warm-Mix Asphalt, Extracted and Recovered RAP and RAS, and Bioasphalt," *Journal of Materials in Civil Engineering*, vol. 23, no. 11, pp. 1569-1574.
- [18] Buttlar, W.G., "Investigation of Mechanisms behind Cracking Observed in IDOT District 1 and 2 Asphalt Pavement Surfaces in 2014," Technical Brief, University of Illinois at Urbana-Champaign, 2014.
- [19] Buttlar, W.G., "Recycled Asphalt Shingle Modified Asphalt Mixture Design and Performance Evaluation," Technical Brief, University of Illinois at Urbana-Champaign, 2015a.
- [20] Buttlar, W.G., "Balanced Performance Testing For the Design of Modern, Sustainable Asphalt Paving Mixtures," Technical Brief, University of Illinois at Urbana-Champaign, 2015b.
- [21] Buttlar, W.G., Hill, B.C., Wang, H., and W. Mogawer, "Performance-Space Diagram for the Evaluation of High and Low Temperature Asphalt Mixture Performance," *Journal of the Association of Asphalt Paving Technologists*, 2015.

D.3. Ground-Tire Rubber

An ever-increasing waste tire stream from vehicles is causing a great concern regarding environmental pollution. The produced CO² from burning waste tires can have a detrimental impact on the environment. The potential for dangerous fires or rampant mosquito breeding in landfills containing discarded tires presents two additional environmental concerns. Therefore, the idea of using ground tire rubber or crumb rubber in pavement to modify asphalt binder properties has garnered much attention over the years. Besides increasing the sustainability by recycling used tires, it is believed that crumb rubber modified asphalt binder can improve the performance and increase the service life of pavements. This chapter presents a literature review on the use of crumb rubber in asphalt pavements in United States and discusses its effect on various parameters that can affect the service life of asphalt pavements by reviewing the reports done by States Department of Transportations (State DOTs). In addition, a comprehensive field investigation which is underway by the Illinois Toll Highway Authority is presented.

D.3.1. Introduction

Currently, there are more than 300 million scrap tires in stockpiles in the U.S., and this amount is increasing every year [1]. Only in 2008, 290 million new tires were made in U.S. to be used for cars and trucks [2]. This enormous amount of waste tires brings severe recycling and disposal challenges with themselves since they are heavy, bulky, and made from several different chemicals. Some of this waste is used as a low cost tire-derived fuel (TDF) which can emit great amounts of CO₂ into the environment. Therefore, recycling waste tires by using them in pavements is a sustainable solution for this problem that can also benefit asphalt if its service life can be increased by the toughness and tenacity of tire rubber and the potentially beneficial effects of carbon black, which is an antioxidant.

According to Yetkin [3], the practice of modifying asphalt using polymers was patented circa 1843. Europe undertook few projects in 1930s and later in 1950s polymer modified asphalt started to gain some attention. More specifically, in 1960s Charles McDonald the head material engineer for the city of Phoenix, Arizona used rubber-modified asphalt to patch cracked roof of trailers when travelling with the US Bureau of Public Roads, currently known as FHWA [4]. Mr. McDonald added ground tire rubber (GTR) to binder at elevated temperatures to increase the flexibility of the mixture. He is widely considered as the “inventor” of crumb rubber modified asphalt in United States. Years later, ASTM defined asphalt rubber as “a blend of asphalt cement, reclaimed tire rubber, and certain additives in which the rubber component is at least 15 % by weight of the total blend and has reacted in the hot asphalt cement sufficiently to cause swelling of the rubber particles” [5]. Regardless of the exact invention date and the definition, several states in United States have performed research on GTR modified asphalt and even use this modification in highway routes in their states. The following sections will analyze and summarize a sampling of these findings.

D.3.2. State DOT Research on GTR

Alaska Department of Transportation (AKDOT)

The state of Alaska was the first to start the application of rubber asphalt binders in 1979 [6]. Placement of seven rubberized pavements totaling 4 lane-km between 1979 and 1981 is reported in the mentioned reference. The main conclusions regarding GTR modified asphalt in this study were:

- GTR modified asphalt exhibits similar fatigue behavior to conventional binders, and;
- The dynamic flexural stiffness is lowered when GTR is implemented

Florida Department of Transportation (FLDOT)

In 1989 Florida Department of Transportation (FLDOT) conducted a study on use of recycled (waste) materials in asphalt pavements [7]. Two major processes for incorporating GTR in asphalt was studied, namely, the wet process and dry process. It was concluded that the addition of GTR to HMA can reduce permanent deformation (rutting). Additional benefits such as low temperature flexibility and resistance to oxidative hardening were also reported. Research on asphalt-rubber RAP (recycled asphalt pavement) was also reported. Problems corresponding to the aged rubber's inability to soften the reclaimed asphalt were reported. It was also reported that addition of rubber to surface mixtures will generally increase the cost of the mix by 10% (mainly due to processing cost of asphalt-rubber binder). However, it was believed that the increase in service life of the pavement would compensate for the increase in cost.

As a result of the enhanced performance of GTR modified asphalt, GTR has been successfully used in highway applications such as crack fillers, stress absorbing membrane interlayers (SAMIs) in Florida. However, the use of GTR was limited to 5 – 10% based on different mixtures, which only results in the use of 10% of the scrap rubber produced annually in Florida. If this calculation is accurate, this process cannot completely solve the issue of scrap tire rubber in Florida. Ten years later the same group published another paper discussing the performance of their sample GTR modified asphalt that was cast in their original report [8]. In this study, the long term effect of GTR modified asphalt binder on the performance of surface mixtures was evaluated. The evaluation was performed on several categories such as ride-ability, rutting, cracking and patching, and skid resistance. Their conclusions were listed as follows:

- GTR modified binder had no effect (detrimental or beneficial) on field performance related to skid resistance;
- With use of Mays ride meter, the wet process resulted in higher ride ratings on open-graded surface mixes;

- The wet process was more beneficial in improving cracking resistance. Wet process rubberized mixtures resulted in 1-6% cracked areas, as compared to 30% for the dry process;
- The optimum rubber content (in terms of reducing fatigue cracking) was found to be 10-15%, and;
- Less rutting was observed in dense-graded mixes when GTR was used.

New York State Department of Transportation (NYDOT)

The New York State Department of Transportation (NYDOT) also performed a study in 1989 to evaluate GTR [9]. One of their first findings was that GTR-modified asphalt had appreciably higher cost, due to the procuring and processing of GTR and the additional work required during mixing and placement. A 20-25% increase in placed mix-ton cost was observed based on the amount of GTR used. It should be noted that in order to be able to use similar mixing and placing equipment as one would do with conventional mixes, the GTR percentage was limited to 3% in their study. It was surmised that amounts higher than 3% might lead to construction problems. However, the authors have also reported that considering adequate equipment and training, mixing and placing GTR modified rubber can likely be performed in a similar manner to that of conventional mixtures. Problems reported in NYDOT report included:

- Difficulties in obtaining proper rubber gradation;
- Higher material and mixing costs;
- Higher placing costs (due to higher temperature requirement of GTR modified asphalt).

Improved performance in terms of improved fatigue properties, resistance to cracking, skid resistance under icy conditions and noise levels was also observed and reported in the NYDOT report. These results, however, were mainly based on laboratory tests. Knowing the improved performance that can be achieved through using GTR in asphalt pavement, the report also discusses the availability of scrap tire rubber.

The available scrap tires (at the time of the study) was deemed to be sufficient to provide 2 percent rubber-modified mixes for 50 percent of the hot-mix asphalt concrete used for highway pavement overlays in New York State.

Virginia Department of Transportation (VDOT)

Based on a report performed by Virginia Department of Transportation (VDOT) [10], four test sections using GTR modified asphalt hot mix were placed in Virginia in a period of 1990 to 1993. The main objectives of the study were to familiarize contractors and VDOT personal with the construction process and compare the performance of different methods of implementing GTR in asphalt pavement. They have reported a cost increase if

64 to 102% more than conventional mixes. However, it is mentioned that one reason for the extremely high cost is that the jobs were relatively small in size of construction.

The authors also concluded that the tested pavements containing GTR performed similarly to conventional pavements. Several issues corresponding to designing the mixes containing GTR were also been reported. It was also reported that mixes containing GTR showed considerably less rutting.

Georgia Department of Transportation (GDOT)

In 1991, the Georgia Department of Transportation (GDOT) undertook extensive research to evaluate the production and placement of crumb rubber hot-mix asphalt. Wet process was used in this examination as superior performance of wet process compared to dry process had been previously observed. On-site blending units were used to combine the ground tire at a rate of 16% by weight of asphalt cement. The test was performed from 1991 to 1995. Their results indicated that:

- GTR modified asphalt can become very brittle over time, confirmed by a large increase in viscosity and decrease in penetration, and by a large amount of transverse reflective cracking;
- Compared with the conventional mixes, GTR modified asphalt did not reduce rutting and was more than twice as expensive to place;
- However, it was shown that GTR modified asphalt could be produced and placed using conventional equipment with a few modifications, and;
- RAP could be added into the mix if rubber dosage percentage was kept below 10%. For one of the test sections, 35% RAP was used successfully with a GTR content of 6%.

Other Studies

Several other states have also performed research on the use of GTR in asphalt pavements including California Department of Transportation [12], Arizona Department of Transportation [13, 14], Wisconsin Department of Transportation [15], Colorado Department of Transportation [16], and Maryland Department of Transportation [17]. Currently in the United States, asphalt-rubber is the largest market for scrap tires, consuming an estimated 220 million pounds, or 12 million tires [18] with California and Arizona using the most compared to other states (over 80%) and Florida being the next largest consumer.

The Federal Highway Administration (FHWA) has been involved in ‘rubber technology’ since the 1970’s [20] and throughout the 1980’s it came up with reports on the asphalt-rubber paving technologies. The FHWA report released in 1992 about the design and

construction of asphalt paving materials with Crumb Rubber Modifier (CRM)² mentions, in detail, the enhancing features of the CRM modifier such as increase in thermal and reflective cracking resistance, increase in rutting resistance, improving the binder durability, and increase in the asphalt-aggregate bond strength. There were reports of mixed performance by the rubber-modified pavements by various DOTs in the 1980s-1990s, but since then the GTR technology has undergone transformations to stake a claim at being a good paving material for interstate highways and other important paving projects.

GTR-modified asphalt binder has been extensively studied and researched. Study conducted by Richard et al. concerned with the effect that particle size, surface area, and grinding method of the GTR on the asphalt binder (21). This study also looked in to the performance of the polymer-modified asphalt rubber mix. Xu et al. (22) did a rheological investigation on the effects of additives like PPA, EVA, elastomers, and plastomers in GTR-modified asphalt. Vahidi et al. studied the effect of GTR and Treated GTR on high-RAP mixes (23). The study included results from a host of mix and binder tests, like Hamburg, MSCR, mix stiffness (E*), Texas Overlay Test, etc. GTR-modification has been used with different binder systems as well as with other additives. Williams et al. looked into the rubber-modified bio-asphalt (24), Akisetty et al. looked into the high-temperature properties of the GTR-modified binders with WMA additives- Aspha-min and Sasobit (25), and Chui et al. conducted a performance evaluation of Asphalt-Rubber SMA (26).

D.3.3. Illinois Toll Highway Authority Study on SMA-GTR

The usage of Ground Tire Rubber (GTR) has proved to be advantageous for the state of Illinois due to its various distinct advantages such as better cracking resistance, and improved durability of the pavements among many others. Extensive research has been done on GTR-modified asphalt, resulting in advancements in the existing GTR technologies. This project focusses on two such new GTR technologies: Elastiko 100 Engineered Crumb Rubber (ECR), a new dry process GTR product, and Evoflex Rubber Modified Asphalt (RMA).

Elastiko 100 ECR, made by Asphalt Plus LLC., is an engineered crumb rubber that can be added to the hot mix asphalt plant through the RAP collar, wherein lies its main logistical advantage. Ingevity's Evoflex RMA comes in pellets engineered with GTR, SBS and other chemicals. Its main advantage is the possibility of engineering the pellet composition to suit individual projects. The project also included testing of mixes with Seneca's terminally blended GTR, which is an established industry standard in Illinois.

The Illinois Tollway constructed test sections for three Ground Tire Rubber (GTR) asphalt modifier technologies on the Reagan Memorial Tollway (I-88) in April 2016. Apart from estimating the performance characteristics of the new GTR technologies, the study also aimed at learning the effect that a softer virgin binder and an increased amount of reclaimed asphalt have on the mix. Accordingly, the GTR technologies were

²The FHWA uses the terminology CRM instead of GTR [9]

incorporated into SMA mixes using a base binder (PG 58-28), a softer binder (PG 46-34), and the softer binder with an increased Asphalt Binder Replacement (ABR) percentage (PG 46-34 with high ABR). The mixture matrix is shown in Table D-19.

Table D-19. Summary of GTR technologies and asphalt binder types

SMA Mixture Matrix for I-88					
All Mixtures use the same base design aggregates					
Placement	Product	Base	Softer AC	Softer AC & increase ABR	Tonnage
Mainline	Seneca GTR	PG58-28 +12	PG 46-34 +12	PG 46-34 +12 & increase ABR*	3 x 300
Mainline	Elastiko 100	PG 58-28 +10% ECR	PG 46-34 +10% ECR	PG 46-34 +10% ECR & increase ABR*	3 x 300
Shoulder	Evoflex RMA	PG58-28 + 10% 725	PG 46-34 +10% 725	PG 46-34 + 10% 725 & increase ABR*	3 x 200**
* ABR increased during design to 47% by increasing RAS %					
** PG58-28 + 10% 725 section increased to 400 TNs to accommodate asphalt binder batch size					

In total, 12 field cores of 150 mm diameter, were taken from each of the test sections for the nine mixes. The location of the cores is shown in Table D-20. Additionally, gyratory-compacted specimens, a minimum of 12 for each mix, were provided by State Testing, LLC. Furthermore, loose mix, binders, and aggregates were sampled.

Table D-20. Location of GTR Test sections on Reagan Memorial Tollway (I-88)

Rubber Modifier	Lane	Modifier Mile Post Limits		Individual Test Section Mile Post Delineations		
		Mile Post Start	Mile Post End	PG 58-28 Base Asphalt Liquid	PG 46-34 Base Asphalt Liquid	PG 46-34 Base Asphalt Liquid & High ABR
Evoflex RMA	EB Outside shoulder	65.2	66.0	65.2-65.5	65.5-65.8	65.8-66.0
Elastiko 100	EB Inside Lane (Lane 1)	60.1	61.3	60.1-60.5	60.5-60.9	60.9-61.3
Seneca GTR	EB Inside Lane (Lane 1)	64.4	66.2*	64.4-64.7	65.5-65.9	65.9-66.2
* No GTR asphalt placed between Mile Posts 64.7 and 65.5						

The Phase-I of the project comprised of tests to determine the low-temperature cracking characteristics of the mixes. Although detailed test results will not be available until Spring of 2017, a brief summary of the main study finds are presented herein. Plant-compacted gyratories and field cores were tested to measure their fracture energy using the Disk-Shaped Compact Tension test at two temperatures (-12°C and -18°C). As a brief overview of the DC(T) results, only one in nine mixes for plant-compacted gyratories failed in the most stringent criteria of 690 J/m² for fracture energy at -12°C; all mixes pass for -18°C. However, the failed mix has a fracture energy value of 688 J/m² which can be considered to be within the range of possible experimental error. All field cores passed the fracture energy criteria at -12°C and only two out of nine mixes failed at -18°C. Hamburg Wheel Tracking test results were provided by S.T.A.T.E. Testing LLC., Chicago. DC(T)-Hamburg plots, or the Performance-Space Diagram, were used as graphic tool for mix evaluation based on low-temperature cracking and rutting potential. The plots revealed that all the mixes would perform well on the field. Further, Acoustic

Emission testing was done with the plant-compacted gyratories and the field cores to determine the embrittlement temperature of the mixes. Embrittlement temperature is also an indicator of the thermal cracking resistance of the mix, like fracture energy. The results show that the two new products Elastiko and Evoflex increase the embrittlement temperature irrespective of the mix structure. AE testing on gyratories revealed that usage of softer binder decreases the embrittlement temperature and addition of recycled asphalt increases it.

Overall, the results of Phase-I of the project look promising and call for a continued investigation in the mix properties. Both Elastiko 100 and Evoflex RMA compare well to Seneca's terminally blended GTR.

D.3.4. Summary of GTR Modification

Based on the literature reviewed, there appears to be a great amount of benefit in using GTR in asphalt pavements. The only issues that seem to impede the use of GTR extensively in the United States are lack of knowledge and training, the relative complexity of mix design, and not having proper equipment to process GTR with asphalt binder. Proper investment and training to address these issues seems to be a necessary step in increasing the use of GTR towards helping mitigate the problems associated with the stockpiling of waste tires. Although the cost of paving when GTR is use increases (a 10% to 100% increase in cost has been reported) better performance and durability of GTR modified asphalt can counteract the increase in the initial cost.

D.3.5. References

- [1] <http://www.solidwastedistrict.com/statistics/tires.html>
- [2] http://waste360.com/Recycling_And_Processing/scrap-tires-201003
- [3] Yildirim, Yetkin. "Polymer modified asphalt binders." *Construction and Building Materials* 21, no. 1 (2007): 66-72.
- [4] <http://pavement.engineering.asu.edu/wordpress/wp-content/uploads/2012/12/Way.pdf>
- [5] ASTM D8-13b, Standard Terminology Relating to Materials for Roads and Pavements, ASTM International, West Conshohocken, PA, 2013, www.astm.org
- [6] Raad, Lutfi, and Stephan Saboundjian. "Fatigue behavior of rubber-modified pavements." *Transportation research record: journal of the transportation research board* 1639 (1998): 73-82.
- [7] Kandhal, Prithvi S., E. Ray Brown, and Robert L. Dunning. Investigation and evaluation of ground tire rubber in hot mix asphalt. No. NCAT Rept No. 89-3. National Center for Asphalt Technology, 1989.

- [8] Choubane, Bouzid, et al. "Ten-year performance evaluation of asphalt-rubber surface mixes." *Transportation Research Record: Journal of the Transportation Research Board* 1681 (1999): 10-18.
- [9] Shook, J. F., H. B. Takallou, and E. Oshinski. "Evaluation of the use of rubber-modified asphalt mixtures for asphalt pavements in New York State." ARE Inc. Contract D005072 (1989).
- [10] Maupin Jr, G. "Hot mix asphalt rubber applications in Virginia." *Transportation Research Record: Journal of the Transportation Research Board* 1530 (1996): 18-24.
- [11] Brown, Dan, et al. "Georgia's experience with crumb rubber in hot-mix asphalt." *Transportation Research Record: Journal of the Transportation Research Board* 1583 (1997): 45-51.
- [12] CalTrans, "Use of Scrap Tire Rubber, State of the Technology and Best Practices," State of California Department of Transportation, Sacramento CA, Report: Caltrans/CIWMB Partnered Research, February 2005.
- [13] Gonzales, G. F. D., "Evaluation of Road Surfaces Utilizing Asphalt-Rubber 1978", Report No. '1979 GG3, Arizona Department of Transportation, November 1979.
- [14] Green, E.L. and Tolonen, W.J., "The Chemical and Physical Properties of Asphalt Rubber Mixtures – Basic Material Behavior," Report No. ADOT-R5-14 (162), Arizona Department of Transportation, July 1977.
- [15] Loh, S., Kim, S., and H. Bahia, "Characterization of Simple and Complex Crum Rubber Modified Binders," Wisconsin Department of Transportation, Report WI/PR-07-01, July 2000.
- [16] Shuler, S.. "Use of Waste Tires, Crumb Rubber, on Colorado Highways." Colorado Department of Transportation, DTD Applied Research and Innovation Branch, (2011).
- [17] Witczak M.W.. State of the Art Synthesis Report. Use of Ground Rubber in Hot Mix Asphalt. Maryland Department of Transportation Report MD-91/01, Jun 1991.
- [18] <http://www3.epa.gov/epawaste/conserva/materials/tires/ground.htm>
- [19] Way, G.B., K. Kaloush, and K.P. Biligiri. "Asphalt-Rubber Standard Practice Guide—An Overview." *Proceedings of Asphalt Rubber* (2012): 23-40.
- [20] U.S.D.O.T. Federal Highway Administration. Design and Construction of Asphalt Paving Materials with Crumb Rubber Modifier . Washington, D.C. : Federal Highway Administration, 1992. State of the Practice.
- [21] W.J. Richard, P. Clayton, T. Pamela, R. Carolina, M. Tyler. Effect of ground tire rubber particle size and grinding method on asphalt binder properties. NCAT, 2012.

[22] O. Xu, L.Cong, F. Xiao, S.N. Amirkhanian. Rheology investigation of combined binders from various polymers with GTR under a short-term aging process, 2015.

[23] Vahidi, S. and W.S. Mogawer, and A. Booshehrian. Effects of GTR and Treated GTR on Asphalt Binder and High-RAP Mixtures. 2014, Journal of Materials in Civil Engineering, Vol. 26, Issue 4.

[24] R. Christopher Williams, J. Peraltaa, Ka Lai N.N. Puga. Development of Non-Petroleum Based Binders for Use in Flexible Pavements – Phase II. Iowa, 2015.

[25] C.K. Akisetty, S.J. Lee, S.N. Amirkhanian. High temperature properties of rubberized binders containing warm asphalt additives. 2007, Construction and Building Materials, pp. 565-573.

[26] Chui-Te Chiu, Li-Cheng Lu, A laboratory study on stone matrix asphalt using ground tire rubber, 2006.

Appendix E. Acoustic Emission Testing

E.1. Acoustic Emission Phenomena

Acoustic Emission (AE) technique (1-8) is a widely used nondestructive testing (NDT) method. It is defined as the sudden release of localized strain energy in the form of mechanical elastic waves in a stressed material. Emitted mechanical waves can be detected and recorded using sensitive piezoelectric sensors mounted on material surface.

The AE testing setup is schematically illustrated in Figure E-1. AE stress waves are detected using piezoelectric sensors, amplified, filtered, and then recorded. The microcracking process as the source of AE, generally generates short-lived AE signals with rise times of the order of 10^{-6} to 10^{-4} ; therefore, amplifier and filters are used to condition AE signals.

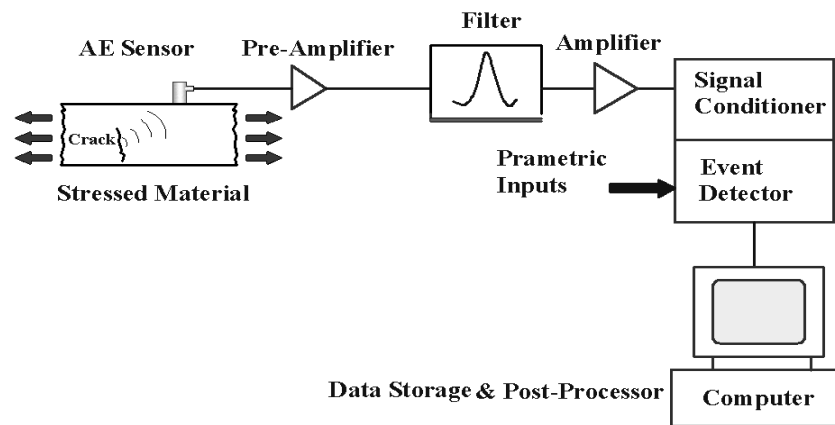


Figure E-1. Schematic representation of Acoustic Emission testing setup

E.2. Developed Acoustic Emission-Based Testing Method

The AE-based testing method is a simple and practical testing method that has been developed under recent NCHRP IDEA projects (#144 and #170) at University of Illinois. The developed method can be used to accurately and rapidly evaluate the low temperature cracking behavior of asphalt materials and characterize the cracking temperature, a.k.a. “Embrittlement Temperature”, of asphalt binders and asphalt mixtures (8-13). In addition to asphalt binders and hot mix asphalt, this technique has been successfully implemented to characterize modern warm mix asphalt and mixtures with high amounts of RAP, to help ensure the durability of these environmentally friendly materials.

Acoustic emission-based asphalt binder and asphalt mixture samples as well as testing set up are shown in Figure E-2. AE asphalt binder sample consists of 6mm thick rectangular shape layer of asphalt binder bonded to granite substrate. To conduct AE test, asphalt binder samples are cooled down from 20°C to -50°C. Differential thermal contraction between granite substrates and asphalt binders induces progressively higher thermal

stresses in the binders resulting in thermal crack formation, which is accompanied by a release of elastic energy in the form of transient waves. Cracking temperature of asphalt binders was predicted by processing and analysis of emitted elastic waves (8-13).

AE asphalt concrete specimens are 50mm thick semicircular samples which are sliced from field cores or laboratory compacted samples. Similar to asphalt binder samples, asphalt concrete samples are cooled down from room temperature to -50°C. Progressively higher thermal stresses in the specimen due to differential thermal expansion coefficients between asphalt mastic and aggregates result in the formation of thermal microcracks in the asphalt mastic, which is accompanied by the release of elastic waves. This manifest itself as a cluster of high amplitude waves during the test.

During conducting AE test, specimen temperature was continuously recorded through using K-type thermocouple placed on the specimen surface. Wideband AE piezoelectric sensors (Digital Wave, Model B1025) with a nominal frequency range of 50 kHz to 1.5 MHz were utilized in order to monitor and record acoustic activities of the sample during the test. High-vacuum grease was used to couple the AE sensors to the specimen surface. Since by nature the acoustic signals are of low energy, the sensor data is immediately fed into a preamplifier to minimize noise interference and prevent signal loss. Signals from AE sensors were pre-amplified by 20 dB using broad-band pre-amplifiers. Then, the signal was further amplified by 21 dB (for a total of 41 dB) and filtered using a 20 kHz high-pass double-pole filter using the Fracture Wave Detector (FWD) signal condition unit. The signals were then digitized using a 16-bit analog-to-digital converter (ICS 645B-8) using a sampling frequency of 2 MHz and a length of 2048 points per channel per acquisition trigger. The outputs were stored for later processing using Digital Wave software (WaveExplorer™ V7.2.6), (8-13).

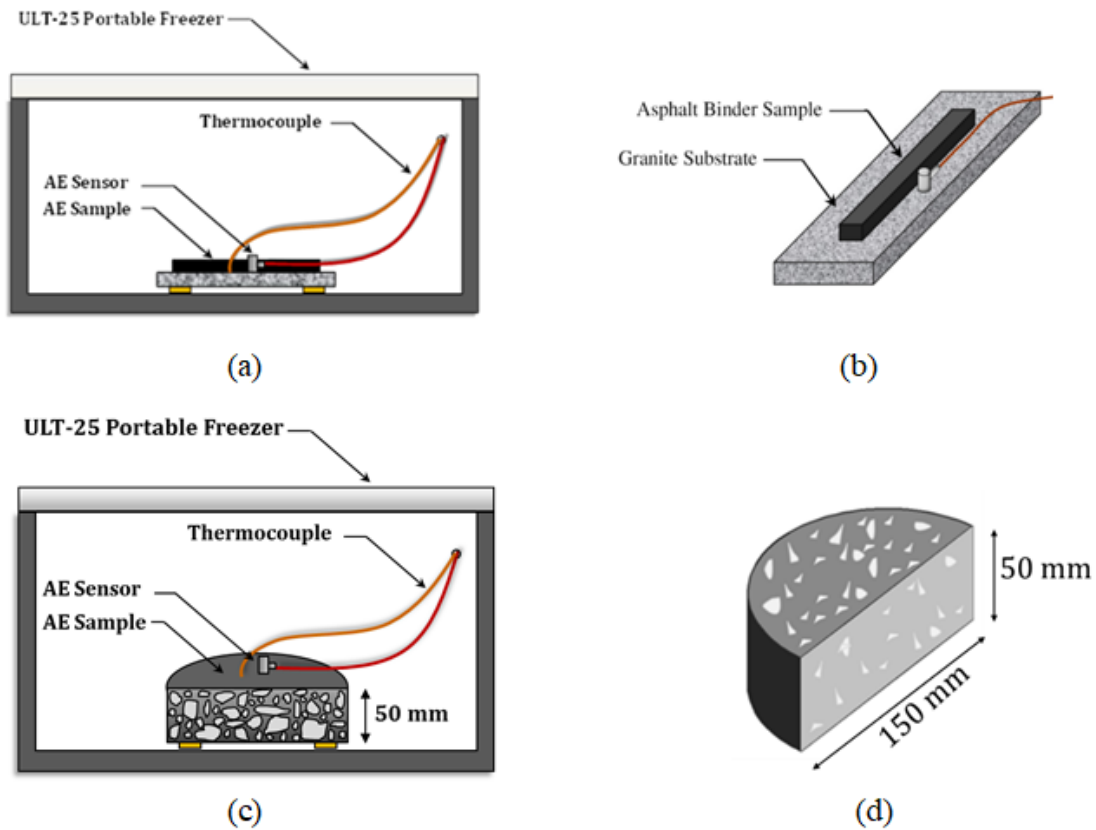


Figure E-2. (a) AE testing setup for asphalt binders (b) AE asphalt binder sample (thin film of asphalt binder bonded to granite substrate) (c) AE testing setup for asphalt mixtures (d) AE asphalt mixture sample

A number of parameters are extracted from the AE test. Analysis of thermally induced AE activity of asphalt mixture specimens is conducted on calculated AE energy, event counts and specimen temperature. The emitted energy associated with each event is calculated by using the following equation shown below, where E_{AE} is AE energy of an event ($V^2 \cdot \mu\text{sec}$) with duration of time t (μsec) and recorded voltage of $V(t)$ (8-13).

$$E_{AE} = \int_0^t V^2(t) dt \quad (1)$$

A typical plot of AE test result for both asphalt materials is shown in Figure E-3. For both asphalt binders and asphalt mixtures, there are three distinct regions in the plot: (a) pre-cracking; (b) transition; and (c) stable cracking regions. The first region is “pre-cracking” region during which material doesn’t undergo any micro-damage and as a result doesn’t exhibit any AE activity. This period occurs prior to the onset of material fracture. The second region, the ‘transition region’, begins when thermal microcracking reveals itself

via relatively high-energy AE events, which occur immediately after the pre-cracking period starts. Progressively higher thermal stresses in the specimen eventually cause thermal microcracks to develop in the asphalt mastic, as well as at the interface between asphalt mastic and aggregates. Microcracks result primarily from a combination of asphalt mastic brittleness (at lower temperatures) and from the action of thermally-induced tensile stresses within the material, perhaps enhanced by the stress concentrations at the interface between the mastic and the aggregates. The AE based embrittlement temperatures are more accurate, i.e., have less variability, than those predicted by the traditional methods (14), which are based upon the rheological material properties of the binder.

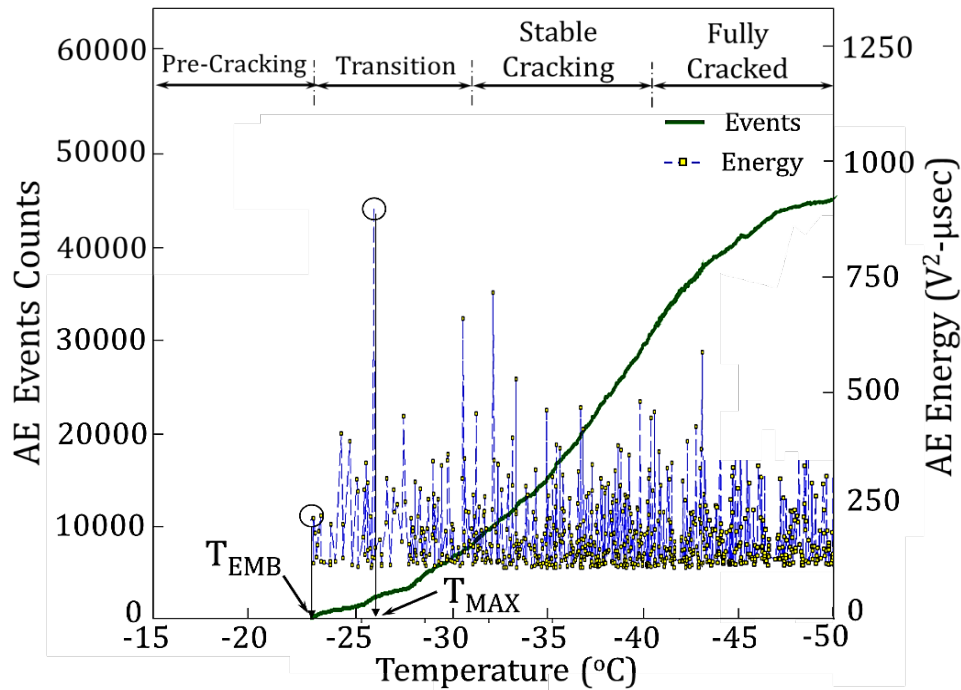


Figure E-3. Typical AE test result for asphalt materials

E.3. Testing Samples and Testing Results

The test specimens were provided by the Missouri Department of Transportation. The specimens consisted of several asphalt binders and asphalt concrete samples that were extracted from cores extracted from roadways in Missouri. Tables E-1 shows the asphalt concrete mixtures tested. The corresponding embrittlement temperatures are presented in Table E-2. The tested asphalt binders were binders extracted from asphalt concrete mixtures around the State of Missouri, see Table E-3. Table E-3 also shows the embrittlement temperatures for the extracted binders.

E.3.1. Asphalt Mixture Test Results

For the acoustic emission tests, the test specimens i.e., asphalt concrete mixture samples, consisted of the two halves of tested Disk-Shaped Compacted Tension Test [DC(T)] samples, i.e., each DC(T) sample produced the AE test samples “x” and “y,” respectively.

The corresponding embrittlement temperatures are included in Table E-1. The data shown in Table E-1 is also shown in a Figure E-4 using a bar chart. As an example, Figure E-5 shows the AE test results for the US54-3-1 test sample.

Table E-1. Asphalt mixture samples tested using Acoustic Emission

Sample Name	Field Core Labels	Virgin Binder	Design ABR RAP (%)	Design ABR RAS (%)
US54-1-6(SPS 10-10-6)	54-1	58-28	-	33
US54-1-7(SPS 10-10-7)	54-1	58-28	0	33
US54-2-1(SPS 10-8-1)	54-2	58-28	33	0
US54-2-2(SPS 10-8-2)	54-2	58-28	33	0
US54-3-1(SPS 10-7-10)	54-3	58-28	18	15
US54-3-3(SPS 10-7-3)	54-3	58-28	18	15
US54-4-2(SPS 10-5-2)	54-4	64-22H	35	0
US54-4-6(SPS 10-5-6)	54_4	64-22H	35	0
US54-7-5	65	64-22	0	0
US54-7-8	65	64-22	0	0
US54-8-5	66	70-22	9	0
US54-8-8	66	70-22	9	0
US63-2-8	--	64-22	20	10
US63-2-10	--	64-22	20	10
MO13-1-4	--	64-22H	17	0
MO13-1-12	--	64-22H	17	0

Table E-2. Acoustic Emission testing results for asphalt mixture samples

Sample Name	Embrittlement Temperatures Specimen X	Embrittlement Temperatures Specimen Y	Average of Embrittlement Temperatures	COV, (%)
US54-1-6	-24.00	-27.30	-25.65	9.10
US54-1-7	-33.00	-27.50	-30.25	12.86
US54-2-1	-28.00	-27.00	-27.50	2.57
US54-2-2	-28.00	-29.00	-28.50	2.48
US54-3-1	-34.00	-35.50	-34.75	3.05
US54-3-3	-33.00	-36.00	-34.50	6.15
US54-4-2	-31.00	-28.00	-29.50	7.19
US54-4-6	N/A	-23.00	-23.00	N/A
US54-7-5	-24.00	-28.00	-26.00	10.88
US54-7-8	-26.50	-23.50	-25.00	8.49
US54-8-5	-24.50	-25.20	-24.85	1.99
US54-8-8	-20.50	-21.00	-20.75	1.70
US63-2-8	-27.50	-29.50	-28.50	4.96
US63-2-10	-25.00	-30.20	-27.60	13.32
MO13-1-4	-28.50	-32.00	-30.25	8.18
MO13-1-12	-34.50	-35.50	-35.00	2.02

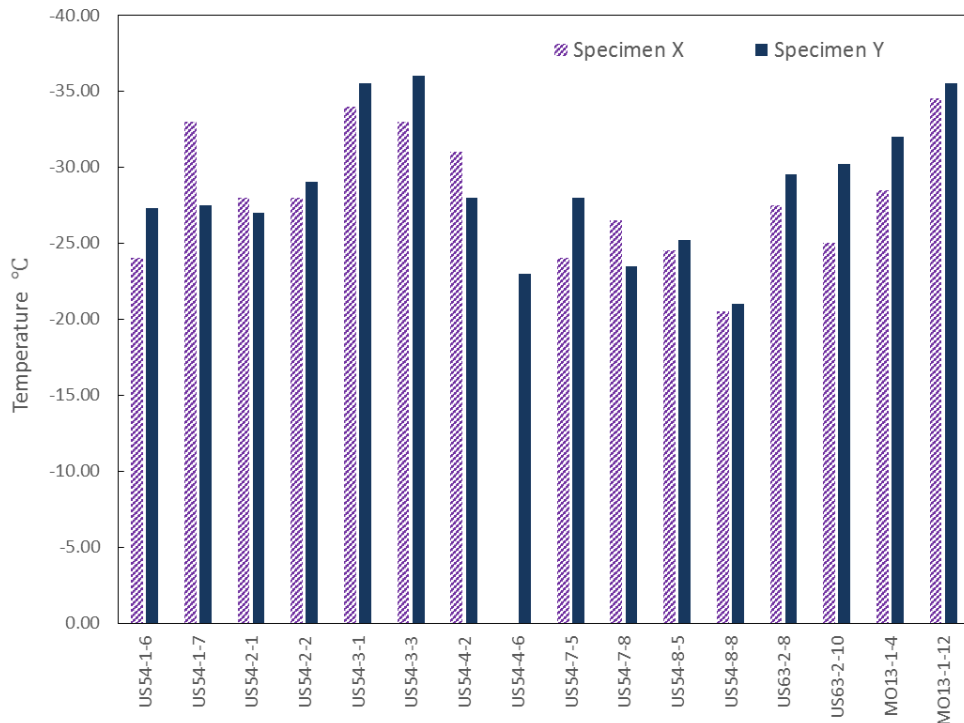


Figure E-4. Embrittlement Temperatures of X and Y Specimens for all mixture samples

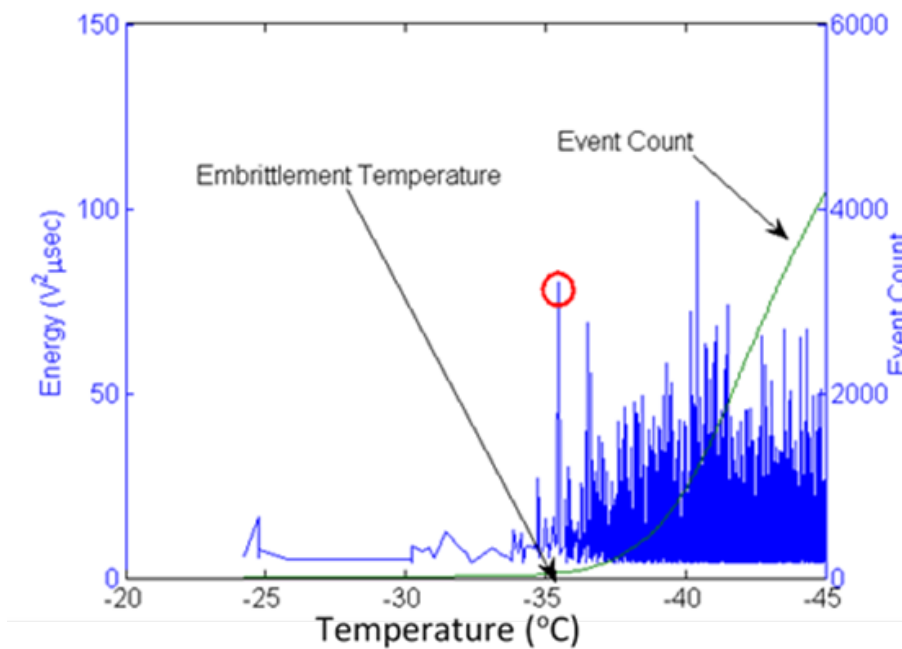


Figure E-5. Acoustic Emission Energy and Event Count versus Temperature for specimen Y of US54-3-1 Sample. Horizontal axis denotes temperature in °C.

E.3.2. Asphalt Binders Test Results

There are a total of five different binder samples. To reduce the experiment bias, three test specimens were made from each binder sample. The resulting embrittlement temperatures are included in Table E-3. Figure E-6 shows a bar chart of the embrittlement temperatures of all the specimens tested. A representative AE testing results for each binder specimen is also shown in Figure E-7 shows the AE response for specimen B of the US63-1 binder sample.

It was observed that the two binders, i.e., binders US54-6 and SPS-10-SEC9, showed a higher variability, i.e., greater COV, in the acoustic emission experimentally obtained embrittlement temperatures than the other binders reported in Table E-2. This higher variability may be explained by the binders not being evenly blended into the test sample.

In addition, it was observed that the binder SPS-10-SEC9 is more viscous, which makes it more difficult to remove the sample from the BBR sample mold. However, it was noted that this difficulty can be easily overcome by (a) increasing the cooling time of the BBR sample mold, provide it does not reach its embrittlement temperature, and (b) wrapping the molding bars in plumber's tape using a longitudinally mode instead of using the traditional method of wrapping the molding bars in an helical mode.

Table E-3. Acoustic Emission testing results for asphalt binder samples

Specimen Name	Sample	Embrittlement Temperatures (°C)	Average Embrittlement Temperature (°C)	COV, (%)
US63-1	A	-42	-42.00	0.00
US63-1	B	-42	-42.00	0.00
US63-1	C	-42	-42.00	0.00
US54-4	A	-36	-37.33	3.37
US54-4	B	-37.5	-37.33	3.37
US54-4	C	-38.5	-37.33	3.37
US54-6	A	-40	-37.50	5.81
US54-6	B	-36.5	-37.50	5.81
US54-6	C	-36	-37.50	5.81
SPS-10-SEC9	A	-41	-38.83	4.87
SPS-10-SEC9	B	-37.5	-38.83	4.87
SPS-10-SEC9	C	-38	-38.83	4.87
MO13-1	A	-34	-33.83	3.72
MO13-1	B	-32.5	-33.83	3.72
MO13-1	C	-35	-33.83	3.72

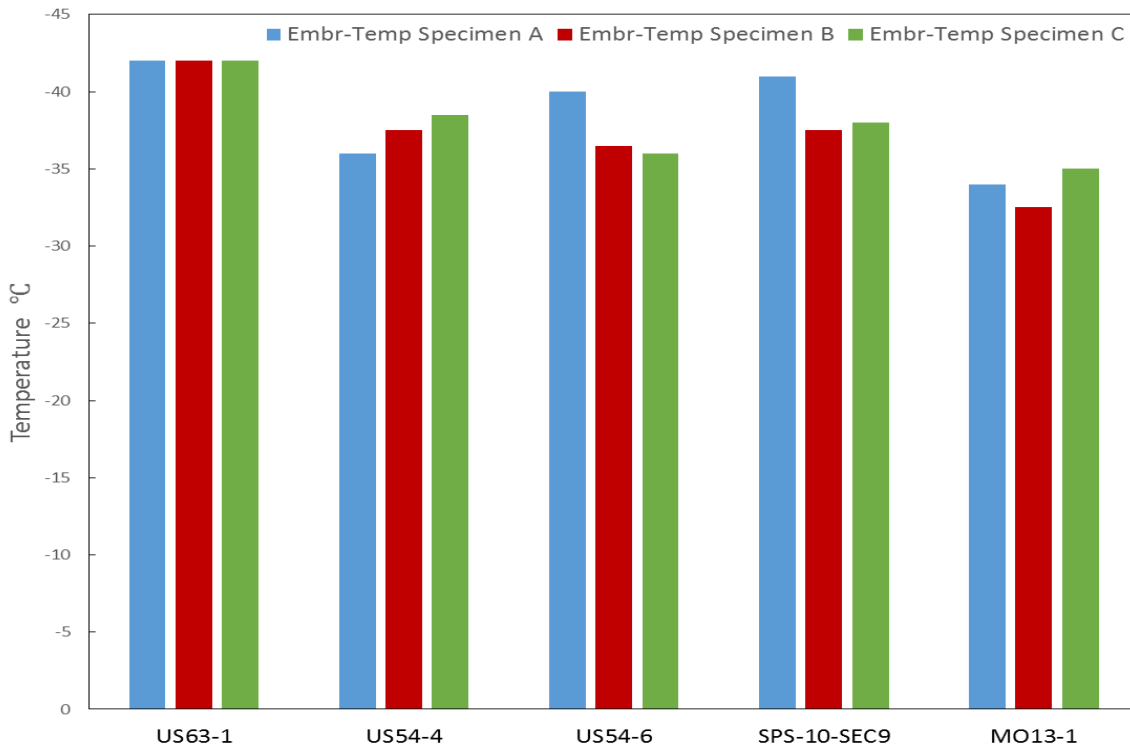


Figure E-6. Embrittlement Temperatures in °C of A, B, C specimens for all binder samples. See Table 3.

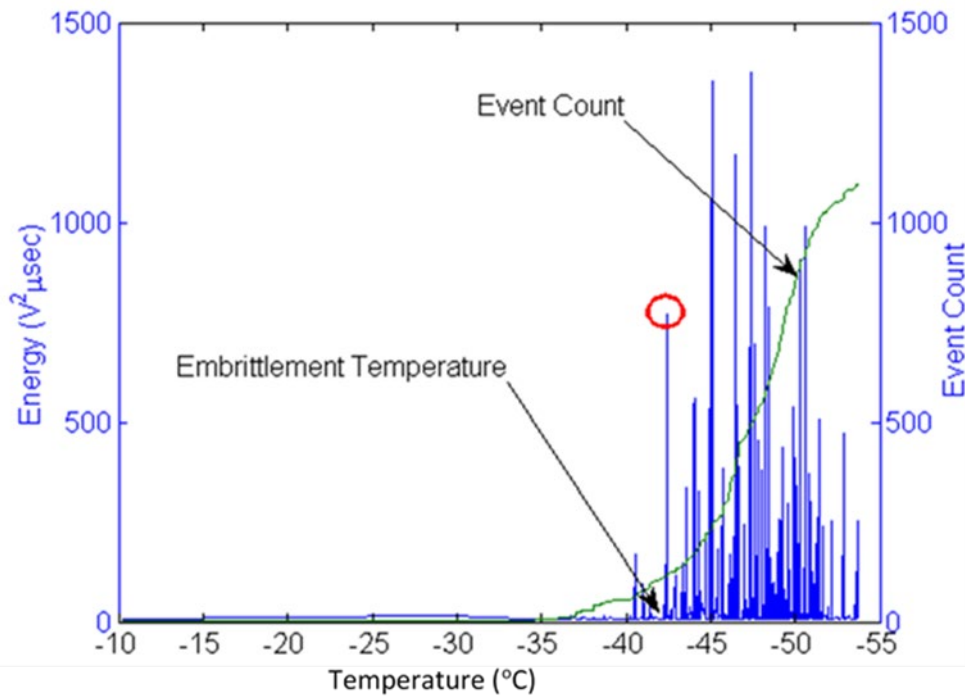


Figure E-7. Acoustic Emission Energy and Event Count versus Temperature for specimen B of US63-1 Binder Sample. Horizontal axis denotes temperature in °C.

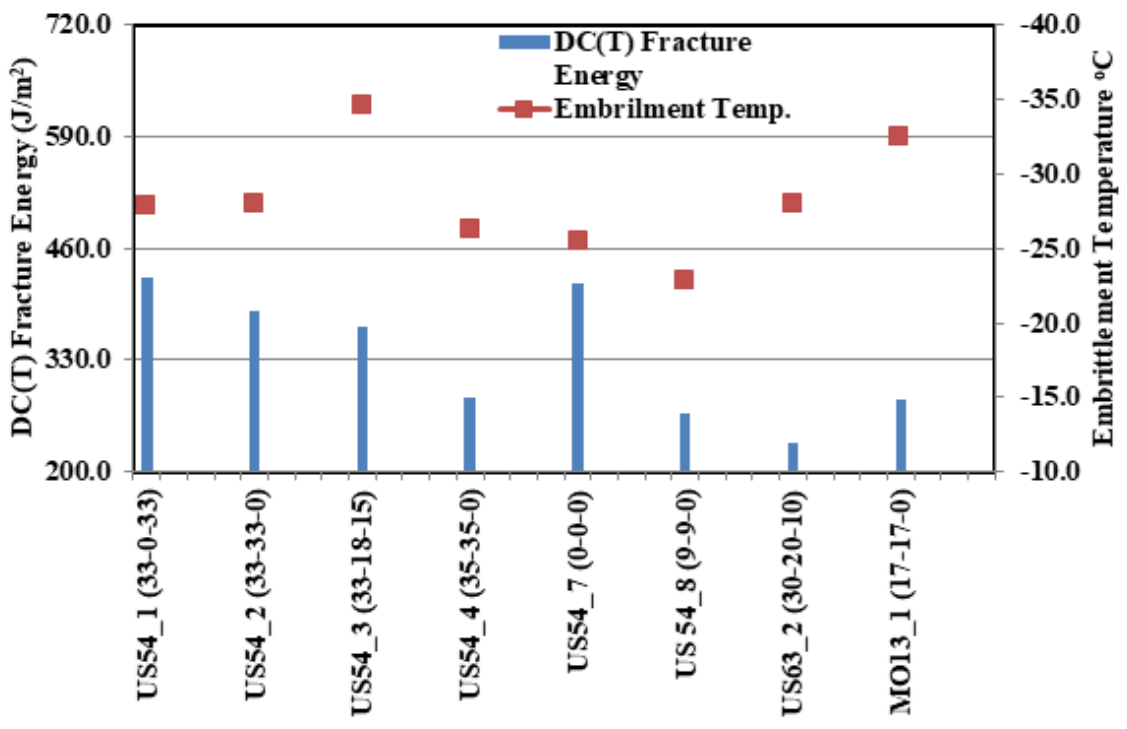


Figure E-8. Embrittlement temperature from Acoustic Emission test compared to the DC(T) fracture energy

Figure E-8 shows comparison between the embrittlement temperatures from AE testing and fracture energies from the DC(T) fracture test. Both the tests characterize the low temperature behavior of asphalt mixtures, but as seen in Figure E-8, the trends are dissimilar. This could be due to the difference in the test procedures; while DC(T) is a mechanical load-displacement type test based on the principles of fracture mechanics, AE test is based on processing signals from the progressively cooling asphalt mixtures. In many cases of AE testing, especially while testing mixtures that have modifiers in them, early isolated signals crossing the set threshold energy level have been observed (14). These isolated signals could be due to presence of a nodule of RAP/RAS or any other modifier such as rubber in the asphalt specimen (14). In cases like these, it becomes difficult to set a particular threshold energy value that's applicable to all the asphalt specimens. This, in turn, results in sometimes missing legitimate energy events during the processing because it was classified as noise, or sometimes accepting a signal and reporting lower embrittlement temperatures when it should have been classified as noise.

E.4. Conclusions

Acoustic emission embrittlement temperatures of asphalt binders and asphalt mixtures were performed on samples provided by the Missouri department of Transportation.

The current AE test differs significantly from existing standard mechanical tests (BBR, DTT, IDT, DC(T), TSRST), and likewise differs from more recently proposed tests, such as the ABCD fracture test, the BBR test for asphalt mixtures, and the modified DENT test of Edwards and Hesp (15). None of the existing or proposed tests has all of the features of the AE-based test, namely:

- Rapid, small, and portable,
- User-friendly computer software with an interactive user interface with the capability to locate AE sources, i.e., cracks.
- Powerful tool to determine the extent of in-situ pavement embrittlement properties loss due to oxidative aging.
- Suitable for both binders and mixtures.
- Independent of sample size and geometry.
- Suitable for in-situ measurements,
- The AE-base method aid in pavement preservation/maintenance by having the potential to determine the optimum timing and method(s) for preventive maintenance and rehabilitation.
- The results obtained have less variability than results typically obtained using traditional methods such as the BBR approach.

E.5. References

- [1] Behzad, B., Buttlar, W.G., and Reis, H., (2011), "An Acoustic-Emission Based Test to Determine Asphalt Binder and Mixture Embrittlement Temperature," NCHRP-IDEA Project 144 Final Report, NCHRP IDEA PROGRAM, University of Illinois at Urbana-Champaign, November 2011.
- [2] William G. Buttlar, G.B., Reis, H., B. Behnia, Sun, Z., and Farace, N., Development and Implementation of the Asphalt Embrittlement Analyzer, NCHRAP IDEA PROGRAM, NCHRP IDEA Project 170, Final Report, University of Illinois at Urbana-Champaign, December 2014.
- [3] T.F. Drouillard, "A history of Acoustic Emission", Journal of Acoustic Emission Vol 14, 1996, pp 1 -34.
- [4] K.M. Holford, "Acoustic Emission---Basic Principles and future directions," Strain 36, 2000, pp 51-54.
- [5] C.B. Scruby "An introduction to Acoustic Emission", Journal of Physics E. Sci. Instru. Vol 20. 1987. pp 946-953.
- [6] Matthew G. Baxter, Rhys Pullin, Karen M. Hullford, and Sam L. Evans, "Delta t Source Location for Acoustic Emission," Cardiff University. 2006. pp 1-9.
- [7] Tinkey, B.V., Fowler, T.J., Klingner, R.E., Nondestructive testing of pre-stressed bridge girders with distributed damage, Technical Research Report 1857-2, 2002, p. 106.
- [8] Behnia, B., Buttlar, W. , Reis, H., Apeageyi, A. "Determining the Embrittlement Temperature of Asphalt Binders Using an Acoustic Emission Approach", the NDE/NDT for Highways & Bridges: Structural Materials Technology (SMT) Conference, New York, August 2010.
- [9] Apeageyi, A.K., Buttlar, W.G., and Reis, H., (2009) "Estimation of low-temperature embrittlement for asphalt binders using an acoustic emission approach" INSIGHT, Vol. 51, No. 3, pp.129-136.
- [10] Dave, E.V., Behnia, B., Ahmed, S., Buttlar, W.G., and Reis, H., (2010), "Low Temperature Fracture Evaluation of Asphalt Mixtures using Mechanical Testing and Acoustic Emission Techniques, AAPT J., Vol. 80, pp. 193-226.
- [11] Behnia, B., Dave, E.V., Ahmed, S., Buttlar, W.G., and Reis, H. (2011), "Effects of Recycled Asphalt Pavement Amounts on Low Temperature Cracking Performance of Asphalt Mixtures using Acoustic Emissions," TRB, No. 2208/2011, pp. 64-71.
- [12] Hill, B.C., Behnia, B., Hakimzadeh, S., Buttlar, W, and H. Reis, "Evaluation of the Low Temperature Cracking Performance of WMA Mixtures," TRR, 2012.

[13] Behzad Behnia, William G. Buttlar, and Henrique Reis (2014) "Cooling Cycle Effects on Low Temperature Cracking Characteristics of Asphalt Concrete Mixtures", Journal of Materials and Structures, DOI 10.1617/s11527-014-0310-y.

[14] Rath, P., 2017. Performance analysis of asphalt mixtures modified with ground tire rubber and related products. University of Illinois, at Urbana-Champaign.

[15] M.A. Edwards, and S.A.M. Hesp, TRR n1962:36-43 (2006).